Elucidating the abilities of MDM2, MDMX and p21 to regulate ferroptosis

Divya Venkatesh

Submitted in partial fulfillment of the
requirements for the degree of
Doctor of Philosophy
under the Executive Committee
of the Graduate School of Arts and Sciences

COLUMBIA UNIVERSITY

2020

Abstract

Elucidating the abilities of MDM2, MDMX and p21 to regulate ferroptosis

Divya Venkatesh

In this thesis, I have explored the role of three genes related to p53, namely p21, MDM2 and MDMX, in regulating ferroptosis, a form of non-apoptotic cell death. Ferroptosis, an iron-dependent mechanism that leads to cell death due to lipid peroxidation, has a large potential to be used as a cancer therapy. My results indicate that p21, the effector of p53-mediated cell cycle arrest, can suppress ferroptosis possibly through its interaction with CDKs. Further, that MDM2 and MDMX, the negative regulators of p53, can act as pro-ferroptosis agents and that this role is independent of p53. Using various approaches to alter their activity, I found that MDM2 and MDMX, likely working in part as a complex, normally facilitate ferroptotic death. They were found to alter the cellular lipid profile to prevent the cells from mounting an adequate defense against lipid peroxidation. For example, inhibition of MDM2 or MDMX lead to increased levels of FSP1 protein and a consequent increase in the levels of coenzyme Q_{10}, an endogenous lipophilic antioxidant. Moreover, I found that PPARα activity is essential for MDM2 and MDMX to promote ferroptosis. My findings also suggest that MDM2-MDMX inhibition might be useful for preventing degenerative diseases involving ferroptosis. Further, that MDM2/MDMX amplification may predict sensitivity of some cancers to ferroptosis inducers. Therefore, I believe that this thesis project has successfully identified several new regulators of ferroptosis and this knowledge can aid better design of therapies centered around ferroptosis.

Table of Contents

List of Tables

List of Figures

Acknowledgments

I am extremely grateful for the many wonderful people in my life, who inspired, supported, mentored and tolerated me throughout my PhD. It truly took an army to make my experience pleasurable while also being successful.

Foremost, I would like to thank both my advisors: Brent Stockwell and Carol Prives, who trusted a fresh eyed undergraduate to establish their collaborative project. I thank Brent, for teaching me to be a critical thinker, nurturing my innovative side and giving me the freedom to explore my ideas, even if they were not always right. I thank Carol for her unwavering support right from indulging my constant impromptu discussions, helping me troubleshoot problems concerning both my professional and personal lives , attaching a high value to my inputs and being an excellent role model of an exceptional scientist as well as mentor. I heavily benefited from being co-mentored, be it in developing a unique perspective from being a part of two distinct labs or getting to attend twice the number of international conferences as any other graduate student.

I was also gifted with the love of the two amazing labs. I am especially thankful to the two lab managers, Ella Freulich and Elise Jiang who truly made sure that I had to worry about nothing other than my experiments. I deeply acknowledge the efforts of my fellow lab members, without whom the success of this project would not have been possible: Nicholas O'Brien, for his unwavering determination and hard work in wading through the multiple challenges that we faced while unraveling the mechanisms at play; Fereshteh Zandkarimi for her timely help in lipidomic analysis and being crucial in helping me draw meaningful conclusions from such complex data; David Tong, for working tirelessly to aid in all our efforts to make the various CRISPR cell lines;

Michael Stokes and Sung-Hwan Moon, Alyssa Klein and Joleen Csuka for their role in helping me generate p21 KO clones, characterize the role of MDM2/X antagonists in effecting cell cycle changes or in the depletion of GSH, respectively.

I also thank our collaborators outside these labs who helped me uplift my project and expand my scientific horizons: Denise Dunn and Donald Lo for extending our data into a neurodegenerative context; Aron Allegra and Christopher Chang for enabling us to effectively measure iron levels with their excellent probe; Angelo D'Alessandro and his team at UC Denver for our initial lipid profiling analysis; Marcus Conrad, for his input and help in connecting our work with the newly discovered ferroptosis suppressor, FSP1 .

I am grateful to all the other present and past members of both these labs as well, not only for their guidance and suggestions to better my project but also for their incredible support that kept me strong through all the ups and downs of this thesis. I thank them for not just being my colleagues, but some of my closest friends and truly my family away from home. I thank my mentees, Eli, Nicholas and Mercedes, mentoring whom gave my life a lot of purpose and who might have actually taught me more than I taught them. I am grateful to Vitalay, for being the best bench mate I could ever have asked for and for keeping me sane to this day (with a lot of help from Brittney); to Ana, Alyssa, Jazmine, Joshua, Carla, Niki, Joleen and Elise, for always being there for me- be it to help me, listen to my complaints or make lab life fun; to Ella, Chen and Tal, whose advice and constant help were paramount to my scientific strides.

I am sincerely thankful to my wonderful committee – Iva Greenwald and Steve Goff , who ensured that every committee meeting was a great open scientific discussion that I looked forward to, and to Scott Dixon for agreeing to fly all the way across the country to advise me on my defense.

I would never have had the strength to do a PhD if it were not for my family. I thank my amazing husband for being patient with me throughout, especially when I was overly critical of some of my striking results despite his reassurances of their scientific merit. I thank my extremely supportive parents, my loving brother, my enthusiastic grandparents, my proud uncles, aunts and parents-in-law for encouraging me to pursue my dreams even if it meant that I would be living in a different country, far away from them. I am fortunate that they all made every possible effort to support and encourage me through my journey.

I have also been blessed with great friends. I thank my other friends in the scientific community for setting examples of great scientists who were also great human beings. I also thank my many "non-scientific friends" for making me smile even when my research did not. I am grateful that they stuck with me even when I had to choose my cells over them at times. I had my own personal armor of people pushing me to do better and yet accepting me with all my limitations.

I want to thank Sarah Kim, Ellie Siddens and Inna Boluk for shielding me from most of the bureaucracy involved in the administrative requirements, so that I could focus all my energy on my research. Finally, I want to thank my mentors at various institutions before my PhD, for nurturing my interest in research and being an integral part of my scientific journey.

Dedication

To my uncle, Gagamama who was like a third parent to me- I derive strength from feeling your love although I sorely miss your presence in my life.

Preface

This dissertation summarizes our efforts into understanding the potential of three p53 related genes, p21, MDM2 and MDMX, in altering the ability of cells to resist death by ferroptosis. Chapter 1 identifies that vast amount of literature relating to ferroptosis, p53, MDM2 and MDMX which provide the foundational basis for developing the project. Chapter 2 pertains to the first part of the project which explores the complex nature of the role of p53 in ferroptosis and identifies potential roles for two p53 target genes, p21 and MDM2 in regulating ferroptotic sensitivity. The portions of Chapter 2 that outline the role of p21 in ferroptosis are part of a manuscript published in *Aging* (2020). Chapters 3 and 4 pertain to the majority of work done during the thesis and are part of a second manuscript published in *Genes & Development* (February 2020). Chapter 3 examines the pro-ferroptotic roles of MDM2 and MDMX, which were found to be independent of p53. Chapter 4 details our efforts into understanding the molecular mechanism controlled by MDM2/X to aid ferroptosis. Chapter 4 also identifies PPARα as a new regulator of ferroptosis, whose activity mediates the ability of MDM2/X to suppress antioxidant defenses of cells, such as CoQ10, in order to promote ferroptotic death. Chapter 5 discusses ideas to further extend the findings of this project in the future.

Chapter 1: Introduction

1.1 Ferroptosis

1.1.1 Discovery and mechanism

Ferroptosis is a form of non-apoptotic death that essentially compromises the oxidative homeostasis of cells in order to kill them. This iron-dependent form of cell death, occurs through an increase in cellular phospholipid peroxidation in the context of a compromised phospholipid peroxide repair system. Specifically, an insult of increased reactive oxygen species (ROS), partly derived from the oxidation of labile iron through Fenton chemistry, in the background of compromised antioxidant defenses of cells leads to this type of death. This disrupted oxidative status of cells leads to rampant lipid peroxidation in membranes, which eventually compromises the integrity of the cells and causes them to perish (Stockwell et al. 2017).

Ferroptosis was originally discovered as a hitherto unknown type of death by two different groups using paralleled approaches: one was a genetic approach showing that the loss of GPX4, an enzyme capable of preventing the accumulation of the deadly peroxidized lipids, induces a non-apoptotic death in mice and that this type of death is also capable of inducing neurodegeneration (Seiler et al. 2008); another was a pharmacological approach using high-throughput drug screens, that discovered some compounds capable of inducing a non-apoptotic death which was dependent on iron regulators and was more lethal to cells harboring a RAS mutation (Yang and Stockwell 2008). Much later this new type of non-canonical death was labeled as “ferroptosis” once it was established as it was dependent on the presence of iron. This death did not share the key hallmarks of any other major types of previously studied death- namely apoptosis, necroptosis and autophagy

(Dixon et al. 2012). Ferroptosis can thus be induced either by using pharmacological modulators or genetic approaches.

1.1.2 Antioxidant defenses compromised in ferroptosis

In this section, the role of key proteins that mediate the cellular antioxidant defenses against ferroptotic killing of cells will be discussed.

Glutathione peroxidase 4 (GPX4) is the only member of the GPX family that is capable of neutralizing lipid peroxides (more information regarding the nature of lipid peroxides is described later in this section). GPX4 is capable of converting the harmful lipid peroxides into harmless lipid alcohols, which are then incapable of propagating the lipid ROS that would otherwise cause the lipid peroxides to accumulate. GPX4 needs to simultaneously oxidize glutathione (GSH is converted to GSSG) in order to reduce the oxidized lipids, thereby making GSH a rate limiting substrate for GPX4 activity (Conrad and Friedmann Angeli 2015). All the different pharmacological inducers of ferroptosis that have since been discovered, do eventually impinge on the activity of GPX4 either directly or indirectly as described below. Additionally, GPX4 expression levels in cells have been found to be correlated with their ferroptosis sensitivity (Yang and Stockwell 2008). This further highlights how central the appropriate functioning of GPX4 is in preventing ferroptosis.

Nuclear factor erythroid 2-related factor-2 (NRF2) is a transcription factor that is well known for its ability to control antioxidant signaling pathways through its target genes. It is in fact considered the master regulator of the cellular antioxidant responses owing to its relevance in various

scenarios that involve the redox balance. Oxidative stress is capable of oxidizing NRF2's negative regulator, KEAP1 to prevent their interaction, thus allowing NRF2 to translocate to the nucleus and effect transcriptional changes. Of relevance to ferroptosis, NRF2's target genes control the synthesis of GSH, as well as iron metabolism; GPX4 is itself a target of NRF2. Therefore, rather unsurprisingly, NRF2 levels in cells can influence their ferroptotic sensitivity and these factors are inversely correlated (Dodson, Castro-Portuguez, and Zhang 2019). Thus NRF2-GPX4 system is one key cellular response against ferroptosis.

Coenzyme Q_{10} (CoQ_{10}), is an endogenous lipophilic antioxidant that can also neutralize the lipid hydroperoxides of the cells. CoQ_{10} is synthesized by the mevalonate pathway; it is produced as one of the branches of the mevalonate pathway, which is often used by cells to generate cholesterol. CoQ_{10} though, is a non-steroidal ubiquinone has been shown to be a quencher of ROS. The reduced form of CoQ_{10} can accept free electrons and this generates the oxidized from of CoQ_{10} (Turunen, Olsson, and Dallner 2004). In addition to its well characterized role in the mitochondrial electron transport chain, CoQ_{10} has also been shown to suppress lipid peroxidation in mitochondrial and non-mitochondrial membranes (Shimada et al. 2016). Recently, two reports have demonstrated that CoQ_{10} functions independently of GPX4 and that these are in fact two parallel antioxidant defense systems against ferroptosis (Bersuker et al. 2019; Doll et al. 2019). These reports also discovered a new suppressor of ferroptosis, AIFM2/FSP1 that has the capacity to regenerate the reduced pool of CoQ_{10} by functioning as an oxidoreductase using NADPH as its substrate. Thus, CoQ_{10} forms the second line of cellular defense against ferroptosis.

1.1.3 Tools available to study ferroptosis

In the last decade the study of ferroptosis has become an emerging field of research across the world. We now have a whole set of tools that can be leveraged to expand the knowledge regarding this type of cell death process.

Ferroptosis inducers: These compounds enable the induction of cell death due to ferroptosis. Four main classes of ferroptosis inducers (FINs) are able to cause cell death through distinct upstream mechanisms (Fig 1.1). The end result of the cellular responses to each FIN is ultimately cellular lipid peroxidation leading to cell death, despite there being different routes to reach this common end point. All these inducers are dependent on the presence of labile iron that can get oxidized to promote the oxidative stress in treated cells (Stockwell et al. 2017).

Class I FINs, inhibit the activity of system X_c^-, the cysteine/glutamate exchange pump. This pump imports cystine in exchange for the export of glutamate. This cystine gets converted to cysteine and eventually glutathione. These FINs thus lead to the depletion of glutathione, which compromises the activity of GPX4 in combatting the devastating accumulation of peroxidized lipids, as glutathione is the substrate needed for this reaction. Examples of class I FINs include erastin, its more potent derivative IKE (imidazole ketone erastin) (Larraufie et al. 2015), as well as chemotherapeutics, sulfasalazine and sorafenib, that have an ability to induce ferroptosis (Dixon et al. 2012; Dixon et al. 2014). Cystine deprivation of cells or preventing the GSH synthesis using BSO (buthionine sulfoximine) are other methods of inducing ferroptosis through the depletion of GSH that is independent of system X_c^- (Stockwell et al. 2017).

Class II FINs (*e.g.*, (1S,3R)-RSL3, hereafter referred to as RSL3) directly bind to and inhibit the activity of GPX4. Since the enzymatic activity of GPX4 is essential to detoxify the lipid hydroperoxides, this inhibition leaves the cells defenseless against the onslaught of lipid ROS (Dixon et al. 2012).

Class III FINs (*e.g.*, FIN56) activate squalene synthase, an enzyme that promotes the synthesis of cholesterol over the other branches of the mevalonate pathway, in turn reducing the production of the intermediates arising from the branches. Since CoQ_{10} is one of the so affected intermediates, this alteration of the mevalonate pathway promotes ferroptosis (Shimada et al. 2016). Inhibiting the mevalonate pathway also blocks the maturation of selenocysteine tRNAs that ensure the presence of selenocysteine in GPX4. The presence of this amino acid in the catalytic pocket is necessary for GPX4's activity (Li et al. 2020). In addition, FIN56 is thought to also cause the degradation of GPX4. Thereby, these class of FINs effectively compromise two different antioxidant defense systems of the cells against ferroptosis (Shimada et al. 2016; Bersuker et al. 2019; Doll et al. 2019).

Finally, Class IV FINs (*e.g.*, $FINO_2$) directly stimulate the oxidation of iron, as well as the loss of GPX4 activity to facilitate the rampant spread of lipid peroxidation (Gaschler et al. 2018).

Ferroptosis inhibitors: Iron chelators and inhibitors of lipid peroxidation are the main ferroptosis inhibitors that can block all the four types of ferroptosis induction described above, as they impinge on the key pathways on which all classes of FINs are dependent. Radical trapping antioxidants (RTAs) like ferrostatin (Dixon et al. 2012) and liproxstatin (Conrad and Friedmann Angeli 2015),

as well as certain naturally occurring lipophilic antioxidants such as Vitamin E are some examples of the blockers of lipid peroxidation. Of note, not all general antioxidants have the ability to behave as ferroptosis inhibitors since their ability to interact with oxidized lipids is crucial for this role. Recently, Derek Pratt's group designed an assay that can verify the ability of RTAs to neutralize lipid hydroperoxides, which can be used to identify effective ferroptosis inhibitors (Stockwell 2019; Shah et al. 2019). Deferoxamine, an iron chelator that is widely used to suppress Fenton chemistry and treat iron-overload based disorders (Mobarra et al. 2016) is also capable of blocking ferroptosis (Dixon et al. 2012).

On the other hand, there are inhibitors of ferroptosis that impinge on other pathways as well. For example, β-mercaptoethanol blocks class I FINS, as it can provide usable cysteine directly to the cells, thereby circumventing the need for system X_c^-; also, since the enzymatic activity of lipoxygenases (LOXs) is key to the formation of lipid hydroperoxides, LOX inhibitors have been previously shown to suppress ferroptosis (Shah, Shchepinov, and Pratt 2018; Seiler et al. 2008). (Stockwell et al. 2017).

Assays to detect the involvement of ferroptosis: Knowledge of the mechanism of ferroptosis induction, enables the use of molecular indicators of this process in cells as well as tissues to determine if the presence of ferroptosis.

As evident from the earlier description of class I FINS, they cause a depletion of GSH and this can easily be measured using a commercially available fluorometric assay (Gaschler et al. 2018). The upregulation of PTGS2 or CHAC1 gene expression can serve as markers of ferroptosis (Zhang et

al. 2019), although their functional relevance is yet unclear. Generally, a cellular death can be considered ferroptotic when it can be rescued by both an iron chelator and an inhibitor of lipid peroxidation, but not by inhibitors of the other major cell death pathways (Stockwell et al. 2017). Another obvious indicator of ferroptosis is change in GPX4 levels (either mRNA or protein levels) or more importantly inhibition of GPX4 activity. This activity can be measured using LC/MS, where the ability of protein lysates, from cells under study, to reduce a provided phospholipid hydroperoxide substrate (such as phosphotidylcholine) is assayed. Alternatively, an absorbance-based assay that measures the amount of NADPH that is reduced in cellular lysates, during the conversion of reduced to oxidized glutathione that is needed for GPX4 to catalyze lipid peroxidation of the provided external substrate, can also be used (Yang et al. 2014).

Many reports have demonstrated iron's relevance to this form of cell death. The formation of lipid peroxides is key to ferroptosis and will be discussed in more detail in the next section. These lipid hydroperoxides mainly form as a result of spontaneous autooxidation catalyzed by iron (Shah, Shchepinov, and Pratt 2018). This is thought to be one key reason that the presence of labile iron, the active form with the catalytic activity, is necessary for ferroptosis.

One of the first reports regarding ferroptosis that described it as an iron dependent process, found that ferroptosis sensitivity was influenced by the levels of transferrin receptor (Yang and Stockwell 2008). This receptor is responsible for the import of transferrin-bound extracellular iron. A more recent report, confirmed that the absence of transferrin in cellular media confers ferroptosis resistance (Gao et al. 2015). Another study has also demonstrated that antibodies against the

transferrin reporter can be used as markers of ferroptosis in both cells and tissues, in either immunofluorescence or flow cytometry-based assays (Feng et al. 2020).

The levels of ferritin, the cellular iron storage protein which keeps iron in an inactive state can also influence rate of ferroptosis (Yang and Stockwell 2008). Autophagy can enhance ferroptotic death by degrading ferritin to release iron (Hou et al. 2016). Therefore, the bioavailability of the transferrin receptor and ferritin protein levels can be used as biomarkers for ferroptosis sensitivity. Further, as previously mentioned, iron chelators are effective ferroptosis inhibitors. The presence of labile iron and ability of class I FINS to increase the amount of labile iron in cells, can also be measured using cellular probes like FIP1 (Aron et al. 2016) and *in vivo* probes such as F-TRX (Muir et al. 2019).

ROS that can oxidize lipids is a major requirement of ferroptosis and this ferroptosis-associated increase in cellular lipid ROS can be detected by the ability of cells to oxidize C-11 Bodipy 581/591, a fluorescent lipid-based dye. C-11 Bodipy 581/591 is red in its native state and it turns green upon being oxidized- this change can be detected either by flow cytometry or live cell imaging (Martinez, Kim, and Yang 2020).

Essentially the state of cellular lipids dictates the outcome of ferroptosis. Phospholipids with polyunsaturated fatty acid (PUFA) tails are more prone to oxidation than those with monounsaturated tails, and are hence the main targets of ferroptosis. In fact, the excessive presence of the latter has been shown to block ferroptosis (Magtanong et al. 2019). The process of oxidation of these polyunsaturated phospholipids can be assayed as hallmarks of ferroptosis. Due to their

oxidation, some intermediates such as 4-hydroxynonenal (4-HNE) and malondialdehyde (MDA) are formed. The presence of these lipid derivates can be measured using flow cytometry or immunofluorescence in cells and immunohistochemistry in tissues. Additionally, the TBARs assay that detects the adducts formed by further reactions of these derivatives can also be used (Feng and Stockwell 2018).

Lastly, lipidomics using mass spectrometry methods is an useful analysis tool that has to potential for being used both to identify the canonical ferroptosis signatures, as well as to glean new information of the type of changes incurred in the cellular lipid metabolism by a novel promoter or inhibitor of ferroptosis. This is still a growing field that needs to overcome many limitations in order to be effective as an untargeted approach. These include (1) the presence of numerous cellular lipid species; (2) the low abundance of most of these lipids, especially the oxidized ones; (3) the ability of small changes in handling of the samples at various phases of processing collection and lipid extraction to cause major perturbations in the lipidomic profile; (4) the analytic complexity due to the huge amount of data obtained and the limited ability of pathway analysis tools to handle lipid-based data. On the other hand, a more hypothesized approach involves enriching for specific lipid species in the samples and then assessing the differences in the abundance of these lipids between test conditions. Given the current limitations stated above, such a targeted approach can provide more definitive results rather than an untargeted approach that analyses changes in the entire lipidome.

Nevertheless, untargeted lipid profiling done in wild-type HT-1080 fibrosarcoma cells treated with erastin/IKE has revealed certain signatures of ferroptosis. There is often a depletion in

phospholipids and triacylglycerides, potentially due to the cleavage of their oxidized PUFA tails when these cells undergo ferroptosis (Zhang et al. 2019). On the other hand, these cells also exhibit an increase in lysophospholipids that are formed after the lipid peroxidation-induced cleavage of the PUFA tails, and in diacylglycerides, which can potentially arise due to the hydrolysis of triacylglycerides. This signature does of course vary with cell type, the presence of mutations and type of ferroptosis induced.

1.1.4 Evidence of involvement of ferroptosis in human disorders

Several reports have linked dysregulated ferroptotic death to various types of diseases. Ferroptotic death has been implicated in multiple neurodegenerative disorders such as Huntington's, Alzheimer's, Parkinson's and ischemic stroke (Wu, Tuo, and Lei 2018). Excessive ferroptosis has also been shown to be a key effector of cardiomyopathy (Fang et al. 2019), renal damage and failure (Friedmann Angeli et al. 2014; Müller et al. 2017) and can potentially mediate the loss of immunity against infection (Matsushita et al. 2015).

Ferroptosis also has the potential to be used as a selective cancer therapy. Cancer cells are generally more reliant on their antioxidant defenses since their enhanced rate of proliferation produces a lot of ROS (Dixon and Stockwell 2014).. They also often have accumulated iron in order to satisfy their energy needs. For example, B- cell lymphomas (DLBCLs) and renal carcinomas are very sensitive to ferroptosis, as they harbor both the above-mentioned dependencies. While DLBCLs are more dependent on system X_c^- , the renal carcinomas require GPX4 activity. Especially in the case of the renal cancers, targeting this dependency might provide a new mode of treatment as they are often resistant to chemo and radio therapy (Yu et al. 2017).

In recent times, there have been several reports that showcase this potential of ferroptosis- IKE nanoparticles were able to suppress tumor growth *in vivo* (Zhang et al. 2019); CD8+ T cells that are activated post immune checkpoint blockade therapy were shown to enhance the rate of ferroptosis in their target tumors and ferroptosis was an essential part of their ability to clear tumors (Wang et al. 2019); FINs were also demonstrated to synergize with radiation to provide a way to target radiation sensitive tumors (Lei et al. 2020; Ye, Chaudhary, et al. 2020). While some chemotherapeutics like sulfasalazine and sorafenib, as previously explained, can have some ferroptotic death associated with their killing effects, it is also conceivable to design combination therapies of FINs with other chemotherapeutics as well. In fact, erastin was able to synergize with some drugs such as cisplatin and doxorubicin to kill some cancer cell lines (Sato et al. 2018).

The involvement of ferroptosis in immunotherapy also suggests that ferroptosis might be part of the natural tumor suppression mechanism in organisms, though this hypothesis is not yet proven. The section detailed below also suggests that ferroptosis might play a role in the ability of p53 to suppress tumor formation.

Therefore, continuing research efforts into identifying more regulators of ferroptosis is the need of the hour. These discoveries will help better frame the therapeutic applications of the pharmacological regulators of ferroptosis in the context of cancer and other disorders.

1.2 p53

Cancer is essentially a result of failure of the attempts of the cellular system at rectifying insults or its own mistakes to prevent unchecked proliferation of such damaged cells. One of the major

lines of defense of the cell that are bypassed in cancer are tumor suppressors such as p53. Indeed the *Tp53* gene is found to be mutated with high frequency in cancer; while the frequency of mutation varies with the tissue of origin, over 50% of most tumors have either lost p53 expression or have acquired a mutation in *Tp53* (Olivier, Hollstein, and Hainaut 2010).

1.2.1 Function as a transcription factor

p53 is a DNA-binding dependent transcription factor and this function is the largest contributor to its most well-known role as a tumor suppressor (Beckerman and Prives 2010) . This is evidenced by the most common mutations in p53 being missense mutations in its DNA-binding domain, which disrupt the ability of p53 to bind to DNA of its target genes in order to control their transcription (Olivier, Hollstein, and Hainaut 2010).

p53 has been shown to directly activate a whole host of target proteins, which help p53 modulate the fate of the cell (Riley et al. 2008). The ability of p53 to directly repress certain downstream targets is yet controversial. While there is some evidence suggesting that p53 can directly repress some targets (Ho and Benchimol 2003), there are others that show that p53 downregulates its targets only through its activation targets (Sullivan et al. 2018). p53 can also alter some signaling pathways in cells through transcription independent mechanisms: p53 can contribute to controlling protein synthesis by associating with some key proteins of the translation machinery (Ewen and Miller 1996); the protein-protein interactions of p53 can promote apoptosis (Moll et al. 2005) and also suppress homologous recombination post DNA damage by inhibiting several members of the repair system (Menon and Povirk 2014).

p53 gets activated in response to various stresses that interfere with its negative regulation in different ways. Upon activation, it affects a whole host of downstream targets, in any of the above-mentioned ways (Fig 1.2) (Beckerman and Prives 2010). Depending on the targets affected, p53 can then mediate various outcomes that have relevance in tumor suppression, as well as other disorders. p53 seems to be able to make a choice on which program to activate and differentially dictate the fate of the cell based on the type and severity of stress (Surget, Khoury, and Bourdon 2013). Thus, p53 is key protein in regulating numerous cellular outcomes most of which are relevant to its function as a major tumor suppressor.

1.2.2 p53 can regulate cell survival

As mentioned earlier, p53 is able to differentially respond to stresses. In terms of acute stresses such as extensive or irreparable DNA damage, for example, it can promote death of the damaged cells. One of the major cell death processes known to be mediated by p53 is apoptosis. As p53 controls numerous pro-apoptotic target genes such as Bax, PIGs, NOXA, PUMA, KILLER/DR5 it can induce both extrinsic and intrinsic apoptotic pathways, even independent of caspase activation (Vousden and Lu 2002; Ranjan and Iwakuma 2016). It can also promote cell death via its activation of targets involved in autophagy such as DRAM (Levine and Abrams 2008). In some cases, p53 can promote senescence in response to severe damage or oncogenic stress through Pml and prolonged p21 activation among others (Qian and Chen 2013). p53 has also been shown to regulate other non-apoptotic cell death pathways such as necroptosis, paraptosis, pyroptosis and even ferroptosis (Ranjan and Iwakuma 2018) (Fig 1.3). On the other hand, when the stress is more moderate, however, p53 usually induces a cell cycle arrest, that is reversible in most cases and allows cells the time to repair their DNA before resuming proliferation (Hoe, Verma, and Lane

2014). The type of arrest is dictated by the choice of downstream target affected by p53. For example, one of the strongest responder of p53, p21 can impose a G1 arrest, whereas downstream targets, 14-3-3σ and GADD45 mediate a G2 arrest (Sionov and Haupt 1999).

The ability of p53 to dictate cellular metabolism can also help determine cell fate independent of the above targets that affect cell survival directly. p53 regulates some target genes with the ability of altering glycolysis and energy generation of cells, that in turn affect the ability of cells to proliferate. p53 controls GLUT1/4 that regulates glucose uptake, TIGAR that is the rate limiting enzyme in glycolysis, SCO2 that mediates oxidative phosphorylation and GLS2 that can alter the Krebs' cycle and the antioxidant potential of cells (Hager and Gu 2013). p53 can also alter cellular lipid metabolism by modulating certain key lipid pathways (Parrales and Iwakuma 2016) such as the downregulation of lipogenesis and the mevalonate pathway (Moon et al. 2019), as well as the upregulation of fatty acid oxidation and lipid uptake (Gnanapradeepan et al. 2018). Some of these roles in metabolism have also been shown to be relevant to the tumor suppressive functions of p53.

1.2.3 Role in multiple disorders

The most well studied role of p53 as a tumor suppressor, stems from its abilities to suppress the unchecked proliferation of cells by the myriad ways listed above. There have been several reports that affirm its role as the guardian against tumor growth ever since the discovery of p53 to be a tumor suppressor as opposed to a proto-oncogene. Li-Fraumeni syndrome patients, who harbor inheritable germline mutations in p53 are cancer prone (Guha and Malkin 2017). Mice that have been engineered to be p53 null are also similarly predisposed to develop cancer, especially sarcomas and lymphomas (Attardi and Jacks 1999). It is also supposed that most human cancers

have lost their p53 function in one of many ways (Vogelstein, Lane, and Levine 2000). Many of them acquire p53 mutations in one of their alleles and subsequently lose their second wild-type p53 allele by LOH, which is also one of the hallmarks of tumor-suppressors (Baker et al. 1990). Those which retain their wild-type p53 often accrue other mutations which inhibit the functionality of p53, such as the overexpression of its negative regulators MDM2 and MDMX (Karni-Schmidt, Lokshin, and Prives 2016). In the recent past, many therapies trying to reactivate wild-type p53 function, either by reverting the mutation or by inhibiting its negative regulators, have shown to have an anti-tumorigenic potential (Wang and Sun 2010; Cheok and Lane 2017) and this remains an ongoing field of study.

While p53 has been extensively studied for its inhibitory roles in cancer due to its effects in triggering apoptosis and blocking cell proliferation in response to stress, it can also have a role in physiological settings. The loss of p53 can negatively affect embryonic development owing mainly to the lack of clearing of cells necessary for the proper maturation of the embryo (Armstrong et al. 1995; Rinon et al. 2011). On the other hand, hyper activation of p53 can have roles in promoting premature-aging (Lessel et al. 2017), death of neurons in neurodegenerative disorders such as ALS (Aleksandra Szybińska, 2017), Huntington's disease (Steffan et al. 2000) and Alzheimer's disorder (Hooper et al. 2007), as well as other developmental syndromes due to improper formation of tissues (Van Nostrand et al. 2014; Bowen and Attardi 2019).

p53 can also regulate various aspects of stem cell growth and cellular differentiation (Jain and Barton 2018). p53 mainly has inhibitory effects on the self-renewal potential of the adult stem cells of hematopoietic and neuronal origin (Meletis et al. 2006; Liu et al. 2009). Loss of p53 activity is

a key factor in being able to successfully generate induced pluripotent stem cells (Lin and Lin 2017). p53 is also able to regulate differentiation of the mesenchymal layer to determine appropriate cellular lineages (Molchadsky et al. 2008).

Given the multiple roles that p53 can have in mediating various cellular processes both in cancer and otherwise, it is not surprising that p53 is capable of altering the response of cancer cells to treatments through its extensive network of downstream transcriptional targets. One of the first studies to show this was able to demonstrate that the ability of 123 different chemotherapeutic drugs to inhibit the growth of NCI-60 cancer cell lines was linked to their p53 status (Connor et al. 1997). Mutations in p53 have been shown to enhance the chemo-resistance of many patient-tumors to a wide range of traditional forms of chemotherapy, including doxorubicin and cisplatin treatments (Hientz et al. 2017).

1.2.4 p53 has a complex role in regulating ferroptosis

As p53 is a crucial factor in controlling the response of cancer cells to drug treatment, in addition to the roles in regulating cellular metabolism, understanding its involvement in the ferroptotic death of cells is of large importance. Indeed, in the recent past, several groups have been studying the ability of p53 to modulate the ferroptotic sensitivity of cancer cells.

The initial set of reports showed p53 as a promoter of ferroptosis through regulation of a number of downstream targets (Murphy 2016). First, p53 can decrease the expression of *SLC7A11*, a component of system X_c^- that is necessary for uptake of cystine by some cells to generate glutathione, the substrate of GPX4 activity needed to suppress ferroptosis (Jiang et al. 2015). This

study also provided evidence that ferroptosis can contribute to the tumor growth and the embryonic developmental defects seen in mice due to the absence of functional p53. Second, glutaminolysis driven by GLS2 was shown to promote ferroptosis in human cancer cells, possibly through its ability to alter cellular metabolism, which in part can lead to ROS production to favor ferroptotic killing (Gao et al. 2015). GSL2 is a p53 activation target (Hu et al. 2010; Suzuki et al. 2010) and in fact, it was also reported that when human cancer cells harbor an African polymorph variant of p53 (P47S), whose ability to induce GLS2 is compromised, they are rendered ferroptosis-resistant (Jennis et al. 2016). This polymorph of p53 is also ineffective at tumor suppression in mice, even though it retains the ability to activate a majority of the transcriptional programs of wild-type of p53, including those that control the induction of apoptosis and senescence. Taken together, these two studies show that p53 can promote ferroptosis through its activation of GLS2. Third, p53 can induce *SAT1*, an enzyme that controls polyamine metabolism, which was found to increase the formation of lipid peroxides to drive this type of cell death in human cancer cells, as well as in xenografts and MEFs. *SAT1* possibly enhances the presence of lipoxygenases in the cell through its effect on metabolism to cause the increase in lipid peroxides (Ou et al. 2016). All these studies suggest that ferroptosis can be a part of the arsenal of weapons used by p53 to execute its role in tumor suppression.

Yet recently, there have been other studies that have provided evidence that p53 can suppress ferroptosis in some contexts. The first report showed that p21, a well-studied p53 target, can delay the onset of ferroptosis either induced pharmacologically or due to cystine deprivation in human and mice cancer cells (Tarangelo et al. 2018). Here, while the mechanism is not fully established, it was supposed that p21 could increase the retention of reduced glutathione even under ferroptotic

conditions. Another report showed that p53 can form a complex with DPP4 and prevents it from accumulating at the plasma membrane by promoting its nuclear localization (Xie et al. 2017). Since only the membrane localized DPP4 can complex with NOX1 to promote the lipid peroxidation of the membranes, this interaction with p53 could suppress ferroptosis in human colorectal cancer cells.

On the other hand, mutant p53 seems to be able to enhance the ferroptotic sensitivity of human cancer cells. Oesophageal cancer cells and xenograft tumors harboring mutant p53 were more susceptible to ferroptosis treatment, due to the ability of mutant p53 to bind and inhibit the function of NRF2 (Liu et al. 2017). Mutant p53 was also reported to be driver of ferroptosis sensitivity across a panel of human colorectal cancer cells (Xie et al. 2017). Since wild-type p53 often has opposing functions as mutant p53, this further suggests that p53 can inhibit ferroptosis.

Thus, while the ability of p53 to regulate ferroptosis has been demonstrated in different models, the directionality of this regulation seems to vary with context. This necessitates the discovery of additional downstream targets of p53 that can regulate ferroptosis. It is possible that p53 chooses to affect different downstream targets based on the context, which then dictate the ferroptotic outcome. It is also possible that oncogenic alterations in these downstream effectors of the p53 network leads to differential modulation of the ferroptosis sensitivity through diverse mechanisms, contributing to either tumor suppression or oncogenesis.

1.3 MDM2 and MDMX

1.3.1 Discovery and importance to cancer progression

Murine double minute 2 (MDM2*)* was originally discovered as a gene present in the extrachromosomal nuclear bodies of a spontaneously transformed murine fibroblast cell line (3T3) (Fakharzadeh, Trusko, and George 1991). The name of this gene hails from the notation of these extrachromosomal bodies as 'double minutes'. *MDM2* was found to be highly amplified in these cells and it was considered a potential causative factor for their transformation. The human ortholog of MDM2 is often referred to as HDM2. MDMX was later discovered as a mouse homolog of the MDM2 protein using cDNA expression libraries (Shvarts et al. 1996) and it has a human ortholog that is also referred to as HDMX/MDM4 (Shvarts et al. 1997).

Soon after the original discovery of MDM2, it was demonstrated that the underlying reason for its role in transforming cells was mostly related to the negative regulation of p53. MDM2 was reported to bind to p53 and inhibit the transcriptional output of p53, as well as being capable of lowering the stability of p53 (Iwakuma and Lozano 2003). On the other hand, MDMX was essentially discovered as a protein that interacts with p53 and that also shared some functions of MDM2 (Shvarts et al. 1996). The presence of gene amplifications of *MDM2* and *MDMX* in tumors harboring wild-type p53 further gave credence to the theory that the overexpression of these MDMs is another route opted by cells to eliminate the function of p53 and turn cancerous (Karni-Schmidt, Lokshin, and Prives 2016). MDM2 is often overexpressed in gliomas and sarcomas, while *MDMX* is amplified in gliomas as well as in head and neck carcinomas (Danovi et al. 2004).

While the above studies demonstrating the ability of MDM2 and MDMX to restrain p53 mainly used *in vitro* systems, there have since been several mouse models that extend this analysis to *in vivo* models as well. The first pair of studies showed that the embryonic lethality of *MDM2*

deficient mice could be rescued by a concomitant deletion of *p53* (de Oca Luna, Wagner, and Lozano 1995; Jones et al. 1995). This suggested that the developmental deficiencies and extensive apoptosis observed in the *MDM2* deficient mice were consequences of unrestrained p53 activity in the absence of MDM2. MDMX null mice also exhibited similar p53-dependent embryonic lethality, but this lethality was found to have a slightly more delayed onset and to involve cell cycle arrest rather than apoptosis (Parant et al. 2001). This supports the idea that MDM2 and MDMX are both needed to effectively restrain p53.

Given the lethality seen in mice lacking either MDM2 or MDMX in a background of wild-type p53, conditional knock-out models were created in order to be able to examine the nature of p53 regulation in adult mice. In radio-sensitive tissues, both the conditional activation of p53 in the absence of MDM2 as well the conditional knockout of MDM2 in the presence of p53 killed the adult mice within a few days (Ringshausen et al. 2006; Zhang et al. 2014). Even in radio-insensitive tissues, although not usually lethal, the loss of MDM2 did lead to the stabilization of p53 and a subsequent increase in activity. Other conditional models with tissue specific expression of MDM2/p53 have further demonstrated the presence of this regulation in all tissues of the mice, but the more proliferative tissues tend to show more damage/death upon loss of this inhibition of p53 (Tackmann and Zhang 2017). On the other hand, the extent of requirement of MDMX for the regulation of p53 seems more tissue dependent and the absence of MDMX in adult mice is reported to be less severe. This could potentially be a due to the loss of MDMX resulting in a blockage of cell proliferation rather than apoptosis as caused by the loss of MDM2 (Marine, Dyer, and Jochemsen 2007).

Thus, MDM2 and MDMX are both considered essential and non-redundant for maintaining p53 homeostasis in normal cells (Shadfan, Lopez-Pajares, and Yuan 2012).

1.3.2 Mechanism of negative regulation of p53 by MDM2 and MDMX

MDM2 and MDMX are the most well-studied inhibitors of p53 activity. They can negatively regulate the activity of p53 in multiple ways, both independently and together (Gu J 2002). MDM2-p53 signaling is essentially a negative feedback loop, as MDM2 is a target of p53. Upon activation, p53 binds to the P2 promoter region of *MDM2* that is adjacent to the transcription start site of this gene and transactivates *MDM2* to produce large amounts of the MDM2 protein (Zhao, Yu, and Hu 2014). MDM2 can then bring back p53 levels to normal, in order to help restore the cellular homeostasis in normal cells and to allow the cell to resume post a p53-mediated arrest due to a mild insult and subsequent DNA repair (Alarcon-Vargas and Ronai 2002).

MDM2 can inactivate p53 in three main ways, which are all contingent on MDM2-p53 binding but are not interdependent (Wade, Wang, and Wahl 2010). By binding to p53, MDM2 blocks the transactivation domains of p53 and alters its conformation. MDM2 can also recruit additional co-activators in order to inhibit the transcriptional activity of p53. Alternatively, MDM2 can potentiate nuclear export of p53 to prevent its access to the promoters of its downstream targets. The key negative role of MDM2 lies in altering p53 stability, by polyubiquitinating it through its E3 ligase function and enabling it to be targeted to the proteasome for degradation (Shi and Gu 2012). This last function of MDM2, benefits from the presence of MDMX, since the MDM2-X heterocomplex is a better degrader of p53, owing to its heightened E3 ligase activity (Gu J 2002). The reasons for the heightened E3 ligase function of the MDM2-X complex will be discussed in

in the following section. Although MDMX does not have any E3 ligase function on its own, it can also inhibit the transcriptional potential of p53 independent of MDM2. Through binding-dependent interactions with the transactivation domain of p53, MDMX can inhibit its ability to interact with DNA (Danovi et al. 2004).

The interactions between MDM2/X and p53 keep the basal levels of p53 low in unstressed cells but upon cellular stress, this interaction is broken mainly though post-translational modifications on either of the partners effected by stress sensors (Wade, Wang, and Wahl 2010). The breakage of this interaction thus allows for the activation of p53 needed to appropriately respond to the cellular insult.

1.3.3 Structure of the MDMs

The MDMs- MDM2 and MDMX are structural homologs. While full length human MDM2 protein has 491 amino acids, the human MDMX protein has 490 amino acids. MDM2 and MDMX share the following key motifs: a p53 binding domain in the N terminus, a relatively unstructured acidic domain, a zinc finger motif and a RING domain towards the C-terminus. MDM2 additionally has a nuclear localization signal, a nuclear export signal in the region between the p53 binding domain and the acidic domain, and a nucleolar export signal in the RING domain. Therefore, MDM2 is often localized in the nucleus, while MDMX is usually localized to the cytoplasm, as it lacks these motifs (Karni-Schmidt, Lokshin, and Prives 2016).

MDM2 has an important function as an E3 ligase, to poly and mono ubiquitinate its targets and this function is crucial to the negative regulation of p53; mouse models harboring a *MDM2* mutant deficient

in E3 ligase function are similarly embryonic lethal as a fully *MDM2* deficient mouse, thereby further demonstrating the necessity of this function for MDM2 to effectively inhibit p53 (Tackmann and Zhang 2017). The RING domain of MDM2 is essential for this E3 ligase activity as it chelates Zinc to help MDM2 transfer ubiquitin from the E2 enzyme onto its target protein (Fang et al. 2000). Although MDMX has a RING domain, it has no E3 ligase activity of its own (Iyappan et al. 2010). By forming a heterocomplex with MDM2, MDMX is considered to enhance the effectiveness of the E3 ligase activity of MDM2 (Wade et al. 2012). Although controversial, MDM2 is thought to be able to ubiquitinate itself and MDMX is supposed to stabilize MDM2 by blocking this ability (Stad et al. 2001). Instead, MDMX might then focus the E3 ligase activity of MDM2 against its other targets, thereby providing one reason for the MDM2-X heterocomplex being a better E3 ligase.

The RING domains of these proteins are crucial for the interaction needed between them to form a heterocomplex. There are some residues beyond the RING domain at the C-Termini of both proteins which are also essential for this complex to be stably formed. Mutations in either protein in one of these two regions have been shown to block the formation of the heterocomplex (Uldrijan, Pannekoek, and Vousden 2007; Huang et al. 2011). While, these mutations in MDM2 alone can also block its E3 ligase activity, the extreme C-terminus of MDMX can rescue the E3 ligase ability of C-terminal mutant of MDM2, thus confirming the importance of the domains of MDMX for the E3 ligase activity of the complex (Wade et al. 2012; Poyurovsky et al. 2007).

1.3.4 p53 independent roles of MDM2 and MDMX

MDM2 and MDMX can possess functions and interactions that are independent of p53. MDM2 in particular has been shown to have pro-oncogenic activities beyond regulating p53 (Bohlman and

Manfredi 2014). MDM2 can bind to a myriad of proteins, either altering their activity or causing their proteasome-mediated degradation (Fåhraeus and Olivares-Illana 2013). MDM2 has been shown to regulate gene expression (Biderman, Manley, and Prives 2012; Jain and Barton 2016), heterochromatin rearrangement (Mungamuri et al. 2016; Wienken, Moll, and Dobbelstein 2017), as well as DNA repair and replication (Melo and Eischen 2012; Eischen 2017) independent of its regulation of p53. Furthermore, this protein has p53-independent roles in regulating EMT and metastasis (Chen et al. 2013; Chen, Wang, Wu, et al. 2017; Lu et al. 2016; Wang et al. 2009), cell survival and growth (Feeley et al. 2017), as well as mitochondrial dynamics (Arena et al. 2018).

While it is less studied, MDMX has also been shown to regulate cellular processes independently of p53. MDMX can enhance tumor progression in some cases by promoting cancer cell growth and genomic instability (Kadakia et al. 2002; Carrillo et al. 2015; Xiong et al. 2017). Supporting the idea that MDM2 and MDMX have p53-independent functions is data from human patients' tumors that do not harbor wild-type p53, but have amplified levels of MDM2 or MDMX or both. It is also noteworthy that both MDM2 and MDMX can be activated by oncogenic stressors and mitogenic signals apart from p53 (Karni-Schmidt, Lokshin, and Prives 2016; Shadfan, Lopez-Pajares, and Yuan 2012).

Intriguingly, in some settings, MDMX may have tumor suppressive roles in limiting cell transformation (Matijasevic et al. 2008) and tumor progression (Mancini et al. 2017), as well as promoting genome stability (Matijasevic et al. 2016). MDM2 has also been found to have tumor suppressor functions in addition to its oncogenic functions (Manfredi 2010). For example, MDM2 has been reported to have growth inhibitory domains (Deb 2002; Deb 2003), which seem to be particularly manifested when MDM2 is ectopically expressed (Ganguli and Wasylyk 2003; Deb 2003).

Of particular interest to this study, MDM2 and MDMX are also capable of regulating cellular metabolism independent of p53. MDM2 was shown to be recruited to the chromatin in response to starvation and oxidative stress. This chromatin-bound MDM2, co-operated with transcription factors ATF3 and ATF4 to control genes involved in serine metabolism (Riscal et al. 2016). Such a regulation served to restore cellular oxidative homeostasis. On the other hand, in a recent pair of studies, MDM2 was shown to regulate the mitochondrial dynamics to promote oxidative stress (Arena et al. 2018; Elkholi et al. 2019). Additionally, in a mouse model of lipodystrophy, MDM2 was shown to control certain aspects of adipocyte differentiation independent of p53. The absence of this control led to various metabolic disorders, many of which were lipid related (Liu et al. 2018). MDM2 has also been shown to regulate certain members of the PPAR family, which are lipid regulators whose relevance to lipid metabolism will be discussed in detail in a later section. By controlling the activity of PPARα (Gopinathan et al. 2009) and the stability of PPARγ (Park et al. 2016), MDM2 can have an influence on the global lipid metabolism of cells. MDMX has also been reported to promote the excessive accumulation of fat in mice (Kon et al. 2018). These reports suggest that MDM2 and MDMX might have a potential in being targeted to treat metabolic disorders.

1.3.5 Tools available to study the functions of MDM2 and MDMX

Since MDM2 and MDMX are the main negative regulators of p53, there have been several approaches taken to target them in an attempt to reactivate p53 for cancer treatment.

As detailed earlier, there have been many genetic approaches comprising of complete or partial knockout of MDM2/X that may be conditional or constitutive in mice, as well as cancer cells. A series of mouse embryonic fibroblast lines with loss of MDM2 and p53, MDMX and p53, as well

as loss of MDM2, MDMX and p53 are also available (Barboza et al. 2008). By extension, MDM2 and MDMX can be targeted using RNA interference for performing transient experiments in both mice and human cells. If these experiments are performed in the absence of p53, then they allow for studying the p53-independent functions of these MDMs.

Further, there are numerous small molecules designed to behave as antagonists of the functions of MDM2 and MDMX (Fig 1.4). Most of these disrupt their ability to interact with p53. Many such inhibitors often bind to the p53-binding pocket of MDM2 to outcompete p53; nutlin-3 is one of the more famous of such inhibitors (Vassilev et al. 2004). RITA is another commonly used inhibitor that competitively binds to p53 instead (Issaeva et al. 2004). There are other small molecules which abrogate MDMX-p53 binding, as well as small molecules or peptides that can simultaneously inhibit the binding of both MDM2 and MDMX to p53 (Karni-Schmidt, Lokshin, and Prives 2016). While these inhibitors are a great collection to study the p53-dependent roles of MDM2/X, they cannot be used to assess the p53-independent roles of these proteins.

In order to study MDM2 and MDMX outside the context of p53, there is need to utilize inhibitors whose mechanism of action is not related to p53. There are two main classes of such antagonists: those that affect protein abundance of either MDM2 or MDMX and those that affect the E3 ligase function of either MDM2 or the MDM2-X homodimer. The MDMX inhibitor NCS207895 (Berkson et al. 2005; Wang and Yan 2011), which lowers the transcription of *MDMX* by preventing RNA polymerase from binding to its promoter and SP-141 that enhances the autoubiquitination and subsequent proteasomal degradation of MDM2 (Wang et al. 2014) are two key inhibitors belonging to the first class. Compounds such as HLI, MPD and Sempervine inhibit

the E3 ligase activity of MDM2 but their effects on the E3 ligase activity of the MDM2-X complex are unclear (Wade, Li, and Wahl 2013). On the other hand, MELs specifically inhibit the E3 ligase activity of the MDM2-X heterocomplex with a much lower inhibition of the E3 ligase activity of the MDM2 homodimer (Herman et al. 2011). While these MEL compounds do not inhibit the complex formation, MMRi compounds inhibit the E3 ligase activity of the MDM2-X complex indirectly by binding to the RING domain of MDMX to prevent the RING-RING interaction between the proteins (Wu et al. 2015).

The varying mechanism of action of these inhibitors provides different ways of targeting MDM2 and MDMX to best suit the needs of the biological question. Apart from the question at hand, the choice of these tools should also be based on their limitations. RITA and the HLI compounds has been shown to have p53 independent roles (Wade, Li, and Wahl 2013). While in the case of HLI, this may be due to impingement on the p53-independent roles of MDM2 but it still needs to be confirmed. Even if not off-target effects per se, the compounds can have effects besides the proposed mechanism and these may interfere with drawing firm experimental conclusions. For example, some inhibitors of the MDM2/X-p53 interaction can also enhance the formation of MDM2 homodimers and MDM2-X heterodimers (Wade, Li, and Wahl 2013). So, these inhibitors may in fact enhance the p53-independent roles of MDM2/X. Additionally, the MMRi compounds also cause the degradation of both MDM2 and MDMX apart from blocking their RING interactions. It is quite possible that the degradation is the main reason for prevention of complex formation, but the exact sequence of events and reasons behind the degradation are yet unknown. This suggests that the MMRi compounds may also affect the functions of MDM2 and MDMX that are independent of each other. Further, the various antagonists can also have other effects based

on the system of use and thus, must be carefully assessed before being used to infer the functions of MDM2 and MDMX.

The presence of these limitations highlights the need to use multiple approaches that include small molecules with different mechanisms complemented with genetic techniques, in order to make robust discoveries. Even though each method has its own limitation, if multiple methods all concur on the core observations then there would be higher confidence in the conclusions. There is a higher likelihood in such inferences being true and not being mere artifacts of the technique used for study.

1.4 PPARα

1.4.1 The PPAR family

The peroxisome proliferator-activated receptors (PPARs) are a family of transcription factors that can sense nutrients and act as nuclear hormone receptors. As mentioned in the previous section, they are capable of regulating global lipid metabolism. These proteins are ligand activated transcriptions factors, which undergo a conformational change upon ligand binding. Then, along with RXR family of proteins, they often form heterodimeric complexes that can bind to the DNA response elements (peroxisome proliferators response elements- PPRE) of their targets to regulate their transcription (Qi, Zhu, and Reddy 2000). The PPARs respond to various stresses including the levels of lipids in the environment, which act as their specific ligands to elicit different downstream responses. There are three main isoforms: PPARα, PPARγ, and PPARβ/δ; their expression is tissue specific and they each activate/repress different downstream targets to regulate different aspects of lipid metabolism as well as energy homeostasis (Fig 1.5). Since all the isoforms share a very conserved DNA binding domain,

their functions can be redundant and complementary, but those of PPARα and PPARγ are usually opposing. Agonistic and antagonistic small molecule ligand mimics that can alter the activity of these transcription factors are mainly used to treat lipid-based disorders (Gervois et al. 2000; Ferré 2004; Kersten 2008; Dubois et al. 2017).

1.4.2 Mechanism of transactivation by PPARα

PPARα was the first of the PPAR isoforms to be studied in depth. While all the PPAR family members have a fairly conserved DNA binding domain, the A/B and E domains of PPARα are responsible for most of its transactivation abilities. While the E domain is a ligand binding domain responsible for ligand-dependent transactivation, the A/B domain promotes a low level of ligand-independent activities and is also suggested to provide the specificity to the different isoforms (Qi, Zhu, and Reddy 2000).

There are three main modes of activation of the targets of PPARα: (1) PPARα-RXRα heterodimer directly binds to the PPRE, where PPARα makes the actual point of contact on the DNA, (2) PPARα co-operates with other co-transcription factors including RXRα that are bound to DNA and (3) PPARα promotes transcription of targets without any form of DNA binding, through secondary signaling mediators (McMullen et al. 2014). Thus, very few of the targets of PPARα, actually display binding of PPARα and this makes identifying direct targets of this transcription factor quite challenging. Additionally, the activation of targets is extremely context specific and the choice of targets varies not only with the type of stress/ligand but also on the cell type (Qi, Zhu, and Reddy 2000). Lipids such as fatty acids and its oxidized derivatives, eicosanoids,

leukotrienes and prostaglandins are naturally occurring ligands of PPARα and their abundance serves as one of the determinants of its function (Kersten 2008).

There are several co-activators and co-repressors of PPARα. Prominent synthetic agonists of PPARα enable the binding of co-activators to further enhance the activity beyond the mere binding of the natural ligands. On the other hand, the antagonists of PPARα alter its conformation to prevent the binding of co-activators and instead enable the recruitment of co-repressors to suppress the transcriptional activity (Qi, Zhu, and Reddy 2000).

1.4.3 Key roles of PPARα

PPARα mainly promotes lipid catabolism in tissues with high rates of metabolism. Thus, it is abundant in liver, heart, muscle, kidneys and fat tissues. So, the pharmacological agonists of PPARα such as fibrates are widely used in the treatment of hyperlipidemia. As mentioned earlier, PPARγ usually has an opposing function to PPARα and it mainly promotes lipid biosynthesis as well as differentiation in macrophages and adipocytes.

PPARα can control multiple aspects of lipid metabolism including dampening lipid uptake and trafficking, enhancing fatty acid oxidation, promoting lipolysis and limiting the storage of triglycerides (van Raalte et al. 2004). PPARα can also lower the synthesis of lipid droplets, triglycerides and cholesterol. Therefore, enhanced PPARα activity promotes clearing of triglycerides both by lowered storage and decreased synthesis. This function is the main basis for using the agonists of PPARα in treatment of dyslipidemia (Auwerx et al. 1996; Tyagi et al. 2011). Since long chain fatty acids are targeted for β-oxidation by targets of PPARα such as acyl coA

oxidase and carnitine palmitoyl transferases, PPARα can also control the synthesis of acyl-carnitines that can act as effective signaling molecules (Song et al. 2010; Chen, Wang, Huang, et al. 2017). While these functions are of particular relevance to this study, PPARα is also involved in the control of biogenesis of several other lipid intermediates and the homeostasis of key lipid regulators of disorders (Kersten 2008).

Apart from being a master regulator of lipids, PPARα also has prominent roles in regulating glucose metabolism, suppressing inflammation and maintaining energy homeostasis (Youssef and Badr 2004; Lefebvre et al. 2006). It can also promote cellular proliferation and mediate the increase in production of ROS (Chen, Wang, Huang, et al. 2017; Teissier et al. 2004). Therefore, it is unsurprising that excessive activation of PPARα can be tumorigenic in certain tissues (Youssef and Badr 2004). Thus, targeting PPARα may provide therapeutic relief to various pathologies (van Raalte et al. 2004).

1.5 Figures

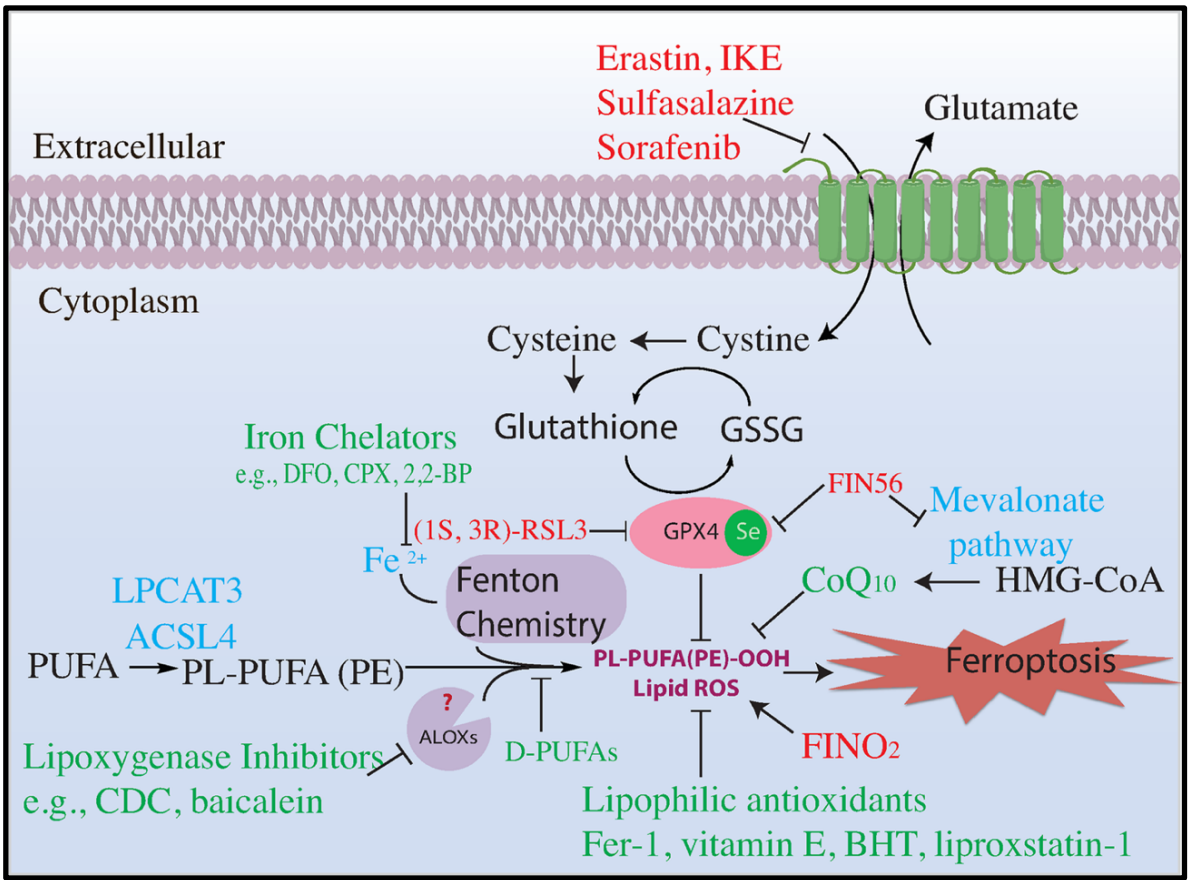

Figure 1.1: The molecular pathways involved in ferroptosis

Schematic summarizing the different upstream pathways affected by the four classes of ferroptosis inducers. It also highlights the mechanism of action of some of the key inhibitors of ferroptosis.

Figure from: Feng H and Stockwell BR, Plos Biology 2018.

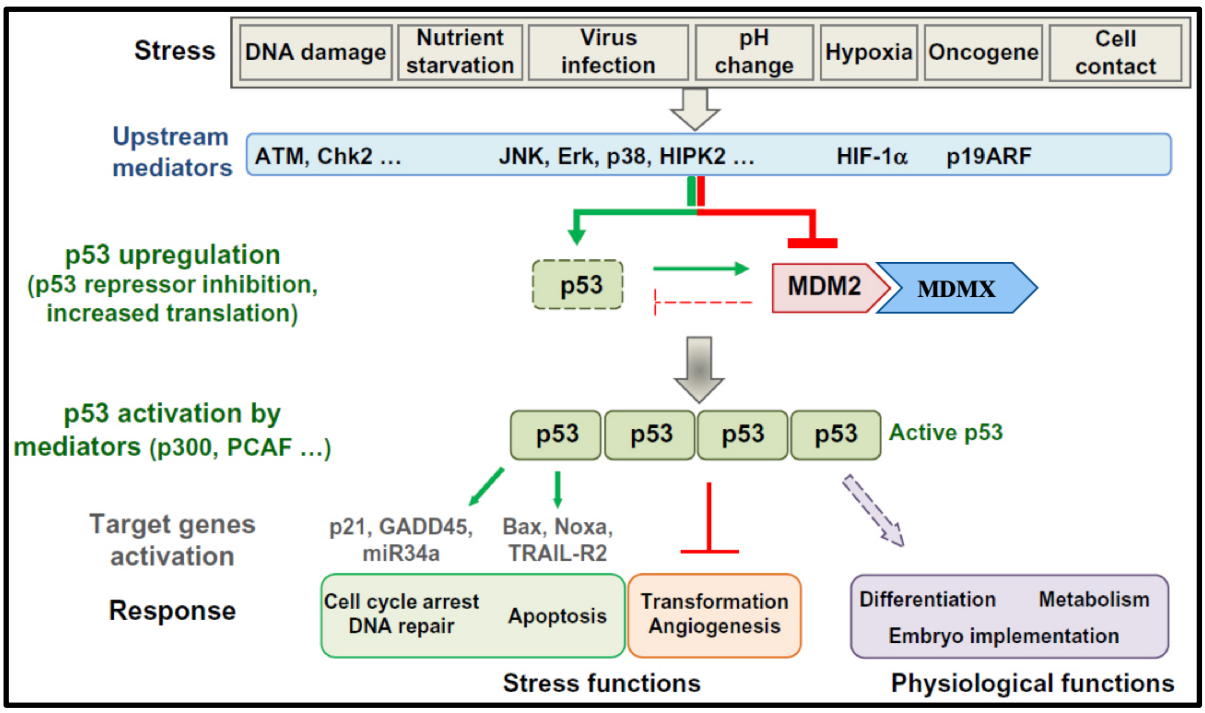

Figure 1.2 Stress-induced transcriptional response of p53

Schematic showing that p53 responds to various forms of stress by activating many downstream programs that differentially alter the cell fate.

Figure modified from: Surget S et al, Onco Targets and Therapy 2013.

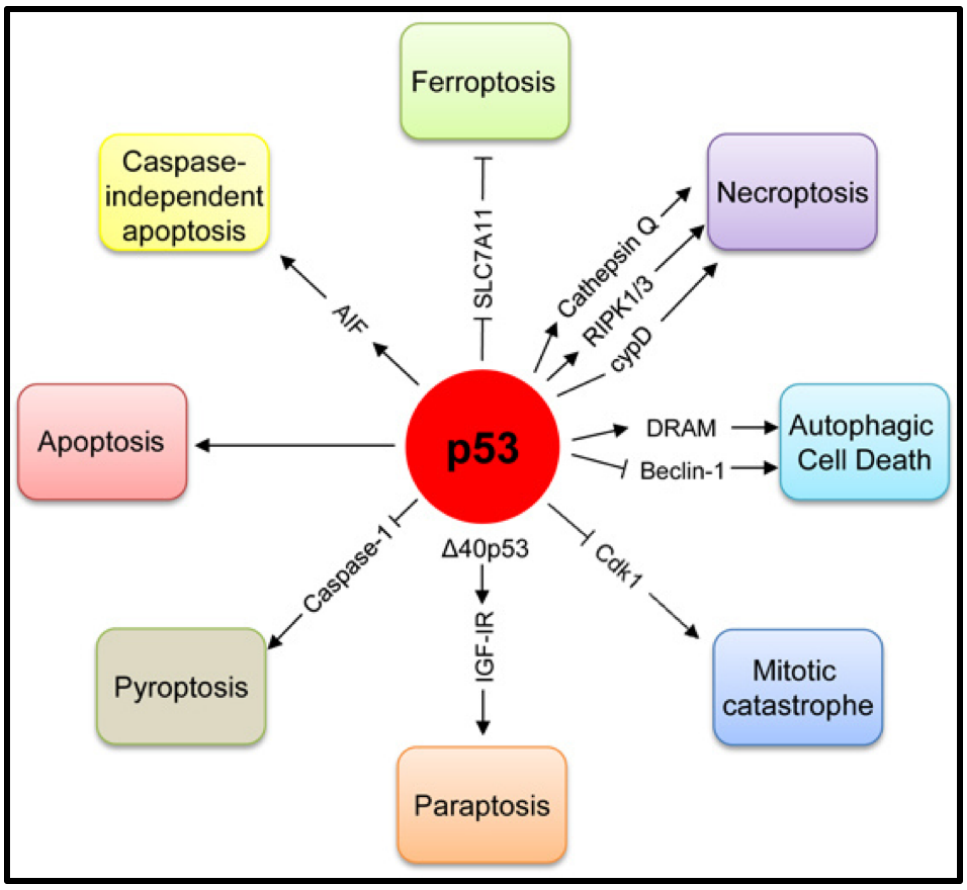

Figure 1.3 Multiple forms of cell death can be regulated by p53

Schematic listing the different types of cell death mechanisms that can be triggered by p53 through different downstream targets in order to influence cell fate.

Figure from: Atul Ranjan and Tomoo Iwakuma, *Int. J. Mol. Sci.* 2016.

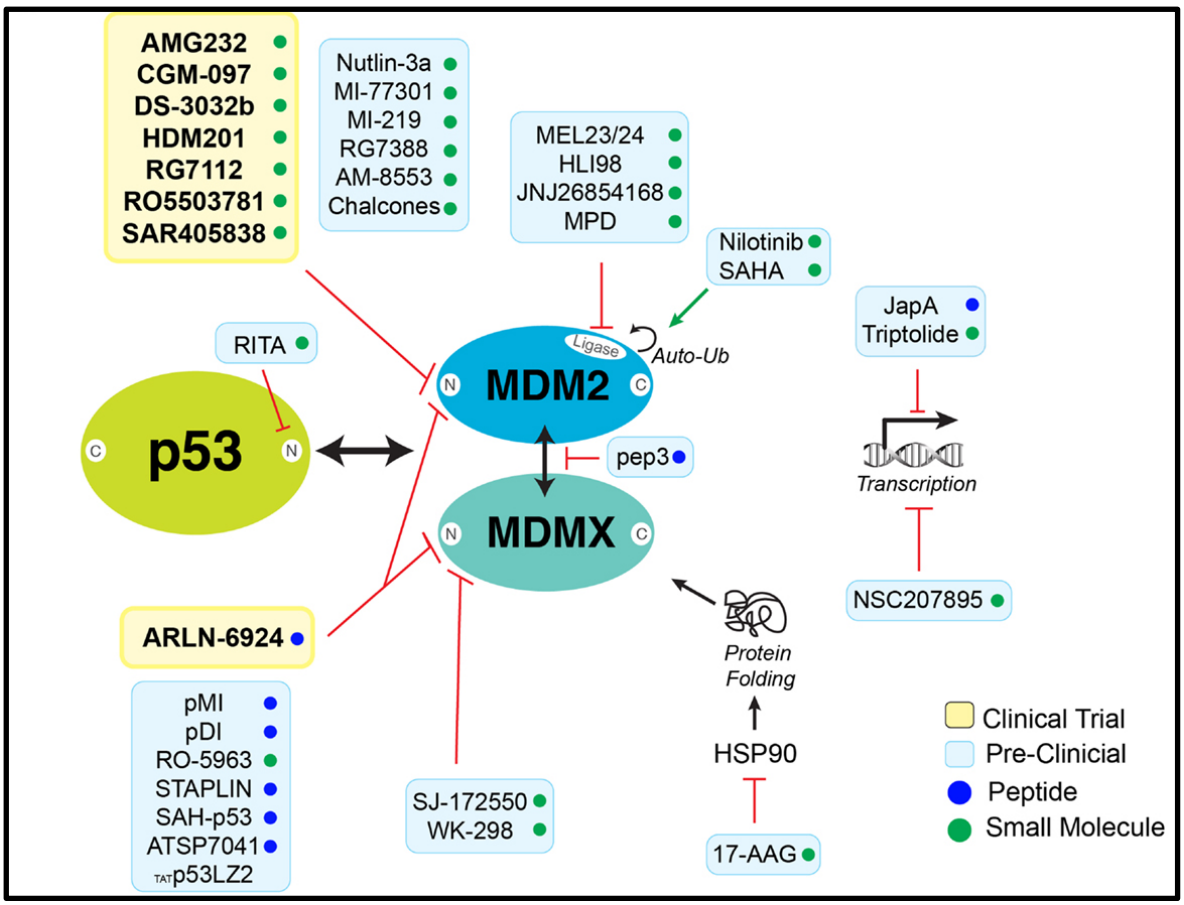

Figure 1.4 Antagonists of MDM2 and MDMX

Schematic highlighting the different aspects of MDM2 and MDMX function that are inhibited by the various inhibitors. These function include those towards the negative regulation of p53 as well as those independent of p53.

Figure from: Burgess A. et al., *Frontiers in Oncology* 2016.

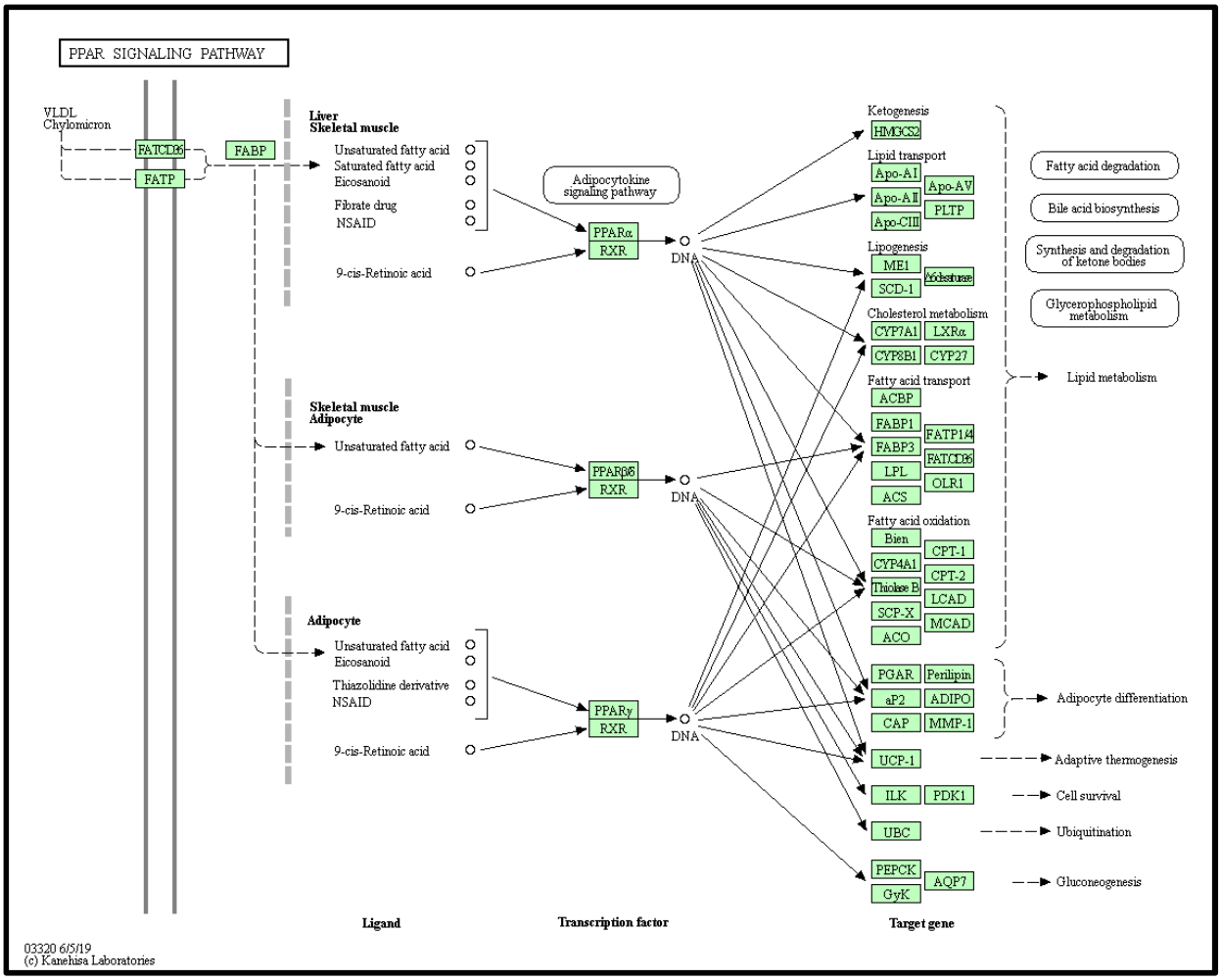

Figure 1.5 Transcriptional map of PPARs

This KEGG pathway depicts that different isoforms of the PPAR family control various aspects of lipid metabolism through multiple downstream targets.

Chapter 2: A role for p53 target genes in mediating ferroptosis

This chapter is mostly adapted from two published manuscripts: Venkatesh et al., p21 can be a barrier to ferroptosis independent of p53, *Aging* (2020); Venkatesh et al., MDM2 and MDMX promote ferroptosis by PPARα-mediated lipid remodeling, *Genes & Development* (2020)

2.1 Introduction

The tumor suppressor, p53 controls the response of cancer cells to drugs through multiple mechanism described in Chapter 1 (Beckerman and Prives 2010). In addition, p53 has links to iron metabolism and regulation of ROS levels, which are key components of the ferroptosis pathway. Cellular iron levels seem to regulate p53 activity through altering its stability. While excessive increase in iron levels seem to destabilize p53 (Shen et al. 2014), the use of iron chelators to treat some tumors can lead to an increase in p53 levels (Liang 2003). On the other hand, p53 also has a bidirectional relationship with the cellular ROS levels (Liu, Chen, and St Clair 2008). Both hypo and hyper physiological levels of p53 can increase ROS levels. In turn increased ROS levels themselves can activate p53. Therefore, it is possible that ferroptotic stress involving an increase in iron and ROS levels (Dixon and Stockwell 2014; Aron et al. 2016), activates p53 and that the activity of p53 then influences the outcome of FINs on cell survival.

While this part of the project was conceived with the above hypothesis in mind, there are now several reports as described in Chapter 1 demonstrating that p53 is indeed capable of regulating ferroptosis. Our own results in the first part of this chapter, looking at the effect of altered p53 status on the ferroptotic sensitivity, also support these papers in concluding that the directionality of the regulation by p53 is complex and context-specific, which is not unlike the other known stress-responses of p53.

In order to better understand how this context specific regulation of ferroptosis is achieved, we decided to investigate the role of some p53 target genes, as most of the differential responses of p53 to other stresses depend on its activation of appropriate target genes. First, we studied p21, a key p53 target which is a cyclin dependent kinase that often mediates p53-induced cell cycle arrest (Warfel and El-Deiry 2013).

Apart from being one of the strongest targets of p53, p21 also has some potential links to ferroptosis. p21 can mediate the p53-ROS signaling pathway by helping sustain higher levels of ROS to effect senescence in some cancer cells (Fitzgerald et al. 2015). High levels of heme-oxygenase-1 have been known to confer a resistance to apoptosis by altering cellular growth possibly due to upregulation of p21 levels (Inguaggiato et al. 2001). It has also been shown that heme-oxygenase can enhance ferroptotic death (Chang et al. 2018; Kwon et al. 2015) but the possibility that p21 could also modulate this is yet to be explored. Of direct relevance to ferroptosis, p21 has been shown to mediate the resistance of liver cells to treatment with sorafenib (Giovannini et al. 2013), a chemotherapeutic kinase inhibitor which has been shown to induce ferroptotic death (Dixon et al. 2014). In fact, sorafenib treatment triggers an induction of p21 and knock-down of p21 can increase cellular killing by sorafenib (Giovannini et al. 2013). Since at least a part of the death due to sorafenib can be attributed to ferroptosis, this strongly suggests a role for p21 in regulating ferroptosis. Our investigation into the ferroptotic regulation by p21 yielded complex results; nevertheless, they suggest that p21 can mediate ferroptosis in certain cases and are in agreement with a more conclusive recent report (Tarangelo et al. 2018). This report as described

in Chapter 1, shows that the p53-p21 axis poses an impediment to the kinetics of ferroptosis in some human cancer cells via the p21-dependent maintenance of the intracellular glutathione pool.

Our results also reveal a potential for cyclin-dependent kinases (CDKs) to be involved in ferroptosis. The major roles of p21 in growth inhibition are mediated by its two main interactions with CDKs and the proliferating cell nuclear antigen (PCNA). The inhibitory effect of p21 on CDKs mediates its effect on the different cell cycle stages, whereas its abrogation of the role of PCNA in the DNA repair process mediates its ability to block DNA replication. These inhibitory effects of p21 on either CDKs or PCNA are binding-dependent. Since both CDKs and PCNA have roles that extend beyond just growth inhibition, p21 is able to control other processes as well (Abbas and Dutta 2009). For example, p21 mediates a significant portion of the ability of p53 to repress transcription (Löhr et al. 2003). These other processes especially in the context of the effects of CDKs may be relevant to ferroptosis given some of the results described in this chapter.

2.2 Results

2.2.1 p53 status is not always a predictor of ferroptosis sensitivity

To evaluate if the role of p53 in ferroptosis is context-specific, we tested a number of human cancer cell lines for their sensitivity to erastin. Consistent with prior reports, we found marked differences in viability of several cancer cell lines (even within those of the same tissue of origin) in response to this compound (Yang et al. 2014) over a 24 h treatment period as summarized in Table 2.1. For example, HCT-116 colon cancer cells and H1299 lung cancer cells were virtually unaffected by erastin after 24 h of treatment. By contrast, both HT-1080 fibrosarcoma cells and SK-Hep1 liver cancer-derived cells were markedly sensitive to erastin (Fig 2.1A). Cell death in these erastin-sensitive cell lines was validated to be via ferroptosis, as it was reversed by ferrostatin-1 (fer-1) (Fig 2.1B). When the time frame of the experiment was extended to 48 h, some cell death in HCT-116 and H1299 cells was observed, and this was also reversed by fer-1 (Fig 2.1C), indicating that their death, while moderate and with a delayed onset, was still via ferroptosis. There was not much difference in the response of HCT-116 cells that harbor wild-type *p53* and *p53*-null H1299 cells. Similarly, two cancer cell lines with impaired wild-type p53 activity (BJeLR and WSU-NHL) were among the more sensitive of the cancer cell lines tested (Table 2.1). These observations were our first indicators that there is no obligate requirement for p53 to be present in its wild-type form for cancer cells to undergo ferroptosis.

Further, we wanted to determine if the loss of p53 in any given cell line would then enhance its sensitivity to ferroptosis. We chose two colon cancer cells with varying ferroptosis sensitivities-RKO and HCT-116, and those for which isogenic cell lines with respect to their p53 status were

already available. These isogenic cell lines were created by the deletion of a functional domain of *p53* (Bunz et al. 2002). In both these cell lines, the loss of p53 made them less sensitive to the chemotherapeutic doxorubicin (Left panels of Fig 2.1D and 2.1E), which is thought to elicit at least part of its effects on cancer cell survival through the eventual activation of p53 (Wang et al. 2004). On the other hand, the loss of p53 only slightly decreased the ferroptosis sensitivity of HCT-116 cells, and the RKO cells actually became more sensitive upon the loss of p53. These results highlight the complexity in defining a set direction of regulation of ferroptosis by p53.

We reasoned that the nuanced role of p53 in ferroptosis might be indirect and perhaps based on the p53 target being activated in response to ferroptosis induction. Therefore, we sought to examine the roles of some known p53 targets in ferroptosis.

2.2.2 p21 may mediate ferroptosis sensitivity in some contexts

Our first choice was to evaluate the role of p21 as it is one of the key downstream targets of p53 and has potential links to ferroptosis. In fact, we actually observed that one key difference between the HCT-116 and RKO cells used above was their relative levels of p21 protein (Fig 2.1F). Then, we observed that upon the induction of ferroptosis using class 1 FINS (erastin or IKE), three different sensitive cell lines (HT-1080, SK-HEP1 and U2OS) showed decreased levels of p21 protein (as well as p53) as a function of erastin concentration (Figs 2.2A-C). Further, there was an increase in p21 protein levels in some resistant cell lines (HCT-116, H1299) (Figs 2.2D-E). This increase in the levels of p21 was p53-independent since it was observed even in the p53 null H1299 cells, as well as the HCT-116 cells that were engineered to lose p53 (p53 KO HCT116).

Since the above results indicated a potential role for p21 in determining the sensitivity of cells to ferroptosis, we wanted to examine if experimentally altering p21 levels would also alter the ferroptosis sensitivity.

In the resistant cell lines, HCT-116 and H1299, our goal was to determine if ferroptosis resistance can be lowered upon loss of p21. We used RNA interference against *p21* in these resistant cells and indeed observed a reduction in the resistance to ferroptosis (Figs 2.2F and 2.2G). We tested the possibility that a more complete and non-transient loss of *p21* might be required to further enhance the sensitivity of these cells, as it was reported that p21 can alter the metabolic pathways involved in ferroptosis (Tarangelo et al. 2018). Indeed, the HCT-116 derived *p21* -/- cell line (Waldman, Kinzler, and Vogelstein 1995), had a much-enhanced sensitivity to ferroptosis compared to its wild-type counterpart (Fig 2.2H).

As a reciprocal approach we aimed to increase p21 levels in the FIN-sensitive cell line, HT-1080 to see if this would decrease ferroptosis. Overexpression of a construct expressing p21 did indeed suppress ferroptosis in these cells (Fig 2.2I). Further, we observed that two key mutant versions of p21, which either mutated the CDK binding domain or the PCNA binding domain differed in this ability to suppress ferroptosis. Specifically, CDK binding-defective version of p21 (Soria et al. 2006) was unable to block ferroptosis, while mutating the PCNA binding region much less impaired p21 in that regard (although the levels of expression of this mutant were lower). This result suggests the possibility that p21 alters sensitivity to ferroptosis by changing the cell cycle and also prompts investigation into a potential role for cell cycle in mediating ferroptosis in the future. It is acknowledged that there is a need to toggle the levels of overexpressed p21 levels to

match those seen under physiological conditions to avoid an excessive alteration of the cell cycle from biasing the results.

2.2.3 MDM2 E3 ligase activity controls the reduction in p21 protein levels upon ferroptosis induction in sensitive cell lines

Given the imperfect setup of the overexpression experiment, we wanted to understand how p21 was being accumulates in the resistant cells upon ferroptosis induction, so that we could then endogenously enhance the p21 protein levels in the sensitive cells. To our surprise, we found that in both sensitive and resistant cells, *p21* expression was upregulated at the mRNA level (Fig 2.3). As controls, increase in the levels of *CHAC1* and *PTGS2* were used as read-out of the presence of ferroptosis induction. This result indicated that ferroptosis induces p21 in a p53-independent manner and that the subsequent loss of p21 protein in the sensitive cells must be a post transcriptional event. Note that there was not a universal reduction in protein levels upon ferroptosis reduction, owing to constant levels of our loading control, as well as the additional control of expected increase in levels of ferritin in ferroptosis (Hou et al. 2016).

MDM2, the key negative regulator of p53, can regulate the stability of p21 in two ways. First, MDM2, as the most well-validated repressor of p53 both directly prevents the ability of p53 to activate its transcriptional targets such as p21 and also functions as the p53 E3 ligase to maintain low levels of p53 protein in unstressed cells, thereby lowering the amount of p53 available to activate transcription of its target (Alarcon-Vargas and Ronai 2002) . Second, MDM2 has also been reported to increase p21 turnover in a p53-independent manner (Zhang et al. 2004; Jin et al. 2003), partially through its E3 ligase activity. So, we thought to use inhibitors of MDM2 as a way

to enhance the endogenous protein levels of p21. We evaluated the effects of two small molecule antagonists of MDM2: nutlin, which binds to the N-terminal region of MDM2 and blocks the primary site of the MDM2-p53 interaction (Vassilev et al. 2004) (Fig 1F), and MEL23 (MDM2 E3 Ligase Inhibitor 23), which blocks the E3 ligase activity of the MDM2 (Herman et al. 2011) (Fig 2.4A).

The addition of nutlin did increase the levels of p21 by activating p53. Although, there was an eventual decrease in p21 levels upon ferroptosis induction, the overall level of p21 even upon ferroptosis induction was higher with nutlin treatment. MEL23 on the other hand was able to significantly reduce the loss of p53 and p21 protein upon ferroptosis, (Fig 2.4B) indicating that in sensitive cells, the loss of p21 protein is mostly due to the involvement of the E3 ligase activity of MDM2 rather than a consequence of the effects of MDM2 on p53. By extension, we hypothesized that both MEL23 and nutlin might be able to suppress ferroptosis in sensitive cell lines owing to the suppression of reduction in p21 levels upon ferroptosis induction. We observed that while nutlin only had a modest suppression of ferroptosis in four different sensitive cell lines, the ferroptosis-suppression with MEL23 was much stronger (Figs 2.4C-F). This striking result indicated that p21 levels might be able to mediate ferroptosis at least in some contexts. However, this finding also suggested that another p53 target, namely MDM2, might have a role in regulating ferroptosis.

2.2.4 Inhibition of the MDM2 E3 ligase activity is able to suppress ferroptosis independent of p21

To evaluate if the role of MDM2 in ferroptosis was actually dependent on p21, a member of the Stockwell lab, Michael Stokes created virus with CRISPR guides against *p21*. Then, Sung-Hwan Moon, in the Prives lab and I created p21 KO clones from two different sensitive cell lines (SK-HEP1 and HT-1080) using the virus and validated that they did not express detectable p21 (Fig 2.5 A). These p21 KO cells lines showed no difference in ferroptosis sensitivity. Contrary to our original hypothesis, MEL23 was able to suppress ferroptosis to the same degree in either of the cell lines even in the absence of p21 (Fig 2.5B and 2.5C). This suggests that one may view the decrease in p21 protein upon ferroptosis induction in sensitive cells as biomarkers of MDM2 E3 ligase activity. It also indicates that cells may be sensitive if they have a high MDM2 E3 ligase activity in response to ferroptosis, which would result in the subsequent degradation of p21. Therefore, it is possible that MDM2 is the true mediator of ferroptosis in the sensitive cell lines.

2.2.5 MDM2 gets dephosphorylated in response to ferroptosis

Given our previous results, we wanted to assay the changes in MDM2 protein levels during ferroptosis. But when we used different MDM2 antibodies which differed in detection of MDM2 protein in ferroptotic cells we obtained strikingly different results (Fig 2.6A). Specifically, a mixture of monoclonal antibodies detected lower protein levels of MDM2 in cells treated with IKE, while the MDM2 signal detected by 2A10 monoclonal antibody increased with the same treatment. Relevantly, it has been previously reported that 2A10 antibody against MDM2 is unable to recognize the form of MDM2 phosphorylated at S395 (Cheng and Chen 2011). On the other hand, the mix of monoclonal antibodies should be able to more accurately recognize the true abundance of the protein despite any of its modifications. This suggested a potential explanation

of why the trends were so different between the two sets of antibodies, namely that phosphorylation, at least at S395 is lost upon induction of ferroptosis.

To validate this line of reasoning, we first confirmed that there was no increase in the mRNA levels of *MDM2* unlike those seen in *p21* (Fig 2.6B). Further, the reactivity of the 2A10 antibody to MDM2 protein from lysates of untreated cells was enhanced by treating the membranes with CIP (calf intestinal phosphatase) that dephosphorylates amino acids (Figure 2.6 C). The MDM2 protein levels on the membranes treated with CIP, now resembled those achieved with the mix of monoclonal antibodies. We used lysates of U87 cells, which have a constitutive expression of phosphorylated Akt as they harbor a *PTEN* deletion, to serve as a positive control to show that the antibody, which only recognizes the phosphorylated Akt loses its reactivity upon the same treatment of the membrane due to loss of the phosphorylated groups.

This result suggests that MDM2 becomes dephosphorylated (at least at S395) upon ferroptosis induction in sensitive cell lines (thereby being detected to a higher extent by 2A10). Such a modification could potentially hyper-activate MDM2. There are reports that stressors like DNA damage potentiate the phosphorylation of MDM2 at S395, in order to activate p53 through blocking the E3 ligase mediated degradation of p53 by MDM2 (Chen 2012).

The results of the first part of the project suggested that MDM2 has the potential to be a new regulator of ferroptosis and that its E3 ligase activity was important for this role.

2.3 Discussion

Our results add to the growing literature on the complex role of p53 in ferroptosis (Gnanapradeepan et al. 2018). Given the highly context-specific directionality in the regulation of ferroptosis by p53, this part of the project focuses on an important next step of studying p53 target genes in ferroptosis. To this end, we have identified p21 and MDM2 as two potential targets for future study.

Based on the data obtained from the wide range of cancer cell lines tested, p21 seems to have a strong potential to be used as a biomarker for ferroptosis sensitivity. Whether this is simply indicative of the role of MDM2 in ferroptosis or due to the role of p21 itself in ferroptosis is yet unclear, and may depend on the type of cell line used.

While the p21 KO HCT-116 cells were markedly more sensitive to ferroptosis, the results were not recapitulated to the same degree by effective RNA interference against *p21*, even in the same cell line. While this could possibly be due to clonal variation arising from the selection process as only a single p21 KO clone was used, there are other explanations based on our results in the HT-1080 cells using overexpressed p21. These results indicate that the ability of p21 to interact with CDKs is important for its role in ferroptosis. The inhibition of CDK activity by p21 can have multiple effects to inhibit cellular growth including altered transcription, the cell cycle and even dedifferentiation to a certain degree (Abbas and Dutta 2009). Even with the limitations of this experiment, it is possible that the p21 KOs had a longer growth period in the absence of p21 for any of these effects to take full effect and therefore had a more pronounced change in ferroptotic

sensitivity than a transient dose of *p21* siRNA. if cancer cells underwent some extent of p21-dependent dedifferentiation in order to become ferroptosis-resistant, then it is likely that these changes would need more time to get reverted. Reports showing that dedifferentiation of melanoma cells as well as further differentiation of neurons enhance ferroptosis sensitivity (Chonghaile 2018; Martinez et al. 2019) lend some support to this theory.

It is also possible that the design of our experiment was not optimized to capture the results of a transient RNA interference experiment. If upon p21 overexpression, the rescue was due to delayed kinetics of ferroptotic cell death, then by extension, the RNA interference experiment could have had an earlier onset of death which might have been missed at the final endpoint that we were measuring. A recently published report, supports this theory and demonstrates effectively that p21 can alter the kinetics of ferroptosis (Tarangelo et al. 2018). We created p21 KO clones of the same cell line (HT-1080) that was used by Tarangelo et al., and these lines did not show any basal changes to ferroptotic sensitivity, also in line with their findings. It is possible that since sensitive cells are capable of eventually lowering p21 levels upon ferroptosis induction, a p21 KO would not make much of a difference. This further supports the idea that p21 can be barrier to ferroptosis and cells that can prevent its accumulation upon ferroptosis will be sensitive. Tarangelo et al. also provide evidence that cell cycle arrest alone is insufficient to suppress ferroptosis, but it is still possible that p21 has a myriad of effects with cell cycle changes just being a subset of them. Taken together, a future study to better understand the molecular regulation of ferroptosis by p21, should evaluate the involvement of CDKs as a key factor.

The results that we obtained with MDM2 in this chapter, set us upon a fruitful journey thus forming the basis for the next two chapters. The possibility that MDM2 might be dephosphorylated in response to ferroptosis, combined with the potential ability of MDM2 to regulate ferroptosis suggests that there might actually be another feedback loop in place akin to the one between p53 and MDM2. This loop would involve FINs activating MDM2 in order to use heightened E3 ligase activity of MDM2 to effectively kill cells, or potentially modulate p53 akin to other stresses like DNA damage. Further work is necessary to understand how exactly this modification is effected and if simply blocking this modification would even be able to suppress ferroptosis.

2.4 Methods

2.4.1 Cells

HCT116, H1299, SK-Hep1, and U2OS cells were maintained in Dulbecco's modified Eagle's medium supplemented with 10% heat-inactivated fetal bovine serum (Gemini Bioproducts, cat# 900-108). HT-1080 cells were maintained in Dulbecco's modified Eagle's medium supplemented with 10% heat-inactivated fetal bovine serum (Gemini Bioproducts, cat# 900-108), and 1% non-essential amino acids (Sigma-Aldrich, cat# M7145). RKO cells were grown in McCoy's 5A modified medium (Gibco, cat# 16600-082) supplemented with 10% heat-inactivated fetal bovine serum (Gemini Bioproducts, cat# 900-108). The HCT116 cells were a gift from Dr. Vogelstein and all other cells were obtained from ATCC. The HT-1080 and SK-Hep1 parental cells are wild-type for p53/p21 and were edited using CRISPR technique (as described below) to obtain the p21 KO clones.

2.4.2 Genome editing using CRISPR technique to generate p21 KO clones

HT-1080 and SK-Hep1 p21 knockout cells were generated using CRISPR/Cas9 genome editing technology. Three guides RNAs targeting exon 1 and 2 of *p21* (*CDKN1A*) were designed using the chop-chop online tool (https://chopchop.rc.fas.harvard.edu/dev/index.php). Guide sequences were purchased as single-strand oligos and prepared for insertion into the lentiCRISPRv2 vector following an established protocol (Sanjana, Shalem, and Zhang 2014). Plasmids containing gRNA insertions were sequenced for validation, and transfected into HEK293T packaging cells, along with envelope plasmids VSV-G and delta 8.9 for lentivirus production. Growth media containing lentivirus was collected and stored at -80 °C until use. To create p21-null cell lines, HT-1080 and

SK-Hep1 cells (7 x 10^5) were seeded in 6-well plates and incubated with the virus for 24 hrs. Successfully transfected cells were selected by using Puromycin 1.5 μg/ml (Santa Cruz Biotech). Single cell colonies were isolated by low density seeding, and validated as null by quantifying p21 protein abundance by western blot using C-19 polyclonal antibody (Santa Cruz Biotechnology). The absence of p21 protein even upon induction of p53 by nutlin (10 μM) was used as a criterion to select the p21 KO clones used.

2.4.3 Drugs and Chemicals

The commercial drugs used are: erastin (Selleckchem, cat# S7242), nutlin-3a (Sigma-Aldrich, cat# 444152), doxorubicin (Sigma-Aldrich, cat#D1515).

MEL23 was obtained from InterBioscreen (Herman et al. 2011).

The following drugs were synthesized in Stockwell lab : IKE as in Larraufie MH et al., 2015(Larraufie et al. 2015) by Yan Zhang, ferrostatin-1 as in Dixon S et al., 2012 (Dixon et al. 2012) by Michael Gaschler.

All the drugs were dissolved in DMSO (Sigma-Aldrich, cat# D8418). The concentrations of drugs used was as follows (unless otherwise mentioned): nutlin- 10 μM, MEL23- 14 μM, ferrostatin-1 (fer-1)- 20 μM.

2.4.4 Quantitative reverse transcription PCR

RNA was isolated from cells using the Qiagen RNeasy minikit. cDNA was generated using the Qiagen Quantitect reverse transcription kit with 0.5 μg of input RNA as measured with a NanoDrop (Thermo Scientific). Real-time PCR was carried out on an ABI StepOne Plus machine

using the power SYBR Green dye (Thermo Scientific). Transcript levels were assayed in triplicate and normalized to *L32* mRNA levels. Relative changes in cDNA levels were calculated using the comparative Ct method ($\Delta\Delta C_T$ method).

Primer sequences:

L32 F: TTCCTGGTCCACAACGTCAAG, L32 R: TGTGAGCGATCTCGGCAC,

p21 F: GGCGGCAGACCAGCATGACAGATT, p21 R: GCAGGGGGCGGCCAGGGTAT,

chac1 F: GAACCCTGGTTACCTGGG, chac1 R: CGCAGCAAGTATTCAGGTGT,

ptgs2 F: TAAGTGCGATTGTACCCGGAC, ptgs2 R: TCTCCAAAGGAGGTTACCTGC,

Mdm2 F: F: TTGGCGTGCCAAGCTTCTCT, Mdm2 R: TACCTGAGTCCGATGATTCC

The p53 primer was premix obtained from Qiagen (Quantitech primer, HS_TP53_1_SG, cat# QT00060235) and the rest was ordered from Invitrogen.

2.4.5 Immunoblot

Cells were lysed with TEB lysis buffer (10mM Tris HCL ph:7.5-8, 137mM sodium chloride, 10% glycerol, 1% NP-40) supplemented with 1mM magnesium chloride, 1mM calcium chloride and complete protease inhibitors (Roche). Protein concentration was assayed using Bio-Rad protein assay dye reagent and results were read using a spectrophotometer.

Protein extracts were run on in-house made Tris-Glycine SDS Polyacrylamide gels. Proteins were then electro transferred at 360mA for 70 min onto a nitrocellulose or PVDF membrane. Membranes were blocked with 5% milk in PBST for 30 min, prior to being incubated overnight with primary antibodies (1:100-1:1000 dilution according to the specific antibody). The

membranes were then washed three times with PBST and incubated with secondary antibody (1:5000 dilution) for 1 h at room temperature. After three more washes with PBST, The WB images were acquired using ECL (Thermo Fisher, Pierce, cat# 32106 or EMD Millipore, Immobilon, cat# WBKLS0050). The primary and secondary antibodies were diluted with 1% milk in PBST.

The following primary antibodies were used: p53 (mAb 1801/mAb DO.1, in-house produced); p21 (C-19, Santa Cruz biotech, cat# sc-397); Mdm2 (2A10, Abcam cat# ab16895 or a mixture of in-house produced mAb 4B11, 3G5, 2A9); Actin (Sigma-Aldrich, cat# A2066); FTH1 (Cell Signaling Technology cat# 3998); Phospho-Akt (Ser473- Cell Signaling Technology, cat#9271S). Actin was used as loading control for all the blots.

For removal of phosphorylated groups

The samples were run in duplicate in two halves of the membrane. Proteins were then electro transferred at 360mA for 70 min onto a PVDF membrane. Membranes were blocked with 5% BSA in TBST for 1 h at room temperature. The membrane was then cut to separate the duplicate halves and they were then placed in separate containers with 3-5 ml of 1X CIP (Alkaline phosphatase from calf intestine) buffer per container. CIP (1 unit per μg of protein present in the membrane) was added to each container and the membranes were incubated for 1 h at 37°C. The CIP and its buffer were obtained from New England Labs, cat#M0290S. The membranes were then incubated overnight with primary antibodies. The primary and secondary antibodies were diluted with 1% BSA in TBST. The rest of the procedure is same is described above.

2.4.6 Transfection: RNA interference

15nM of siRNA was used for each well in a 6-well plate. Lipofectamine RNAiMAX (Thermo Scientific) was used as the transfection reagent for all siRNA experiments (according to the manufacturer's instructions). After 18 h, the media was changed and cells were treated with drugs 24 h post transfection. The cells were plated prior to transfection such that they are only 80% confluent by the end of the drug treatment period.

The following siRNAs were used: siLuciferase (Urist et al. 2004), sip21 #1 (HS_CDKN1A_6 Flexitube siRNA from Qiagen), sip21 #2 (HS_CDKN1A_7 Flexitube siRNA from Qiagen).

2.4.7 Transfection: Ectopic expression of proteins

Plasmids were transfected into cells using Lipofectamine 3000 (Thermo Scientific) according to the manufacturer's instructions, with a ratio of 1 μg:1.7 μl lipofectamine reagent. After 18 h, the media was changed and cells were treated with drugs 24 h post transfection. The cells were plated prior to transfection such that they are only a maximum of 80% confluent by the end of the drug treatment period.

The plasmids for full length and mutants of p21 were obtained from Dr.Vanessa Gottifredi's lab (Soria et al. 2006).

Note: Cells became more resistant to ferroptosis inducers post transfection. In order to obtain cell death post transfection, 3 key factors need to controlled: cell density must be lower than normal,

lipofectamine reagent needs to be washed off as soon as possible, and a much higher dose of FINs must be used to induce ferroptosis.

2.4.8 Cell viability assay

For the dose response curves, 1800 cells were plated in 36µl per well of a 384 well plate on day 1. Drugs were dissolved in DMSO and a 12 point, two-fold series was prepared. The drugs were then dissolved 1:33 in media and 4 µl was added to each well of the plates on day 2. After 24-48 h of drug treatment (based on the cell line), the viability of cells was measured using the 1:1 dilution of the CellTiter-Glo Luminescent reagent (Promega, cat# G7573) with media, which was read on Victor 5 plate reader after 10 minutes of shaking at room temperature. The intensity of luminescence was normalized to that of the DMSO control. The experiments were performed twice in biological duplicates each time.

The inhibitors tested (MEL23, nutlin, fer-1) were added at a constant concentration as specified, to each dilution of the lethal compounds and corresponding amounts of DMSO was added to the control FIN treatment alone.

For viability assays when the experiment was performed in 6-well plates, cells were harvested using trypsin (0.5 ml per well) and the media was saved from each well. The trypsinized cells were resuspended with the saved media and 2-3 aliquots (0.05 ml each) sampling different regions of this this suspension were taken into a 96-well plate to serve as technical replicates for the measurement. CellTiter-Glo Luminescent Viability assay was used to measure the viability of

these aliquots. The rest of the culture was used to extract protein to be analyzed using western blots.

2.4.9 Statistical analysis

Prism (version 8, GraphPad) was used to make all the graphs in the paper and for performing all the statistical analysis shown. The GraphPad style (0.1234(ns), <0.0332(*), < 0.0021(**), <0.0002(***)) was used to represent the p values. The p values were calculated by ANOVA and appropriate multiple testing correction was done where required.

2.5 Tables

Table 2.1 Cancer cell lines differ in their proclivity to undergo ferroptosis.

The cells lines have been broadly categorized based on the relative amount of cell death observed in response to class 1 FIN, erastin.

Sensitive	Moderate	Resistant
BJeLR*- *impaired p53* (engineered fibrosarcoma)	RKO (Colon carcinoma)	HCT116 (Colorectal carcinoma)
HT-1080 (Fibrosarcoma)	U2OS (Osteosarcoma)	H1299*- *p53 null* (Non-small cell lung carcinoma)
SK-Hep1 (Hepatic adenocarcinoma)	HEPG2 (Hepatocellular carcinoma)	MCF-7 (Breast adenocarcinoma)
DoHH-2 WSU-NHL*- *mutant p53* SUDHL6 (Diffuse large B cell lymphoma)	HBL (Diffuse large B cell lymphoma)	LY7 (Diffuse large B cell lymphoma)

2.6 Figures

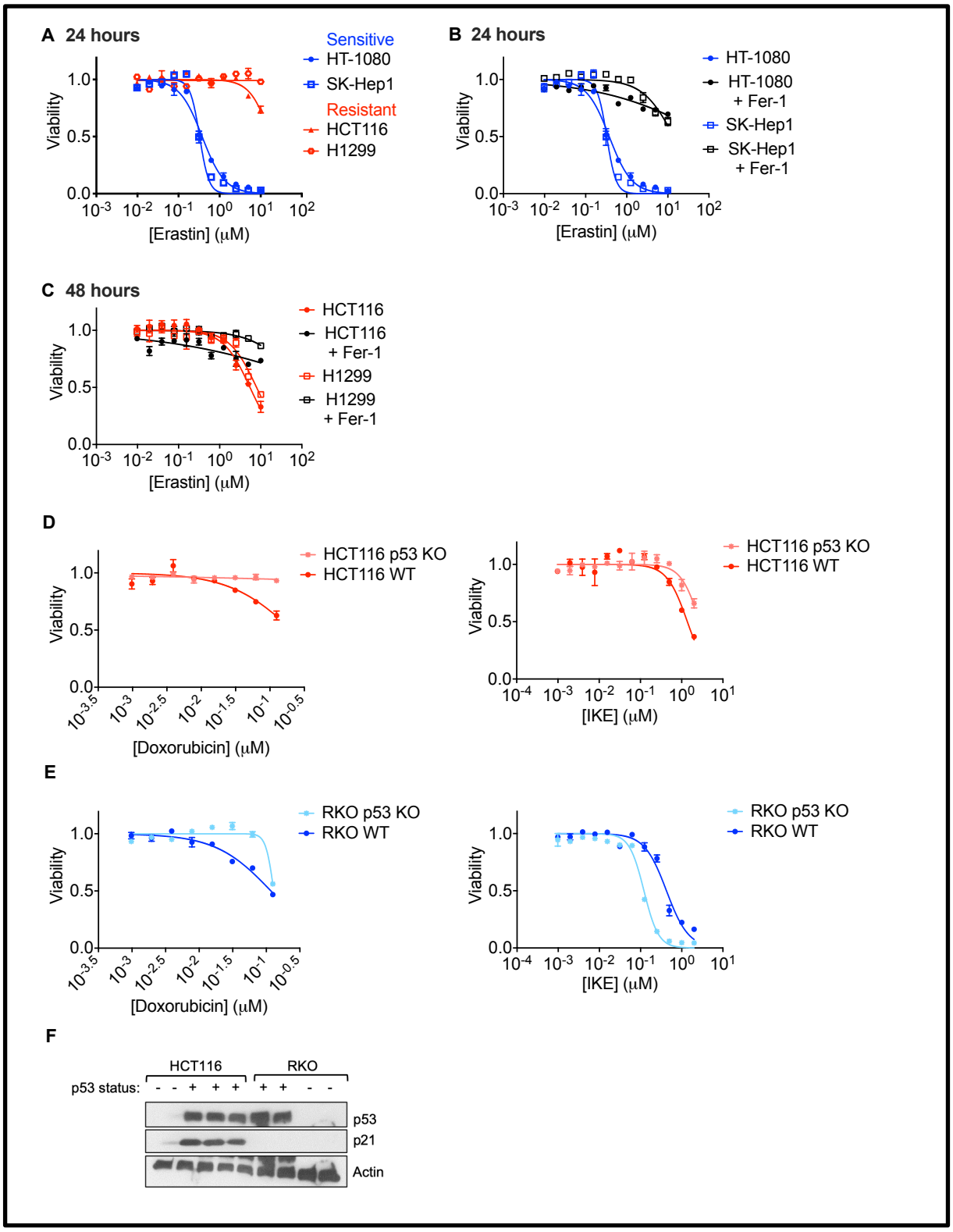
A 24 hours
Sensitive
HT-1080
SK-Hep1
Resistant
HCT116
H1299
Viability
[Erastin] (μM)
B 24 hours
HT-1080
HT-1080 + Fer-1
SK-Hep1
SK-Hep1 + Fer-1
C 48 hours
HCT116
HCT116 + Fer-1
H1299
H1299 + Fer-1
D
HCT116 p53 KO
HCT116 WT
[Doxorubicin] (μM)
[IKE] (μM)
E
RKO p53 KO
RKO WT
F
HCT116
RKO
p53 status: - - + + + + - -
p53
p21
Actin

Figure 2.1 p53 does not always promote ferroptosis in different cancer cell lines

(A) Dose response of HT-1080, SK-Hep1, HCT116, and H1299 cells to erastin treatment of 24 h. (B, C) Effect of fer-1 on the dose response of cells to erastin. (B) Viability of HT-1080 and SK-Hep1 cells after 24 h of treatment. (C) Viability of H1299 and HCT116 after 48 h of treatment. (D, E) Drug response of isogenic cell lines based on p53 status in (D) HCT-116 and (E) RKO to either doxorubicin (left panel) or erastin (right panel) treatment for 24 h.

(F) Comparison of p21 protein levels between HCT-116 and RKO cells. Multiple replicates of the wild-type and p53 KO cell lines cultured in separate dishes were used.

The data in (A-C) represent the mean ± SE for two out of four independent experiments, in (D, E) represent the mean ± SE for two independent experiments. The viability data have been normalized to that of the DMSO control.

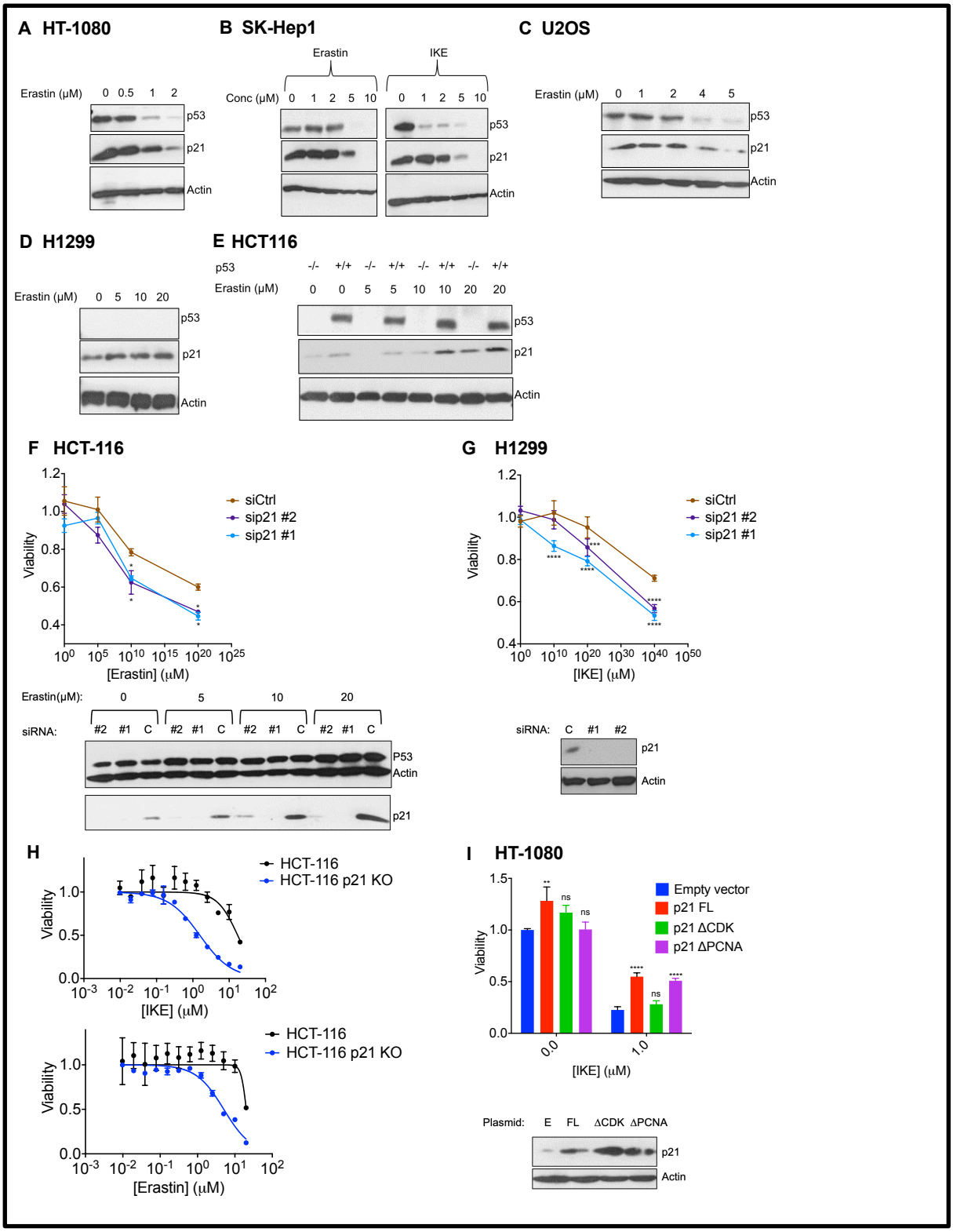

Figure 2.2 p21 has a role in regulating ferroptosis sensitivity

(A-E) Impact of treatment with erastin/IKE on the protein levels of p21 and p53. (A) HT-1080 cells, (B) SK-Hep1 cells and (C) U2OS cells were treated for 16 h whereas (D) H1299 cells and (E) HCT116 cells (+/+ and -/- isogenic lines with respect to p53 status derived by Vogelstein's group) were treated for 48 h.

(F, G) Effect of knockdown of p21 using two different siRNAs (#1, #2) on the degree of death elicited by erastin. Cells transfected with an siRNA against luciferase (siCtrl/C) were used as control. The bottom panels of (F, G) show the corresponding changes in p21 protein levels. (F) HCT-116 cells and (G) H1299 cells were transfected with siRNA for 24 priors and then treated with erastin/IKE for 48 h.

(H) Comparison of ferroptosis sensitivity of HCT-116 derived p21 KO clone to its wild-type counterpart when treated with a dose curve of erastin/IKE for 48 h.

(I) Left panel: Viability of HT-1080 cells transfected with various versions of p21 protein or an empty vector plasmid was measured after treatment with IKE for 48 h. The bottom panel depicts the corresponding protein levels of p21.

The data in (F) represent the mean ± SE for two out of four independent experiments, in (G-H) represent the mean ± SE for two independent experiments, in (I) represent the mean ± SD for one of two independent experiments. The viability data have been normalized to the DMSO control in (F-H) and to their respective untreated control in (I).

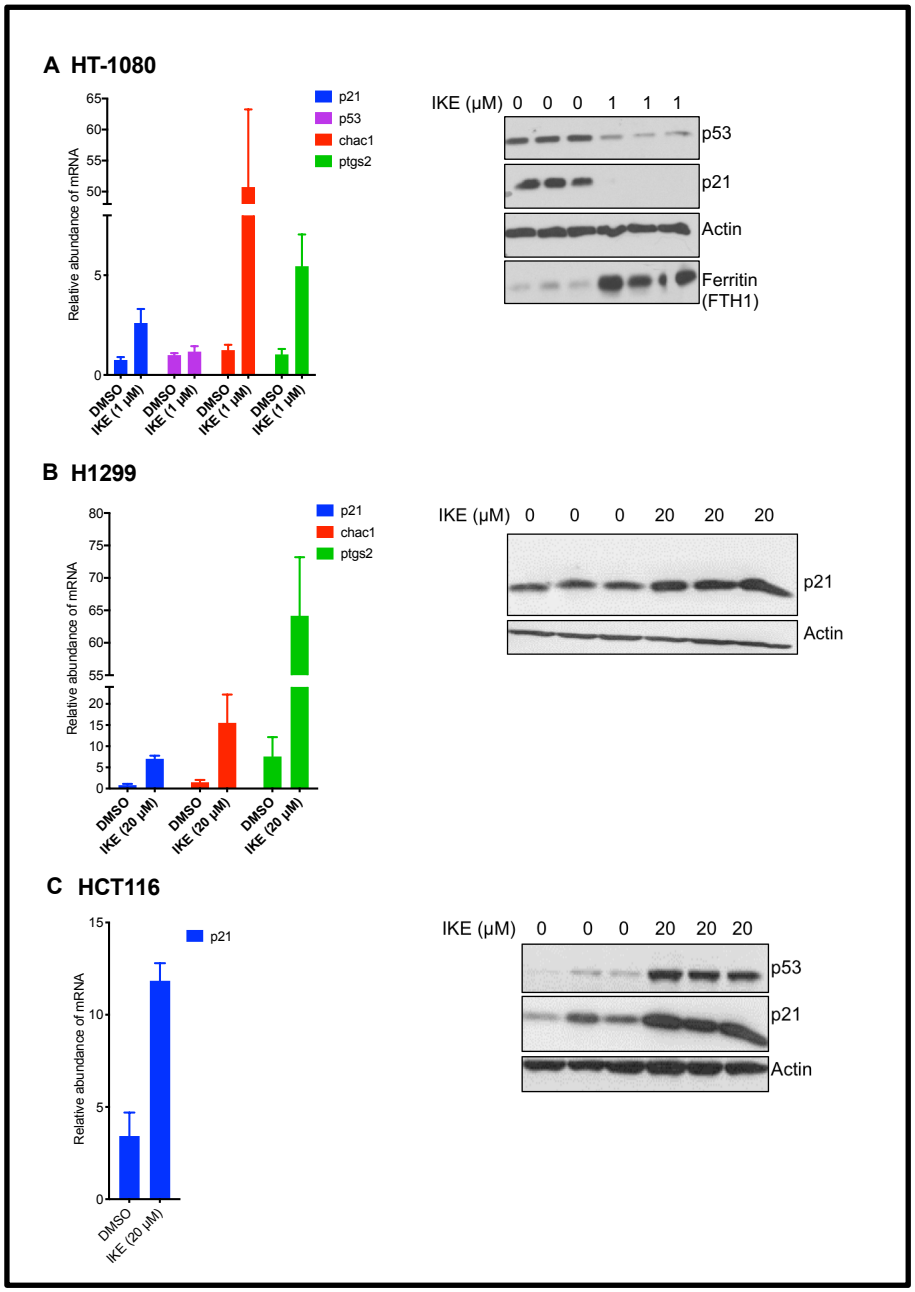

Figure 2.3 p21 is differentially regulated at the post-transcriptional level between cells that are sensitive and resistant to ferroptosis

(A-C) Left panels: Impact of IKE treatment on the mRNA levels of p21. (A) HT-1080 cells were treated for 16 h while (B, C) H1299 and HCT-116 cells were treated for 48 h. *PTGS2* and *CHAC1*

mRNA levels measured in (A, B) serve as markers of ferroptosis. Right panels: the corresponding protein levels in the cells used in the left panels are shown.

The data in left panels of (A-C) represent the mean ± SE for three biological replicates with two technical replicates each.

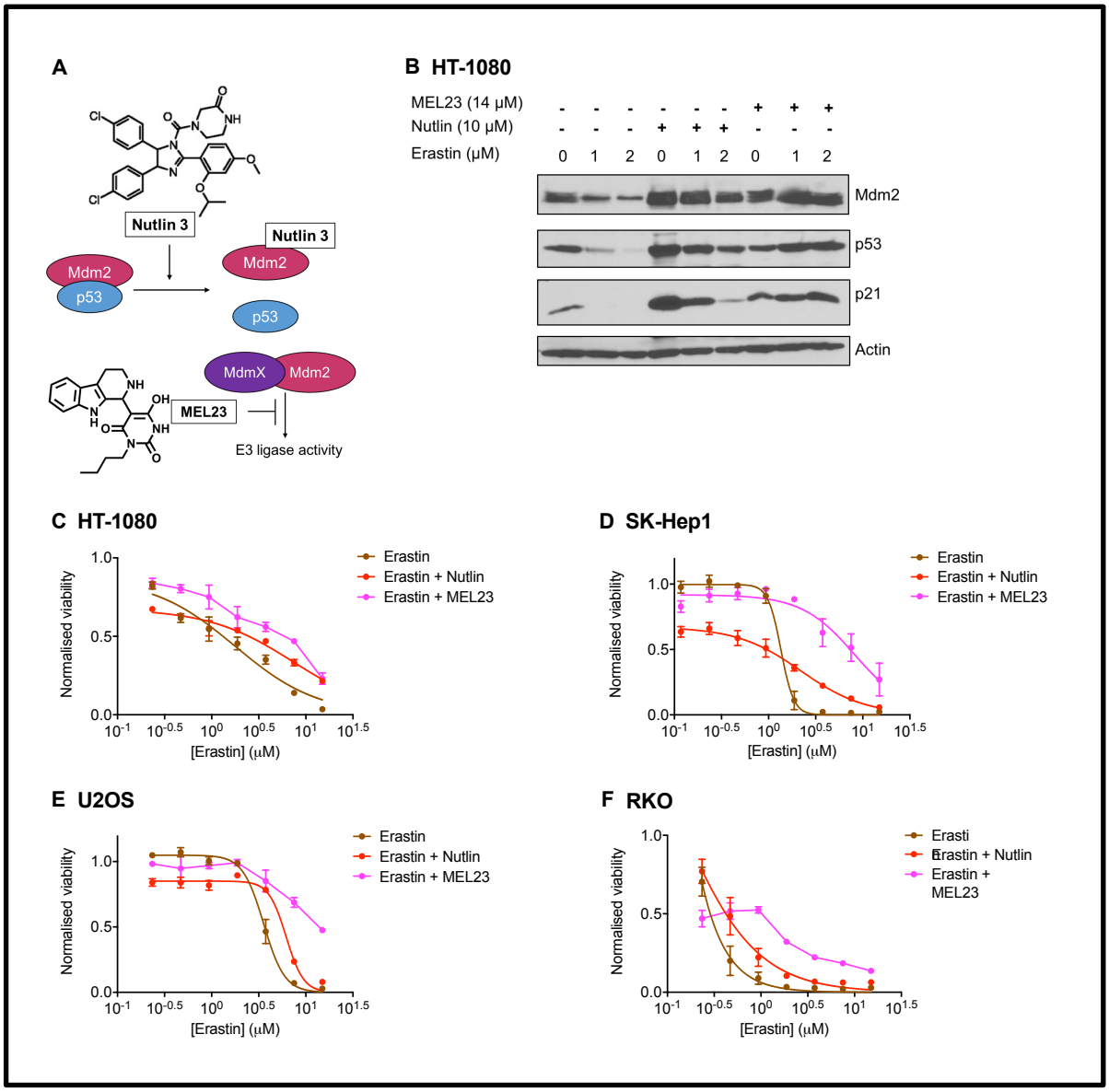

Figure 2.4 Lowered reduction of p21 protein levels may suppresses ferroptosis in sensitive cancer cell lines

(A) Cartoons of known structure and mechanism of action of (top panel) nutlin (Vassilev et al. 2004) and (bottom panel) MEL23 (Herman et al. 2011) .

(B) Protein levels of Mdm2, p53 and p21 in HT-1080 cells when treated with erastin for 16 h with or without the addition of nutlin or MEL23.

(C-F) Dose response to erastin treatment of 24 h when co-treated with nutlin and MEL23 in (C) HT-1080 cells, (D) SK-Hep1 cells, (E) U2OS cells and (F) RKO cells.

The data in (C-F) represent the mean ± SE for two out of four independent experiments. The viability data have been normalized to the DMSO control.

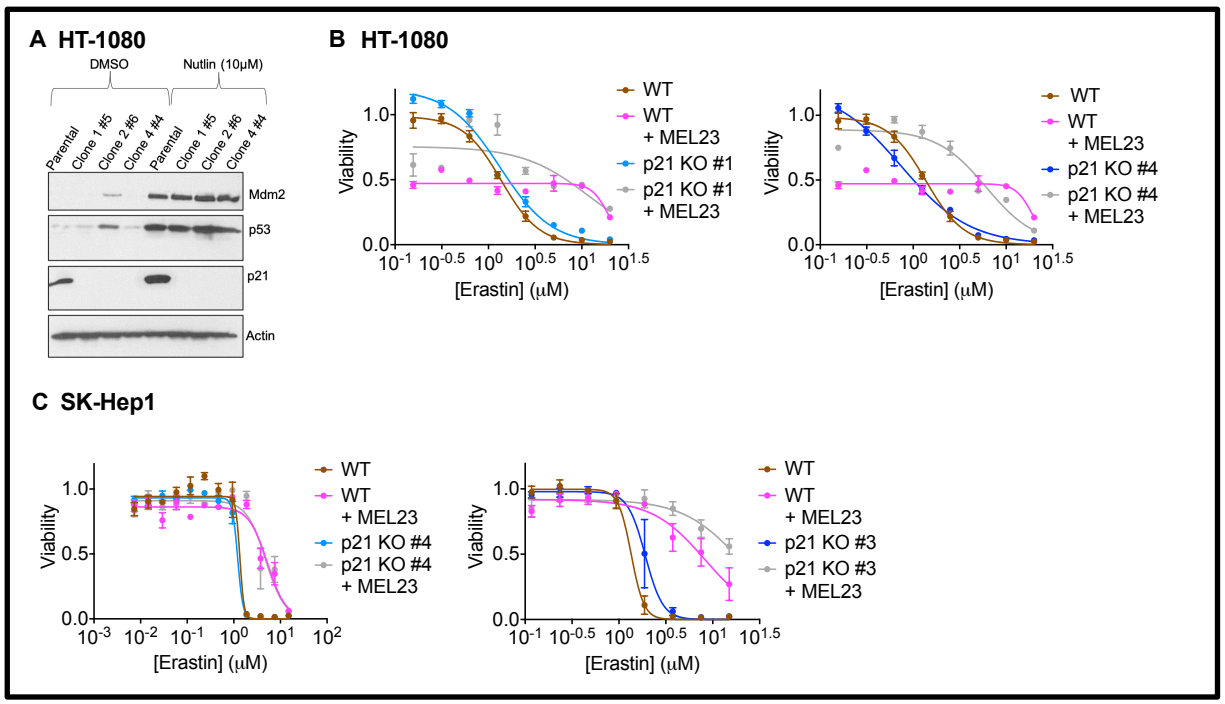

Figure 2.5 Loss of MDM2 E3 ligase desensitizes cells to ferroptosis, independent of p21

(A) MDM2, p53, and p21 protein levels of HT-1080 derived p21 KO clones upon nutlin treatment. (B, C) Effect of MEL23 on the dose-response to erastin in (B) HT-1080 derived cells and (C) SK-Hep1 derived cells.

Cells in (A-C) were treated with drugs for 24 h. The data in (B, C) represent the mean ± SE for two of four independent experiments. The viability data have been normalized to the DMSO control.

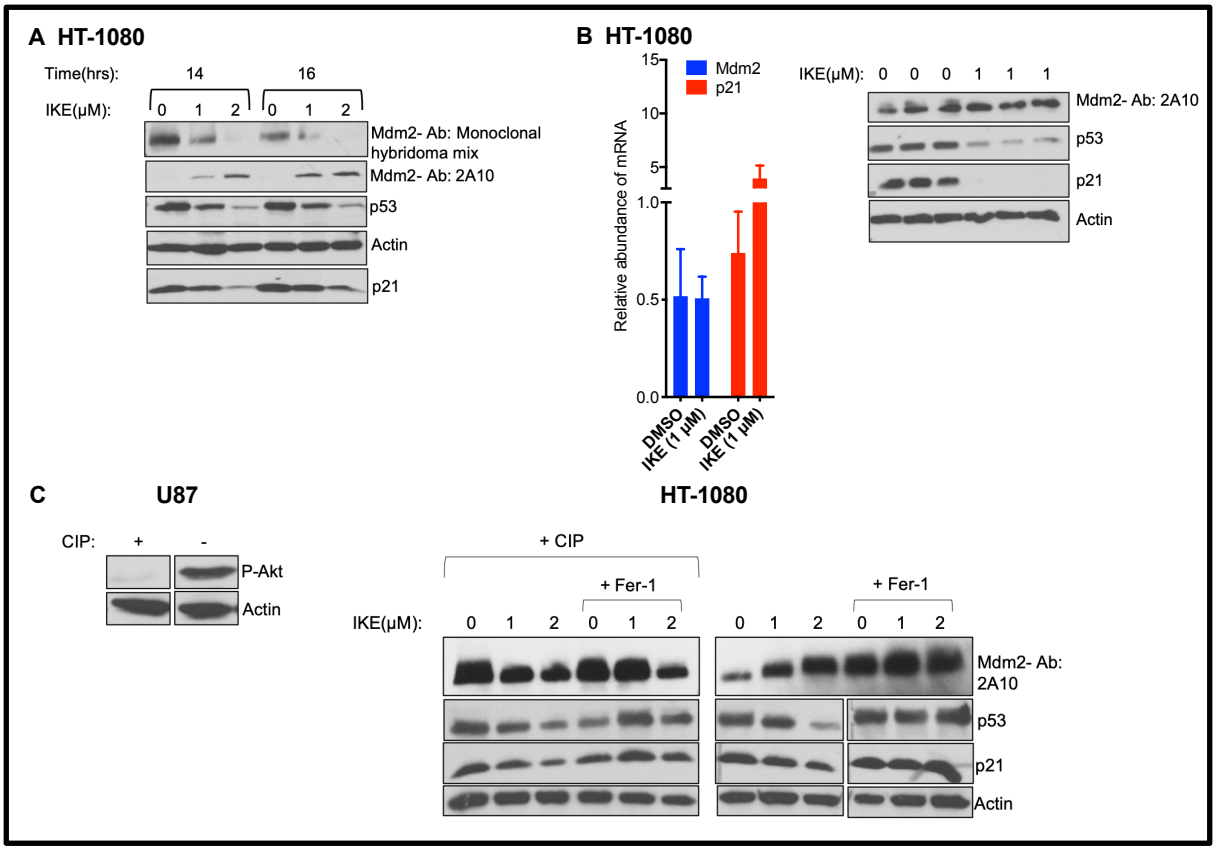

Figure 2.6 MDM2 gets dephosphorylated in response to ferroptosis

(A) Protein levels under ferroptosis treatment are shown to depict the differential detection of MDM2 protein based on the antibody used.

(B) Left panel: *MDM2* mRNA is measured upon ferroptosis induction. Right panel: the protein levels of the corresponding samples are shown. The cells were treated with IKE for 16 h.

(C) Effect of alkaline phosphatase (CIP) treatment of membranes. Left panel shows U87 lysates used as control. Right panel depicts lysates from HT-1080 cells treated with IKE, with or without fer-1 for 16 h.

The data in left panel of (B) represent the mean ± SE for three biological replicates.

Chapter 3: MDM2 and MDMX promote ferroptosis in a p53-independent manner

A large portion of this chapter is adapted from a published manuscript: Venkatesh et al., MDM2 and MDMX promote ferroptosis by PPARα-mediated lipid remodeling, *Genes & Development* (2020)

3.1 Introduction

Recently p53 independent roles of MDM2/X are being explored as summarized in Chapter 1, but the role of the MDM2-X complex has mainly been studied in the context of p53. In fact, while there are several drugs that attenuate the ability of MDM2/X to inactivate p53, most them aim to inhibit their binding to p53 or the E3 ligase activity of only MDM2 (Karni-Schmidt, Lokshin, and Prives 2016). In an earlier collaboration, Brent's and Carol's labs were the first to design compounds called the MELs, one of which was used in the previous chapter. In fact, these compounds specifically inhibit the E3 ligase activity of the MDM2-MDMX complex preferentially over that of the MDM2 homodimer (Herman et al. 2011).

p21 is the only other known target thought to be regulated by the MDM2-X complex, independent of its effects on p53 (Jin et al. 2008; Zhang et al. 2004). The results of our previous chapter indicate that MDM2, and possibly the MDM2-X complex can modulate ferroptosis independent of p21. In this chapter we extend this to show that MDM2, as well as MDMX are able to promote ferroptosis, at least partly because of their ability to form a complex. Since this role is independent of p53, our results address the niche of exploring the role of the MDM2-X complex outside the realm of p53.

In this chapter, we demonstrate that MDM2 and MDMX are strong regulators of ferroptosis as their roles can be shown in different cancer settings (established human cancer cell lines of

different origins and patient cellular models). We are also able to extend the ability of MDM2 and MDMX to promote ferroptosis to the context of neurodegeneration in rat brain slices.

3.2 Results

3.2.1 p53 is not required for suppression of ferroptosis caused by the inhibition of MDM2

In the first part of the project as described in Chapter 2, MDM2 was determined to have the potential to be a new player in ferroptosis. While it confirmed that this was a p21 independent role, it was necessary to examine if this was simply a p53 dependent function of MDM2.

Prives lab member David Tong, generated multiple clones of p53 knock-out (KO) from HT-1080 and SK-Hep1 cells using CRISPR/Cas9 technology (Fig 3.S1A). These cell lines were then tested for their respective responses to a range of erastin concentrations (Figs 3.1A and 3.1B). Consistent with previous reports (Murphy 2016), these p53 KO derivatives were more resistant to erastin compared to their wild-type counterparts. Nevertheless, the HT-1080 and SK-Hep1 p53 KO clones were still more sensitive to erastin than were cells classified as resistant (such as H1299 or HCT116) in Chapter 2. This p53 independent death was through ferroptosis as it was reversed by fer-1, as well as by deferoxamine (DFO), which is an iron chelator that prevents ferroptosis (Dixon et al. 2012) (Figs 3.1C, 3.1D, 3.S1B, 3.S1B and 3.S1F-3.S1I). Neither fer-1 (Figs 3.S1D and 3.S1J) nor DFO (Figs 3.S1E and 3.1S1K) had any effect on the responses of parental (WT) or p53 KO clones of HT-1080 and SK-Hep1 cells that were treated with staurosporine (STS), which elicits an apoptotic response (Belmokhtar, Hillion, and Ségal-Bendirdjian 2001). Thus, while in these cell lines p53 moderately sensitizes to ferroptosis, its presence is not required for ferroptosis. So now we could examine if the ferroptosis suppressive effects of nutlin and MEL23 were p53 independent.

In the p53 KO cells, nutlin had little effect on cell death (Figs 3.1E, 3.S2A and 3.S2B), while, as was seen in the parental (WT) counterparts, MEL23 substantially decreased the extent of ferroptosis (Figs 3.1G, 3.S2C and 3.S2D). Similar results with MEL23 and nutlin were obtained in SK-Hep1-derived p53 KO clones (Figs 3.1F, 3.1H, 3.S2F-3.S2I). Note that MEL23 did not prevent apoptosis induced by STS treatment in any of these cell lines (Figs 3.S2E and 3.S2J), indicating that the effect of MEL23 does not extend to apoptosis.

The results with MEL23 suggested that MDM2 might promote erastin-mediated cell death with or without p53. As nutlin functions to block the p53-MDM2 interaction, it would not necessarily be capable of inhibiting p53-independent functions of MDM2, perhaps explaining its inability to suppress erastin-induced cell death in p53 KO cells (insight into the suppression of ferroptosis by nutlin in parental cells expressing wild-type p53 is provided below).

We validated the specific effect of the drugs by showing that that RNA interference against MDM2 in p53 KO HT-1080 cells also prevents ferroptosis. In these experiments, we induced ferroptosis with IKE, a more potent inhibitor of system X_c^- (Figs 3.1I and 3.1J). We obtained similar results by depleting MDM2 using RNAi in SK-Hep1-derived cells (Figs 3.S2K, 3.S2M, 3.S2N, 3.S2P, 3.S2Q and 3.S2S) As another control, ablation of MDM2 did not alter cell death upon treatment with STS (Figs 3.S2L, 3.S2O and 3.S2R). In summary, these results demonstrate that MDM2 depletion or inhibition can selectively block ferroptosis, but not apoptosis, even in cancer cells lacking p53.

3.2.2 MDMX promotes sensitivity to ferroptosis independently of p53, alone and in complex with MDM2

We previously reported that MEL23 blocks the E3 ligase activity of the MDM2-MDMX heterodimer, preferentially over that of the MDM2 homodimer (Herman et al. 2011). Since MEL23 reduced sensitivity of cells to ferroptosis, we reasoned that lowering levels of the MDMX protein would reduce MDM2-MDMX complex formation and thereby might similarly suppress ferroptosis. We sought to deplete MDMX protein using the MDMX inhibitor NCS207895 (Berkson et al. 2005; Wang and Yan 2011), which represses expression from the *MDMX* promoter (Fig 3.2A), and by using *MDMX* RNA interference, both of which result in lower MDMX protein levels. Indeed, treatment of cells with MEL23 or NCS207895, but not nutlin, prevented ferroptosis in both HT-1080 parental (Fig 3.2B) and HT-1080-derived p53 KO (Figs 3.2C, 3.S3A) cell lines. Similar results were obtained in SK-HEP1 parental (Fig 3.S3B) and SK-HEP1-derived p53 KO cells (Figs 3.S3C and 3.S3D).

Confirmation that MDMX is required for a ferroptotic response was obtained using experiments showing that either parental HT-1080/SK-Hep1 cells or their p53 KO derivatives underwent significantly less ferroptosis when depleted of MDMX by siRNAs (Figs 3.2D, 3.2E, 3.S4A-3.S4D). Notably, the suppressive effects of MEL23 or siMDMX are not transient and do persist to a certain degree for at least 48 h after treatment (Figs 3.S4E-3.S4G). Thus, MDMX is required for erastin-induced ferroptosis in these cell lines, and this function of MDMX does not require p53.

These data raised the question as to why nutlin treatment reduced ferroptosis in cells with wild-type p53 (Figs 3.1 and 3.S2). Consistent with previous reports (Patton et al. 2006; Wade et al.

2006; Xia et al. 2008), the levels of MDMX were markedly reduced upon nutlin treatment in the parental HT-1080 cells (Fig 3.2B). By contrast, nutlin treatment did not reduce levels of MDMX in HT-1080 p53 KO cells (Figs 3.2C and 3.S3A). Similarly, in parental SK-Hep1 cells (Fig 3.S3B), nutlin treatment resulted in reduced MDMX protein abundance, which was not observed in p53 KO SK-Hep1 cells (Figs 3.S3C and 3.S3D). By contrast, and as expected, MEL23 led to accumulation of MDMX, as reported previously (Herman et al. 2011), by preventing its degradation by the MDM2 E3 ligase in both parental and p53 KO cells. Therefore, we hypothesize that the ability of nutlin to partially rescue viability in cells harboring wild-type p53 (but not KO cells that do not express p53) was due to its effect on the levels of MDMX protein. This finding, which suggests why nutlin was able to reduce ferroptosis in the presence of wild-type p53, provides further evidence that MDMX drives ferroptosis sensitivity.

The ability of MEL23 to suppress ferroptosis, in conjunction with the need for both MDM2 and MDMX to promote ferroptosis, led us to test whether the complex formed between MDM2 and MDMX mediates the ferroptosis sensitivity of cells, as opposed to the possibility that MDM2 and MDMX have independent functions. Towards this end, we ectopically expressed either wild-type MDMX or the MDMX variants MDMX (C463A) and MDMX (ΔC5), which lack the ability to bind to MDM2 (Uldrijan, Pannekoek, and Vousden 2007; Huang et al. 2011) (Fig 3.S4H). Overexpressed wild-type MDMX markedly increased cell death induced by erastin (Fig 3.3) which could be suppressed by fer-1 (Figs 3.S4I and 3.S4J) in both HT-1080 and SK-Hep1 cells. This is consistent with the idea that MDMX is itself a target of the MDM2-MDMX complex and hence a limiting factor in the activity of the complex.

Overexpression of either mutant of MDMX produced significantly less ferroptosis, such that while both MDMX mutant proteins did cause an increase in cell death due to erastin, neither was as effective as wild-type MDMX despite being expressed at similar or even greater levels than wild-type MDMX (Figs 3.3, 3.S4I and 3.S4J). Attempts to overexpress MDM2 and perform comparable experiments were not technically successful.

These results indicate that the MDM2-MDMX complex plays a role in facilitating ferroptosis, but also suggest that MDMX may have additional functions beyond being a part of the MDM2-MDMX heterodimer. Together with the finding that MEL23 is known to inhibit the MDM2 E3 ligase mainly when in complex with MDMX, we infer a primary role for the MDM2-MDMX complex in promoting ferroptosis.

We tried to extend our study to include other small molecule inhibitors of MDM2/X or specifically their complex. Indeed, our p53 KO clones (derived from either cell line) had lowered ferroptosis sensitivity due to any of the currently available inhibitors that we tried, which further strengthened our conclusion. But each inhibitor has its own disadvantages, which sometimes interfered with accurate interpretation of the data (Table 3.1). Therefore, we chose to use MEL23 and the MDMX inhibitor for further study as their disadvantages did not seem to limit their scope of use in the context of ferroptosis.

3.2.3 The MDM2-MDMX complex can promote ferroptosis in patient-derived glioblastoma models and rat brain slices

To examine whether MDM2 and MDMX can mediate ferroptosis in other contexts, we expanded our study to include patient-derived glioblastoma (GBM) cellular models, as well as an organotypic brain slice culture model of Huntington's disease. It was reported that patient glioblastoma models vary in their sensitivities to the ferroptosis inducer RSL3 (Quartararo et al. 2015). We compared the sensitivity of two GBM patient-derived models with high expression of *MDM2* (Ye, Reznik, et al. 2020), but with wild-type *TP53* versus two patient-derived cell models with normal expression level of *MDM2* and wild-type or mutated *TP53* (Fig 3.4A). We found that these two sets of GBM models (high versus normal expression of MDM2) had different responses to RSL3 (Fig 3.4B); specifically, the models with high MDM2 expression had ~50 times greater sensitivity to RSL3-induced ferroptosis. This trend in sensitivities of these models was specific to ferroptosis, as their response to apoptosis inducers, staurosporine and doxorubicin, was similar (Figs 3.4C and 3.4D). Notably, we were able to prevent cell death in both sets of GBM models with the co-addition of MEL23 (Figs 3.4E and 3.4F). The models with high expression of MDM2 exhibited a stronger inhibition of RSL3-induced death upon co-treatment with MEL23, such that, upon MEL23 treatment their response to RSL3 became similar to that of the wild-type MDM2-expressing models. These results suggest that MDM2, and likely the MDM2-MDMX complex, are able to drive the sensitivity of glioblastoma cells to ferroptosis.

Our collaborators Denise Dunn and Donald Lo, then examined the role of the MDM2-MDMX complex in the medium spiny neurons (MSNs) of the striatum of rats using a postnatal brain-slice model of Huntington's disease (Reinhart et al. 2011). These brain explants have been previously shown to lose a large portion of healthy MSNs when the first exon of mutant HTT (mHTT-Q73) is co-transfected with yellow fluorescent protein (YFP), as compared to the number of MSNs with

YFP transfection alone (Kaplan et al. 2015; Reinhart et al. 2011). Since fer-1 can suppress ferroptotic death in this model (Skouta et al. 2014), we used it as a positive control to rescue the death of these MSNs with mutant HTT. We observed that MEL23 was also able to prevent mutant-HTT-induced death of these MSNs, even at low concentrations (Fig 3.4G). This suggests that MEL23 is an inhibitor of ferroptosis in rat neurons, and that MDM2 and MDMX might mediate ferroptosis even in the context of neurodegeneration.

Our results demonstrate that MDM2 and MDMX are bona fide regulators of ferroptosis and that they promote this type of death independent of p53. Further, we believe that the MDM2-X complex is crucial for full efficiency of death by ferroptosis.

3.3 Discussion

One main strength of this study is that we have used various ways to inhibit MDM2/X- small molecule inhibitors of MDM2 and MDMX, siRNA-mediated ablation of these proteins, and ectopically expressed MDMX variants- which eliminate a possibility of drawing a conclusion based on any potential off-target effects of just one method. The results so obtained gives us confidence in concluding that MDM2 and MDMX can regulate ferroptosis in a p53-independent manner. This study also provides a repertoire of tools for any future study of p53-independent roles of MDM2/X in cancer.

Identifying a role for MDM2 and MDMX in ferroptosis may provide insight into therapeutic applications of ferroptosis inducers and inhibitors. The data presented here suggest that cancers with high levels of the MDM2-MDMX heterocomplex (and its E3 ligase activity) might be suitable targets for therapy involving ferroptosis inducers. Our results showing that the MDM2-MDMX complex can mediate the ferroptosis sensitivity of patient-derived glioblastoma cell lines further corroborates this hypothesis. There have been extensive efforts to develop nutlin-like compounds to treat cancers with wild-type p53 (Warner et al. 2012; Atatreh et al. 2018); one possible approach is to pair such compounds with other chemotherapeutics to achieve a more profound cancer control (Zanjirband, Edmondson, and Lunec 2016; Deben et al. 2015). Given the discovery of p53-independent roles of MDM2 and MDMX, cancers with amplifications in MDM2 and MDMX (even in the absence of wild-type p53) (Pishas et al. 2015; Wade, Li, and Wahl 2013) might benefit from therapies that act as antagonists of MDM2 and MDMX. Yet such therapies would likely not benefit from being combined with FINs or chemotherapeutics that induce ferroptosis, such as sorafenib (Lachaier et al. 2014) and sulfasalazine (Stockwell et al. 2017). In regard to such

combinations, our data indicate that combining MDM2-MDMX antagonists with ferroptosis inducers would in fact be counter-productive.

The results reported here could also aid in designing therapies for neurodegenerative disorders, ischemia, and organ damage, which have been shown to involve ferroptosis (Stockwell et al. 2017): MDM2-MDMX inhibitors might be used as inhibitors of degeneration in these diseases, as has been suggested for fer-1 (Yang and Stockwell 2016). In support of this concept, we found that MEL23 has a robust neuroprotective effect in the brain slice model of Huntington's disease. MDM2 has also been shown to regulate kidney function, predominantly through its effects on p53, but also via p53-independent roles in modulating post-ischemic kidney injury (Mulay et al. 2012). Since there is mounting evidence that ferroptosis mediates kidney injury (Martin-Sanchez et al. 2017) and failure (Friedmann Angeli et al. 2014; Müller et al. 2017), our data provide additional support for the notion that MDM2 (and MDMX) antagonists might have potential in treating kidney dysfunction.

While most of this work was done in the absence of p53, we did find that the suppression of MDM2 and MDMX was effective in reducing the degree of ferroptosis in cells with functional p53. Especially in the context of the class II FIN RSL3, there seems to be a further desensitization to ferroptosis by inactivation of the MDM2-MDMX complex beyond the effect of loss of p53. We therefore suggest that MDM2 and MDMX may also be able to mediate the role of p53 in ferroptosis perhaps in different ways that are specific to particular classes of FINs. This mediatory role of the MDMs needs to be further evaluated to better understand the entirety of their role in ferroptosis.

Finally, MDM2 and MDMX may have context-dependent tumor suppressor functions in addition to their well described oncogenic functions mediated by inhibition of p53 (Manfredi 2010). Our results suggest a mechanism for this observation, namely that MDM2 and MDMX can act as tumor suppressors by facilitating ferroptosis. Given that mounting evidence suggests that ferroptosis is a tumor suppressive mechanism (Jiang et al. 2015; Ou et al. 2016; Wang et al. 2016; Jennis et al. 2016; Murphy 2016; Zhuang and Gan 2019), our data provide a new hypothesis for the field to explore.

3.4 Methods

3.4.1 Genome editing using CRISPR/ cas9 technology to generate p53 KO clones

HT-1080 and SK-Hep1 p53 KO cells used were wildtype for p53 and they were cultured as in 2.4.1. These cells ($7x10^5$) were transfected with 2 μg of p53 CRISPR/Cas9 KO plasmid (Santa Cruz Biotech). Two days later, cells were treated with nutlin-3A (10 μM) for 10-12 days to inhibit proliferation of cells with wild-type p53, thereby enriching for p53 KO cells. Single-cell clones were selected via limiting dilution, and p53 KO clones were confirmed by Western blotting using FL-393 polyclonal antibody. The presence of indels in targeted exons 4, 5, and 7 was verified by DNA sequencing.

3.4.2 Immunoblot

The same methodology as described in 2.4.5 was used. Actin or GAPDH was used as the loading control.

The following primary antibodies were additionally used: MDM2 (D1V27, CST cat#86934 or N20, Santa Cruz biotech, cat# sc-813); MDMX (Bethyl laboratories cat# A300-287A or mAb 8C6, produced in Dr. Jiandong Chen's lab); GAPDH (CST cat# 5174S).

3.4.3 Chemicals

The following chemicals were additionally used apart from those listed in 2.4.3: MDMX inhibitor NSC207895 (Calbiochem, cat# 444158), staurosporine (Selleckchem, cat# S1421), deferoxamine (Calbiochem, cat# 252750).

The fixed concentrations of compounds used was as follows (unless otherwise mentioned): nutlin, 10 μM, MEL23, 14 μM, ferrostatin-1 (fer-1), 20 μM, deferoxamine (DFO), 90 μM, MDMX inhibitor, 5 μM.

3.4.4 Transfection-siRNA

The same methodology as described in 2.4.6 was used.

The following siRNAs were used: siLuciferase (Urist et al. 2004), siMDMX #1 : si_102_MDMX (Chen et al. 2005), siMDMX #2: Hs_MDM4_4 FlexiTube siRNA (QIAGEN, Valencia, CA, USA), siNegative control from silencer select (ThermoFisher, cat# 4390843), siMDM2#1 from silencer select (ThermoFisher, cat# s8630) and siMDM2#2 from silencer select (ThermoFisher, cat# ss224037).

3.4.5 Transfection- plasmids

The same methodology as described in 2.4.7 was used.

MDMX wild-type plasmid was obtained from Jiandong Chen's lab, MDMX C463A was obtained from Dr. Zhi-Min Yuan's lab(Huang et al. 2011) and MDMX Δ5 was obtained from Dr. Karen Vousden's lab (Uldrijan, Pannekoek, and Vousden 2007).

Note: Cells became more resistant to ferroptosis inducers after transfection when using Lipofectamine series of reagents. In order to observe cell death post transfection, three key factors

were controlled: cell density was kept low, Lipofectamine was washed off as soon as possible, and a higher concentration of FINs was used to induce ferroptosis compared to non-transfected conditions. On day 1, 1 x 10^5 cells were plated in 2 mL in each well of a 6-well plate for HT-1080-derived cells and 2 x 10^5 cells were plated for SK-Hep1-derived cells. The cells were transfected in the late evening of day 2. The cells were washed and the medium was changed after an overnight incubation with transfection reagent. On the evening of day 3, FINs were added. IKE was used instead of erastin to achieve more potent ferroptosis induction. For SK-Hep1 cells, a confluent 10 cm dish was transfected with siRNA (20 nM of siRNA). 24 h post-transfection, cells were harvested, counted and plated into 384-well plates. Cells were simultaneously plated into 6-well plates to be harvested on the same day as the cell viability assay was performed, to measure the efficiency of knockdown.

3.4.6 Huntington's brain slice assay

This assay was performed as previously described in (Kaplan et al. 2015).

3.4.7 Immunoprecipitation

The cells were lysed as described in 2.4.5 and immediately used for the next steps. All of the following steps were performed at 4°C. Equivalent amounts (180 μg) of each cell lysate were subjected to immunoprecipitation with specific antibody for 2 h. Then, 40 μL of protein G beads (GE Healthcare) that were pre-blocked with bovine serum albumin (BSA) (New England BioLabs) was added for another 1 h. Then the beads were washed 3 times with 500 mL of lysis buffer (without the protease inhibitors). The proteins were eluted by adding protein sample buffer and incubating for 10 min at 95°C. Immunoblotting analysis was performed as described in 2.4.5.

For MDM2 IP: 1 million HT-1080 p53 KO cells were plated in 10 cm dishes. The next day, they were transfected with 300 ng of the MDMX variants (WT, C463A, Δ5) using Lipofectamine 3000 (Thermo Scientific) for 48 h before harvesting. TEB lysis buffer was used for the steps described above. We used 4 μg of the purified D1V27 (CST cat#86934) antibody against MDM2.

3.4.8 Cell viability assay

For dose response curves and 6 well experiments the same methodology as described in 2.4.8 was used.

For siRNA experiments in SK-Hep1-derived cells: 1,400 cells were plated for SK-Hep1 wild-type cells, while 1,000 cells were plated for the SK-Hep1-derived p53 KO cells (clone 2 and clone 4). The rest of the viability assay procedure remained the same.

For viability assays performed in 6-well plates, cells were harvested using trypsin (0.5 ml per well) and the medium was saved from each well. The trypsinized cells were resuspended with the collected medium and 2-3 aliquots (0.10 ml each) sampling different regions of this suspension were taken into 96-well plates to serve as technical replicates for the measurement. CellTiter-Glo Luminescent Viability assay was used to measure the viability of these aliquots. The rest of the culture was used to extract protein to be analyzed using western blots.

3.4.9 Statistical analysis

Prism (version 8, GraphPad) was used to make all the graphs in the paper and for performing all the statistical analysis shown. The GraphPad style (0.1234(ns), <0.0332(*), < 0.0021(**), <0.0002(***)) was used to represent the p values. The p values were calculated by ANOVA and appropriate multiple testing correction was done where required.

3.5 Tables

Table 3.1 Multiple inhibitors of MDM2/X tested for their ferroptosis suppressive abilities

All the inhibitors listed were able to suppress ferroptosis independent of p53, but since they each have different limitations, we chose to pursue the two whose disadvantages did not directly interfere with the context of ferroptosis.

MDM2/X antagonist	Mechanism of action	Disadvantages	Discovery paper
MEL23	Specific to E3 ligase activity of the MDM2-X complex.	Exact binding location is unclear. Basal cell death makes it toxic at higher concentrations.	Herman et al., 2011
MDMX inhibitor	Lowers MDMX protein directly.	Increases labile iron levels in the cells undergoing ferroptosis. Basal cell death makes it very toxic at higher concentrations.	Berkson et al., 2005
MMRi compounds	Blocks the formation of the complex.	Is a very potent iron chelator during ferroptosis.	Wu et al., 2015
SP141	Promotes auto ubiquitination of MDM2.	Expected changes in MDM2 and MDMX protein levels are not seen at the time of rescue.	Wang et al., 2014
PROTAC against MDM2	Degrades MDM2, by actively targeting it to the cullin 4A E3 ligase system	Markedly increases basal cellular viability.	Li et al., 2019

3.6 Figures

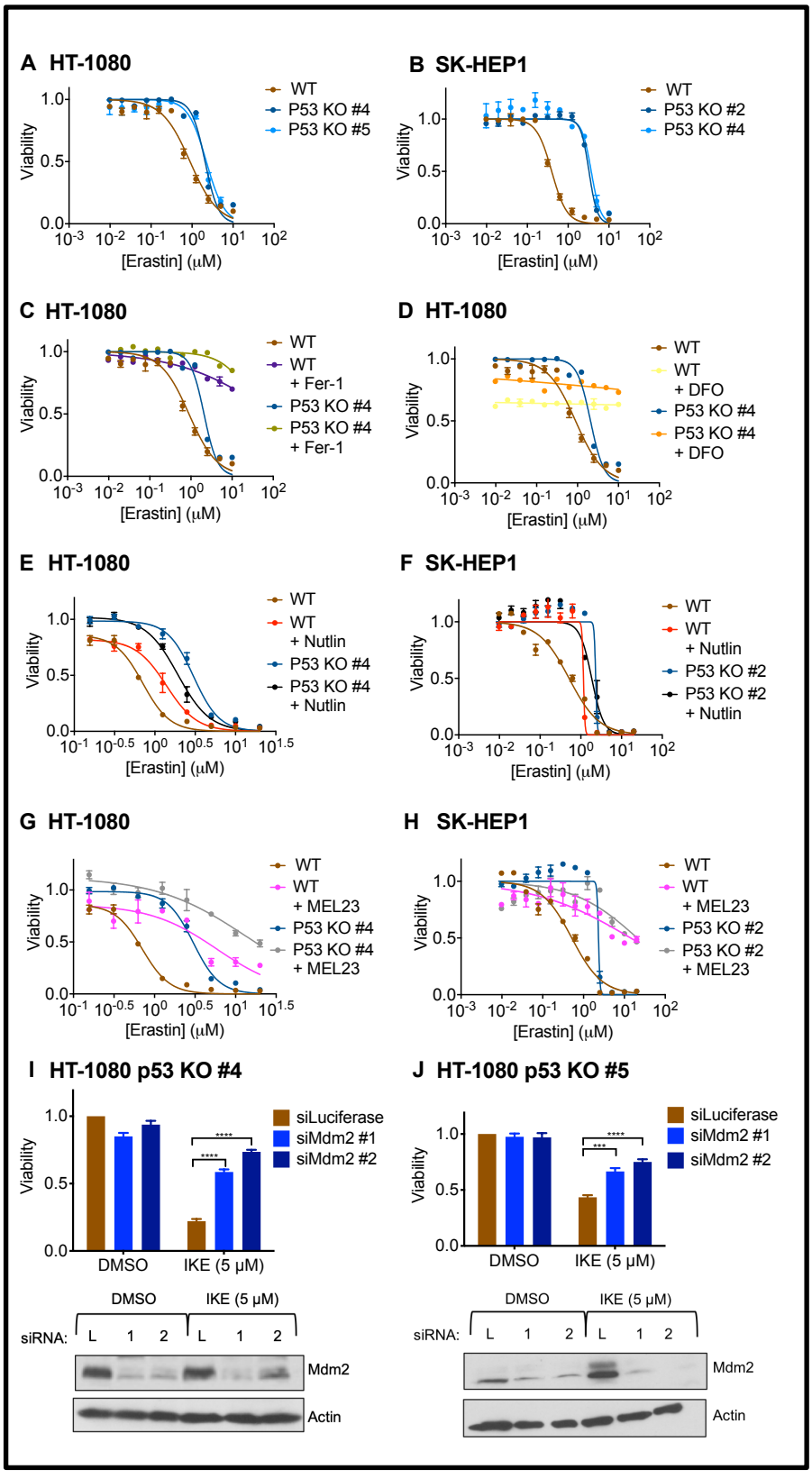
A HT-1080
WT
P53 KO #4
P53 KO #5
Viability
[Erastin] (μM)
B SK-HEP1
WT
P53 KO #2
P53 KO #4
C HT-1080
WT
WT + Fer-1
P53 KO #4
P53 KO #4 + Fer-1
D HT-1080
WT
WT + DFO
P53 KO #4
P53 KO #4 + DFO
E HT-1080
WT
WT + Nutlin
P53 KO #4
P53 KO #4 + Nutlin
F SK-HEP1
WT
WT + Nutlin
P53 KO #2
P53 KO #2 + Nutlin
G HT-1080
WT
WT + MEL23
P53 KO #4
P53 KO #4 + MEL23
H SK-HEP1
WT
WT + MEL23
P53 KO #2
P53 KO #2 + MEL23
I HT-1080 p53 KO #4
siLuciferase
siMdm2 #1
siMdm2 #2
DMSO
IKE (5 μM)
siRNA:
L 1 2 L 1 2
Mdm2
Actin
J HT-1080 p53 KO #5

Figure 3.1 p53 is not required for suppression of ferroptosis caused by inhibition of MDM2

(A, B) Dose-response of wild-type and p53 KO cells to erastin in (A) HT-1080 derived cells and (B) SK-Hep1 derived cells.

(C, D) Inhibition of erastin-induced HT-1080 cell death by (C) fer-1 and (D) DFO

(E-H) Effect of MDM2 antagonists (nutlin and MEL23) on the dose-response of two different cells lines to erastin treatment. (E) HT-1080 derived cells and (F) SK-Hep1 derived cells treated with the combination of nutlin and erastin. (G) HT-1080 derived cells and (H) SK-Hep1 derived cells treated with the combination of MEL23 and erastin.

(I, J) Suppression of ferroptosis by the knockdown of MDM2 in two HT-1080 derived p53 KO clones. The top panel shows the viability of cells treated with a lethal dose of IKE when transfected with either the siRNA against Luciferase or one of two different siRNAs against MDM2. The bottom panel shows the corresponding decrease in the protein levels of MDM2 upon RNA interference against Luciferase (L) or MDM2 (1 and 2). The transfection was done using 15nM of siRNA and the cells were treated with IKE 24 h after transfection.

Cells in (A-H) were treated with drugs for 24 h. Cells in (I, J) were treated with drugs for 18 h. The data in (A-H) represent the mean ± SE for two out of four independent experiments. The viability data in (I, J) represent the mean ± SE for four independent experiments. The viability data have been measured using ATP based CellTiter-Glo reagent and have been normalized to the DMSO control.

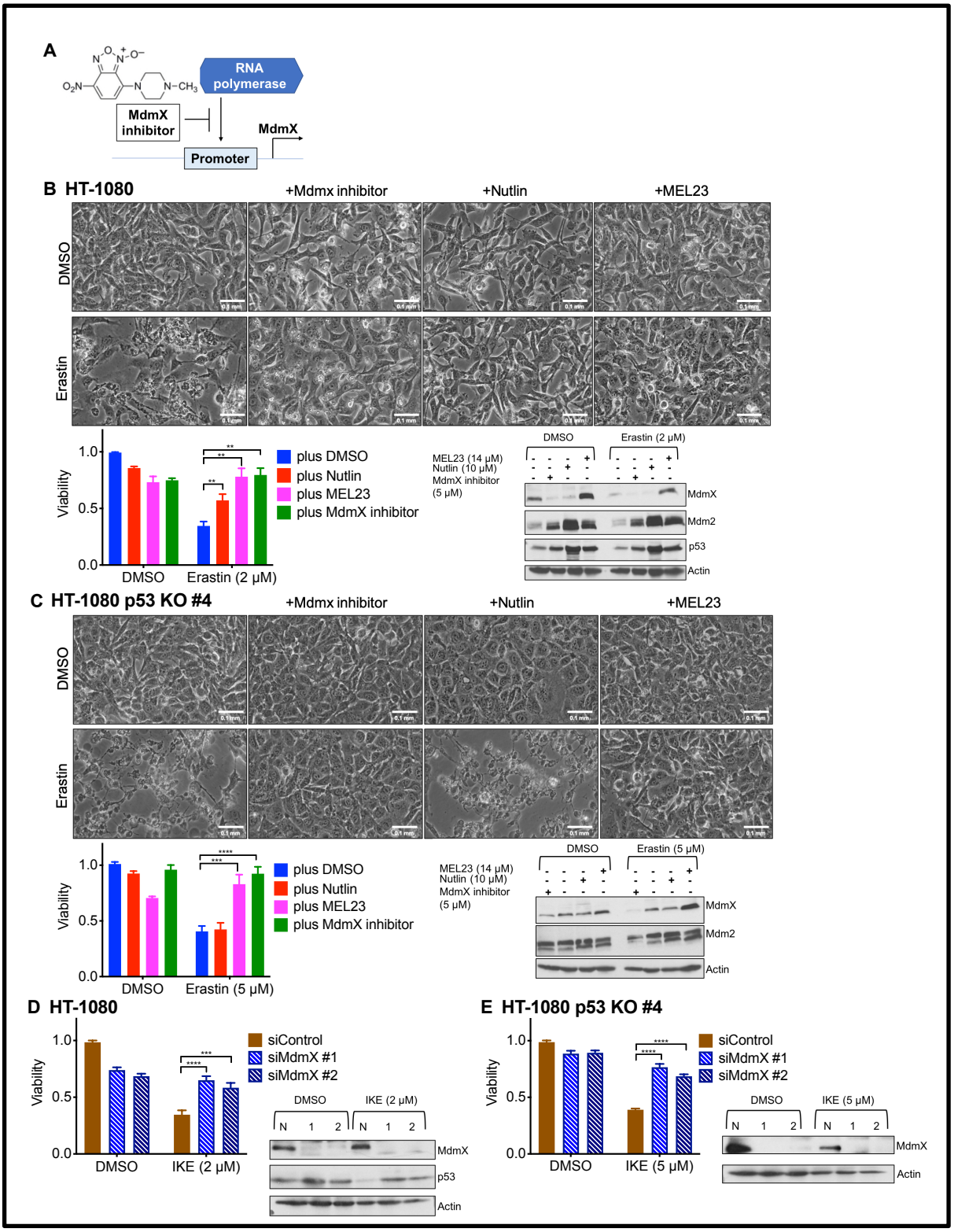

Figure 3.2 MDMX promotes sensitivity to ferroptosis independently of p53

(A) Cartoon of the known structure and mechanism of action of the MDMX inhibitor (Berkson et al. 2005; Wang and Yan 2011).

(B, C) Effect of MDM2 and MDMX antagonists (MEL23, nutlin, and MDMX inhibitor) on the lethality of erastin in HT-1080 derived cells. This effect was analyzed using microscopic images taken at 10X magnification (top panel) and cell viability (bottom left panel). The corresponding MDM2/X protein levels were also measured (bottom right panel).

(D, E) Suppression of ferroptosis by the knockdown of MDMX in HT-1080 derived cells. The left panel shows the viability of cells treated with a lethal dose of IKE when transfected with either the scrambled siRNA negative control or one of two different siRNAs against MDMX. The right panel shows the corresponding decrease in the protein levels of MDMX upon RNA interference against the control (N) or MDMX (1 and 2). The transfection was done using 15nM of siRNA and the cells were treated with IKE 24 h after transfection.

Cells in (B, C) were treated with drugs for 16 h. Cells in (D, E) were treated with drugs for 18 h. The viability data in (B, C) represent the mean ± SE for two independent experiments. The viability data in (D, E) represent the mean ± SE for three independent experiments. The viability data have been measured using ATP based CellTiter-Glo reagent and have been normalized to the DMSO control.

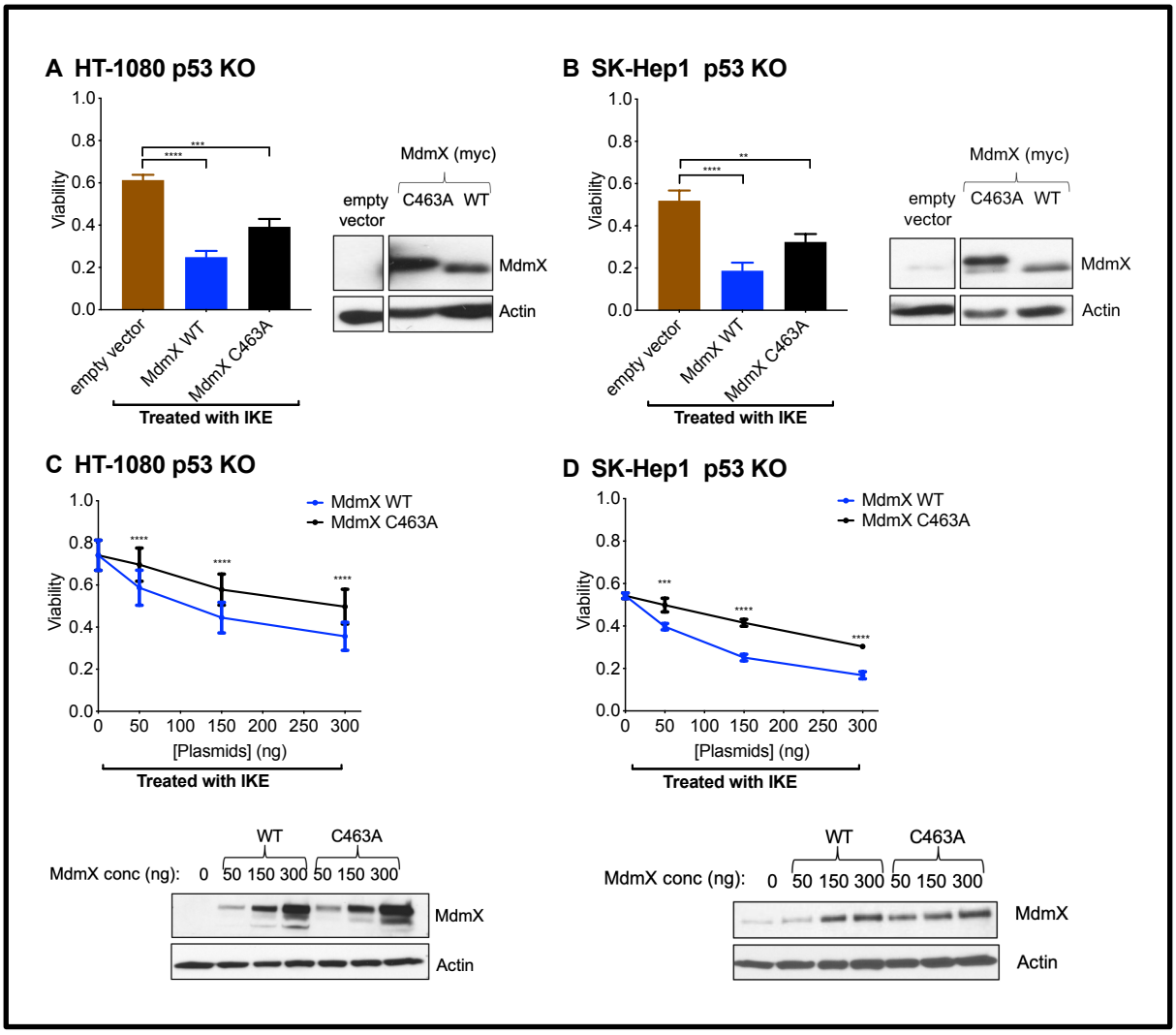

Figure 3.3 Wild-type MDMX is more effective at sensitizing cells to ferroptosis than MDM2 binding-deficient mutants of MDMX

(A-D) Effect of overexpression of MDMX variants (WT and C463A) on the lethality of IKE in p53 KO clones derived from two different cells. The transfection was done using 300µg of plasmid of each variant in (A) HT-1080 derived cells and (B) SK-Hep1 derived cells. The transfection was done using a dose-curve (0-300µg) of each variant in (C) HT-1080 derived cells and (D) SK-Hep1 derived cells. The right panel of (A, B) and the bottom panel of (C, D) show the corresponding

expression levels of the MDMX variants. The cells were treated for 18 h with IKE (5μM) 24 h after transfection.

The viability data in (A-D) represent the mean ± SE for three independent experiments. The viability after drug treatment has been measured using ATP based CellTiter-Glo reagent and is normalized to the viability of the DMSO control under each transfection condition respectively.

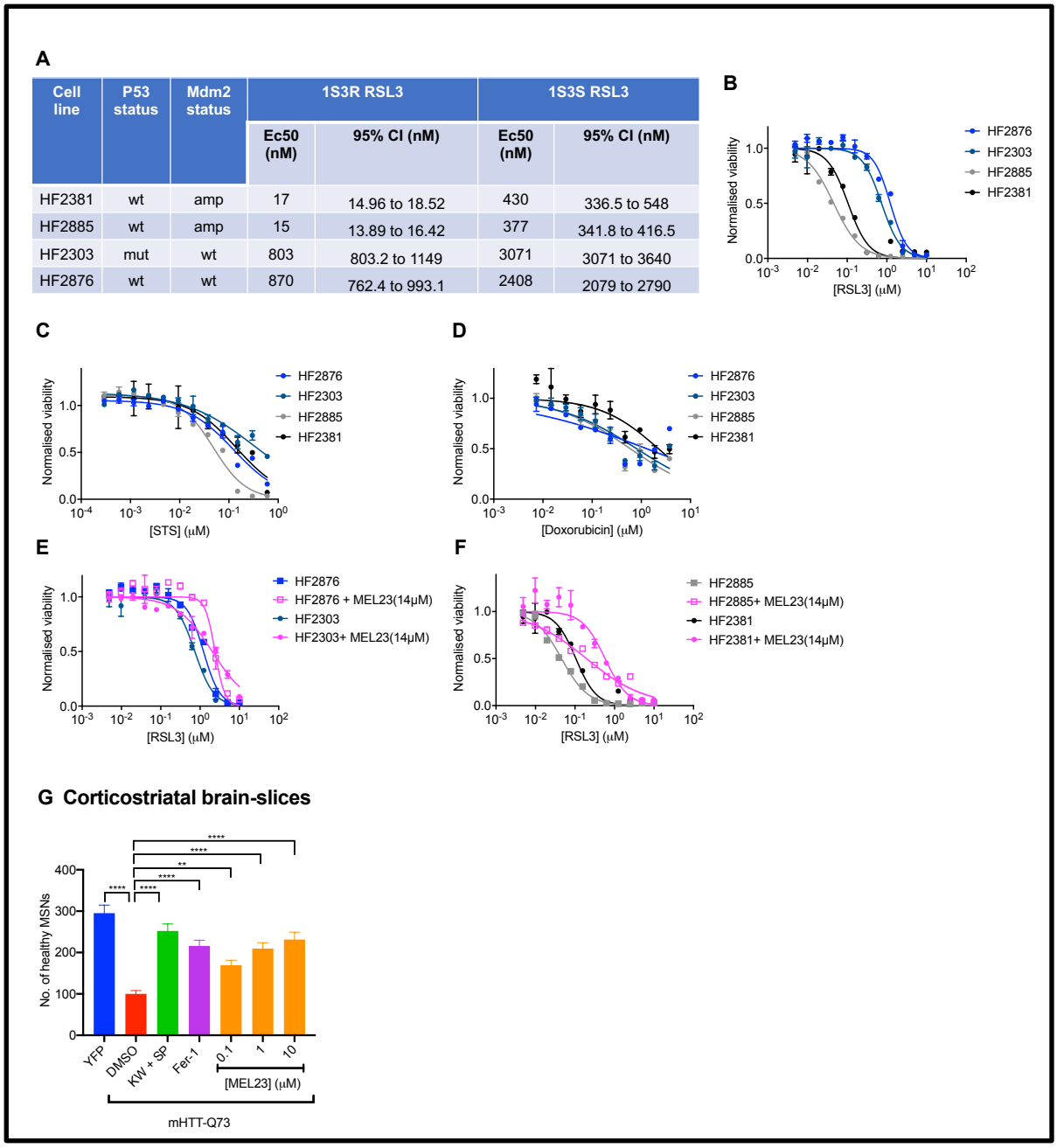

Cell line	P53 status	Mdm2 status	1S3R RSL3		1S3S RSL3	
			Ec50 (nM)	95% CI (nM)	Ec50 (nM)	95% CI (nM)
HF2381	wt	amp	17	14.96 to 18.52	430	336.5 to 548
HF2885	wt	amp	15	13.89 to 16.42	377	341.8 to 416.5
HF2303	mut	wt	803	803.2 to 1149	3071	3071 to 3640
HF2876	wt	wt	870	762.4 to 993.1	2408	2079 to 2790

Figure 3.4 The MDM2-X complex can promote ferroptosis in patient-derived glioblastoma models and rat neurons

(A-F) The MDM2-X complex mediates the sensitivity of four different patient-derived glioblastoma models to RSL3. (A) RSL3's EC50, MDM2 and p53 status for the glioblastoma

models. Dose response of the glioblastoma models to (B) RSL3, (C) staurosporine (STS), and (D) doxorubicin. MEL23 is able to inhibit the sensitivity of (E) MDM2 wild-type glioblastoma models and (F) MDM2 amplified glioblastoma models to RSL3 treatment.

(G) MEL23 is able to suppress the mutant Huntingtin (mHTT) protein induced neurodegeneration of rat striatal medium spiny neurons in a brain slice model of Huntington's disease. Rat corticostriatal brain slice explants were co-transfected with the first exon of the mHTT (Q73) and YFP transfection was used as a control. Brain slices were treated with either DMSO, a positive control mixture of 50μM KW-6002 and 30μM of SP600125, fer-1 as a second positive control, or a three-point concentration-response curve for MEL23.

Cells in (A-F) were treated with drugs for 24 h. The data in (A-F) represent the mean ± SE for two out of four independent experiments. The data in (G) represent the mean ± SE from one of two representative experiments, with at least 24 samples assessed per condition. The viability data have been measured using ATP based CellTiter-Glo reagent and have been normalized to the DMSO control.

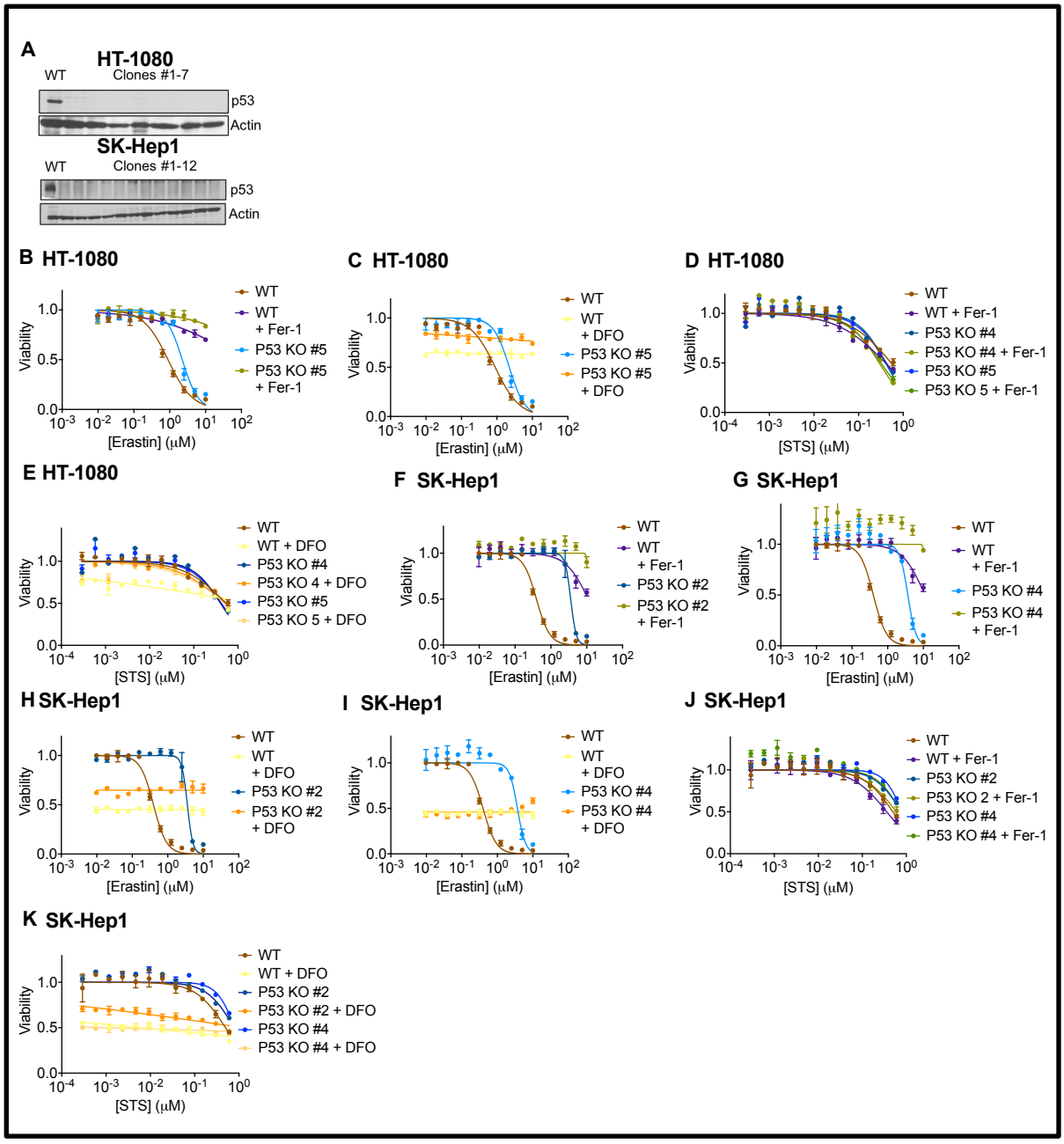

Figure 3.S1 p53 knock-out clones are moderately less sensitive to ferroptosis (Related to Figure 3.1)

(A) p53 protein levels in the CRISPR edited p53 KO clones derived from HT-1080 and SK-Hep1 cells.

(B-K) Dose-response of two different cell lines to erastin and STS when co-treated with fer-1 or DFO. HT-1080 derived cells were treated a combination of fer-1 and (B) erastin or (D) staurosporine (STS). HT-1080 derived cells were treated a combination of DFO and (C) erastin or (E) STS. SK-HEP1 derived cells were treated with a combination of fer-1 and (F, G) erastin or (J) STS. SK-HEP1 derived cells were treated a combination of DFO and (H, I) erastin or (K) STS.

Cells in (B-K) were treated with the drugs for 24 h. The data in (B-K) represent the mean ± SE for two out of four independent experiments. The viability data have been measured using ATP based CellTiter-Glo reagent and have been normalized to the DMSO control.

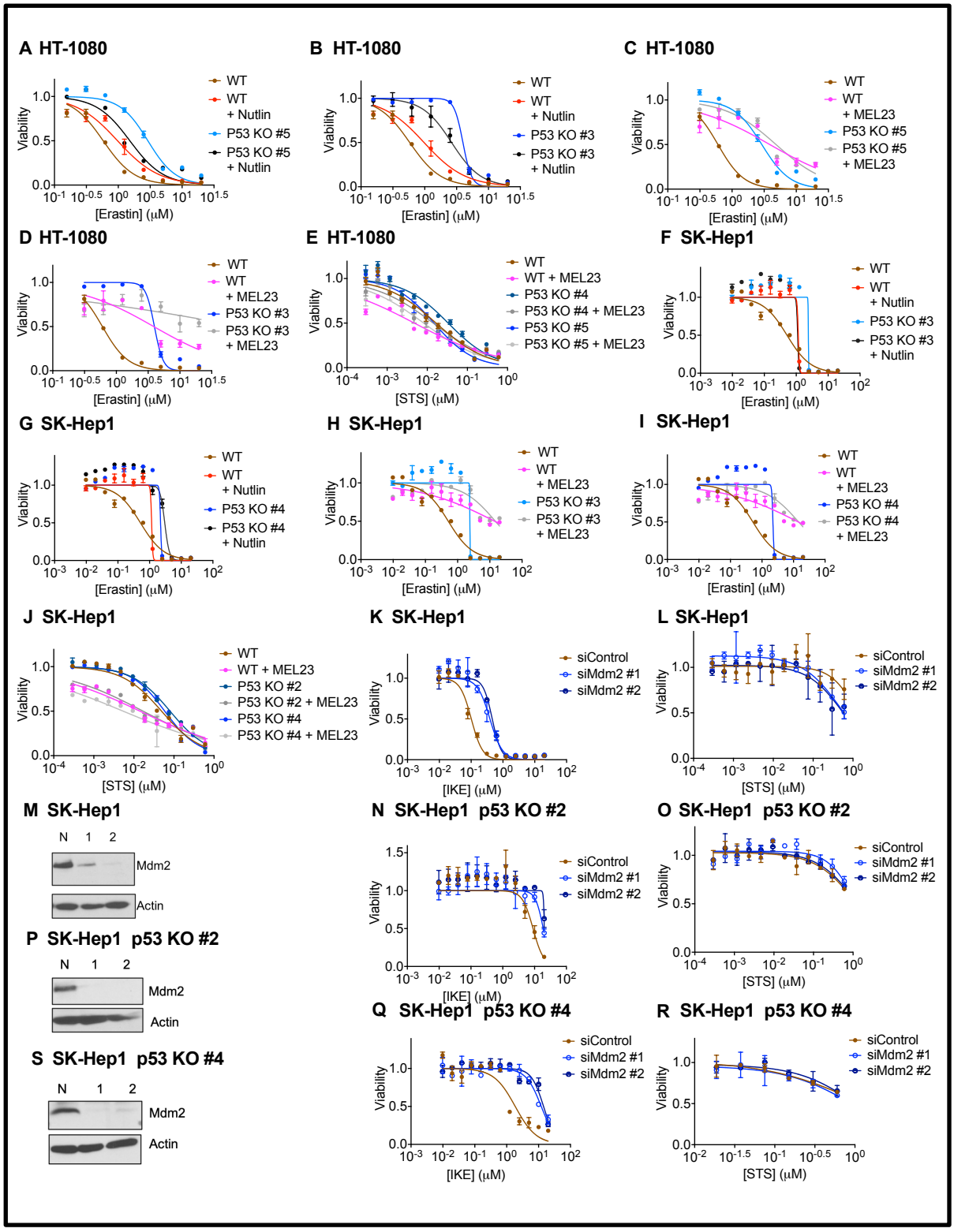

Figure 3.S2 MDM2 can suppress ferroptosis independent of p53 (Related to Figure 3.1)

(A-J) Effect of MDM2 antagonists (nutlin and MEL23) on the dose-response of two different cells lines to erastin and STS treatment. (A, B) HT-1080 derived cells and (F, G) SK-Hep1 derived cells treated with the combination of nutlin and erastin. (C, D) HT-1080 derived cells and (H, I) SK-Hep1 derived cells treated with the combination of MEL23 and erastin. The lethality of STS is unaffected by MEL23 in (E) HT-1080 derived cells and (J) SK-Hep1 derived cells.
(K-S) Suppression of ferroptosis by the knockdown of MDM2 in SK-Hep1 derived p53 KO cells. The transfected cells were treated with a dose-curve of either (K, N, Q) IKE or (L, O, R) STS. (M, P, S) The corresponding decrease in levels of MDM2 protein in the cells transfected with either a scrambled siRNA negative control (N) or one of two different siRNAs against MDM2 (1 and 2). The transfection was done using 20nM of siRNA and the cells were treated with drugs 48 h after transfection.

Cells in (A-R) were treated with drugs for 24 h. The data in (A-L, N, O, Q, R) represent the mean ± SE for two out of four independent experiments. The viability data have been measured using ATP based CellTiter-Glo reagent and have been normalized to the DMSO control.

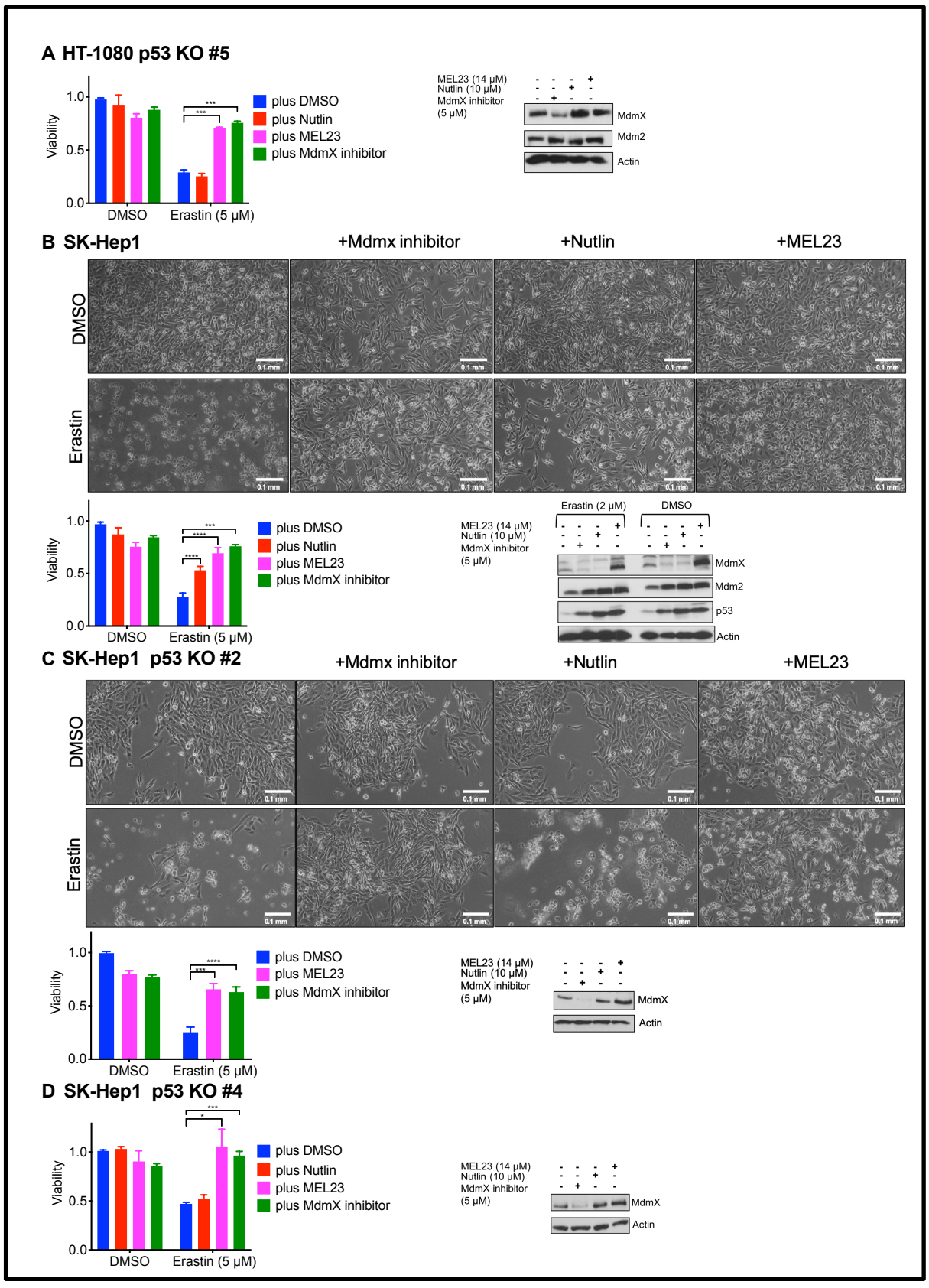
A HT-1080 p53 KO #5
Viability
1.0
0.5
0.0
DMSO
Erastin (5 μM)
plus DMSO
plus Nutlin
plus MEL23
plus MdmX inhibitor
MEL23 (14 μM)
Nutlin (10 μM)
MdmX inhibitor (5 μM)
MdmX
Mdm2
Actin
B SK-Hep1
+Mdmx inhibitor
+Nutlin
+MEL23
DMSO
Erastin
0.1 mm
Erastin (2 μM)
DMSO
p53
C SK-Hep1 p53 KO #2
D SK-Hep1 p53 KO #4

Figure 3.S3 The presence of p53 is not essential for the ability of MDMX to promote ferroptosis (Related to Figure 3.2)

(A-D) Effect of MDM2 and MDMX antagonists (nutlin, MEL23, and MDMX inhibitor) on the response of cells to 16 h of erastin treatment. Cell viability of (A) HT-1080 derived p53 KO cells and (B-D) SK-Hep1 derived cells when treated with erastin in combination with the antagonists is shown. The top panel images in (B, C) correspond to the cells used to measure viability shown in their respective bottom panels. The images were captured at 10X magnification. The protein levels in the right panels of (A, D) and bottom right panels of (B, C) correspond to the samples for which cell viability was measured.

The viability data in (A-D) represent the mean ± SE for three independent experiments. The viability data have been measured using ATP based CellTiter-Glo reagent and have been normalized to the DMSO control.

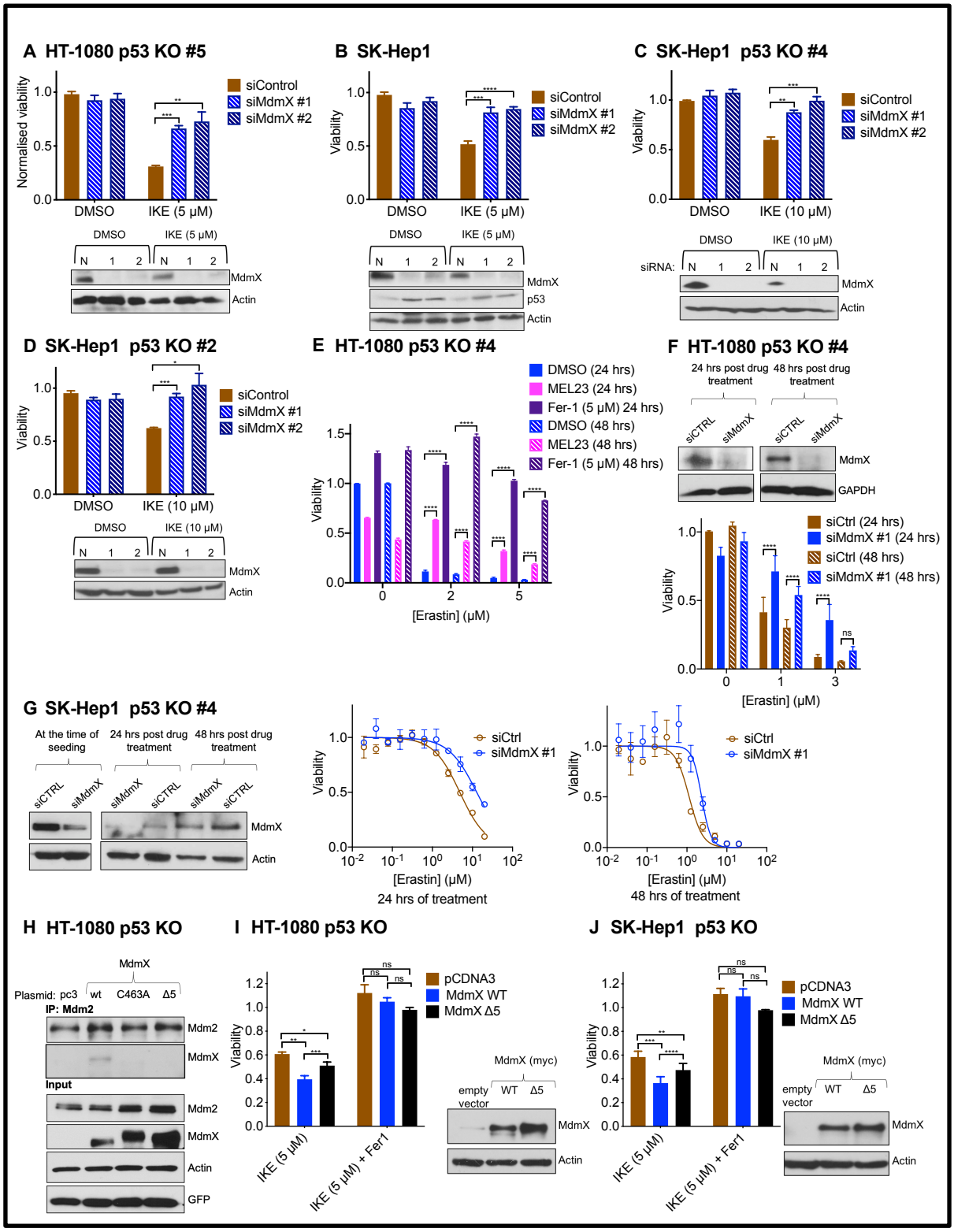
A HT-1080 p53 KO #5
Normalised viability
siControl
siMdmX #1
siMdmX #2
DMSO
IKE (5 μM)
MdmX
Actin
B SK-Hep1
Viability
p53
C SK-Hep1 p53 KO #4
IKE (10 μM)
siRNA:
D SK-Hep1 p53 KO #2
E HT-1080 p53 KO #4
DMSO (24 hrs)
MEL23 (24 hrs)
Fer-1 (5 μM) 24 hrs)
DMSO (48 hrs)
MEL23 (48 hrs)
Fer-1 (5 μM) 48 hrs)
[Erastin] (μM)
F HT-1080 p53 KO #4
24 hrs post drug treatment
48 hrs post drug treatment
siCTRL
siMdmX
GAPDH
siCtrl (24 hrs)
siMdmX #1 (24 hrs)
siCtrl (48 hrs)
siMdmX #1 (48 hrs)
G SK-Hep1 p53 KO #4
At the time of seeding
24 hrs of treatment
48 hrs of treatment
H HT-1080 p53 KO
Plasmid: pc3
wt
C463A
Δ5
IP: Mdm2
Mdm2
Input
GFP
I HT-1080 p53 KO
pCDNA3
MdmX WT
MdmX Δ5
MdmX (myc)
empty vector
WT
IKE (5 μM)
IKE (5 μM) + Fer1
J SK-Hep1 p53 KO

Figure 3. The protein levels of MDMX dictate the sensitivity to ferroptosis (Related to Figure 3.2 and 3.3)

(A-D, F, G) Suppression of ferroptosis by the knockdown of MDMX in cells. The effects of RNA interference against *MDMX* (1 and 2) was compared to that against the scrambled siRNA negative control (N). In (A-D), the top panels show the viability of cells treated with a lethal dose of IKE for 24 h, after 24 h of transfection. In (F), the bottom panel shows the viability of cells treated with a lethal dose of Erastin for 24 and 48 h, after 24 h of transfection. In (G), the right panels show the viability of transfected cells treated with a dose-curve of Erastin for either 24 or 48 h, after 48 h of transfection. HT-1080 derived cells were used in (A, F) and SK-HEP1 derived p53 KO cells were used in (B-D, G). The bottom panels of (A-D), the top panel of (F) and the left panel of (G) show the corresponding decrease in the protein levels of MDMX at the respective time points. The transfection was done using 20nM of siRNA.

(E) The suppressive effects of MEL23 and fer-1 on the cellular response to erastin at 24 and 48 h in HT-1080 derived p53 KO cells.

(H) Immunoprecipitation using MDM2 antibody in HT-1080 derived p53 KO cells shows the ability of the various MDMX variants (WT, C463A, Δ5) to be bound to MDM2.

(I, J) Effect of overexpression of MDMX variants (WT, Δ5) on the lethality of IKE in p53 KO clones derived from two different cells. (I) HT-1080 derived cells and (J) SK-Hep1 derived cells were treated with a combination of fer-1(10μM) and IKE after transfection with either MDMX variant. The right panels show the corresponding expression levels of each MDMX variant. The transfection was done using 300μg of plasmid of each variant.

Cells in (I, J) were treated for 18 h with IKE, 24 h after transfection. The viability data in (A-D) represent the mean ± SE for three independent experiments, in (E, F, I, J) represent the mean ± SE for two of three independent experiments, in (G) represent the mean ± SE for two independent experiments. In (A-G), the viability data have been normalized to the DMSO control. For (I, J), the viability under drug treatment is normalized to the viability of the DMSO control under each transfection condition respectively. The viability data have been measured using ATP based CellTiter-Glo reagent.

Chapter 4: MDM2/X lower PPARα activity to dampen the antioxidant defenses of cells against ferroptosis

A large portion of this chapter is adapted from a published manuscript: Venkatesh et al., MDM2 and MDMX promote ferroptosis by PPARα-mediated lipid remodeling, *Genes & Development* (2020)

4.1 Introduction

Although p53 has been implicated in the control of many cell death pathways (Ranjan and Iwakuma 2016), the p53 independent role of MDM2/X in such regulation is largely unexplored. Our previous chapter has been the first study to show that regulating ferroptosis is a p53 independent property of the MDM2/X complex. Since this is such a novel role of MDM2/X, it became important to characterize the molecular pathway involved.

In the previous chapters, we eliminated the only known targets of the MDM2/X complex, namely p53 and p21, as not being essential for the role of the complex in ferroptosis. Lack of other known targets of the MDM2-X complex prevented us from being able to quickly pinpoint a potential mechanism of action. The two approaches that were then used to identify the mechanism of regulation of ferroptosis by MDM2/X, are described in this chapter. First, we evaluated if any of the known modulators of ferroptosis were under the control of MDM2/X. Since no such targets were found, we instead started evaluating some of the known targets of MDM2 with potential ties to ferroptosis (based on their known biological roles) without any successful hits. We then asked which ferroptosis checkpoint is affected by the inhibition of MDM2/X to identify the level of regulation involved. As described in Chapter 1, the different FINs effect cell death by impinging on different upstream pathways and these form the basis of the different checkpoints of ferroptosis which can be manipulated to alter the final outcome. Evaluating the effect of MDM2/X antagonists

on the different classes of FINs led us to conclude that one of the more downstream checkpoints was being affected. This finding led us to perform an untargeted lipidomic analysis. While such an analysis has been previous performed in the context of wild-type p53 cells treated with erastin/IKE, our profiling of p53 KO cells treated with erastin in combination with MDM2/X antagonists revealed novel alterations to the lipid compositions of cells. These changes prompted us to study the roles of the PPAR family in ferroptosis. A previous study showed that MDM2 was able to strongly regulate the activity of PPARα (better than that of PPARβ/δ, while PPARγ's activity was unaltered) (Gopinathan et al. 2009). This report taken together with the changes that we observed in the lipid composition being hallmarks of PPARα activity, caused us to mainly focus on this isoform.

Our results show that PPARα is indeed the modulator of the ability of MDM2/X to alter the lipid metabolism of cells undergoing ferroptosis. We also show that MDM2/X and PPARα activity are upstream regulators of a newly discovered ferroptosis regulator, FSP1 that functions to enhance the antioxidant response of cells to ferroptosis (Bersuker et al. 2019; Doll et al. 2019). Therefore, we believe that MDM2 and MDMX dampen the antioxidant defenses of cells to promote death due to ferroptotic insult.

4.2 Results

4.2.1 Promotion of ferroptosis by MDM2 and MDMX is not dependent on the cell cycle

In the previous chapter, our results showed that the role of MDM2/X is independent of p21, a key regulator of the cell cycle (Warfel and El-Deiry 2013). But even in the absence of p53, MDM2 has been reported to promote cell growth and survival in some settings (Feeley et al. 2017), and these effects need not be dependent on p21. In line with this, David Tong in the Prives lab was unable to create stable MDM2 or MDMX knock-out cells with CRISPR/Cas9 using either HT-1080 or SK-Hep1 derived p53 KO cells. This supports the notion that MDM2 and MDMX are necessary for cell survival in these cancer cell lines, even when lacking p53.

MEL23 and the MDMX inhibitor were able to prevent ferroptotic cell death, even after 7-8 h of treatment (Fig 4.1A left panel). At this time point, we did not find significant changes in the cell cycle analysis performed by a member of the Prives lab, Alyssa Klein, which were common to the two MDM2-MDMX inhibiting compounds that had similar effects on ferroptosis (Fig 4.1A right panel). Taken together, these results indicate that the impact of blocking MDM2-MDMX complex activity on ferroptosis is independent of p21 and is not merely a by-product of cell cycle changes.

4.2.2 MDM2 and MDMX regulate a hitherto-unknown mediator of ferroptosis

We first examined if some of the known ferroptosis regulators could be modulating the role of MDM2/X in ferroptosis, but none of these seemed to be involved in mediating the role of MDM2/X (Table 4.2). Instead, our results indicated that there might be a novel mechanism involved.

As an alternative approach, we examined multiple previously known targets of MDM2 that have a potential link to ferroptosis. While our analysis revealed potential new regulators of ferroptosis that can be further studied, as well as some hitherto unknown targets of the MDM2-X complex, none of the targets tested seemed to modulate this role of MDM2/X in ferroptosis (Table 4.2).

4.2.3 Inhibition of MDM2 and MDMX protects cells from ferroptosis caused by all classes of FINs

To gain insight into the role(s) of MDM2 and MDMX in promoting ferroptotic cell death, we aimed to identify the point in this process that was affected by MDM2 and MDMX inhibition. This was accomplished by testing the impact of both MEL23 and the MDMX inhibitor on the response to other classes of FINs, which induce ferroptosis through different mechanisms, with the help of two Prives lab members, Everett Kengmana and Nicholas O'Brien (Fig 4.1B). Importantly, both compounds were able to suppress ferroptosis induced by all of the FINs, with the degree of rescue being the highest with class I FINs. Notably, these effects also did not require p53, although RSL3 was better suppressed in the presence of p53 (Figs 4.1C, 4.S1A-4.S1C). Thus, MDM2 and MDMX were not limited to promoting ferroptosis induced by system X_c^- inhibition; their roles extend to ferroptosis induced by all known mechanisms. We surmised that MDM2 and MDMX facilitate the lethal phospholipid peroxidation that is commonly affected by all four classes of FINs. Consistent with this conclusion, we confirmed that depletion of GSH, a characteristic of class I FINs, was not prevented by either of the MDM2 or MDMX inhibitors using an assay optimized in the Stockwell lab by Joleen Csuka (Figs 4.1D and 4.S1D). On the other hand, lipid peroxidation, which is a hallmark of all classes of FINs, was blocked by these same inhibitors (Figs 4.1E and 4.S1E). This

supports the likelihood that MDM2 and MDMX facilitate lipid peroxidation, a common requirement for all FINs.

In order to further examine the mechanism by which MDM2 and MDMX promote ferroptosis, we first focused on HT-1080 cells and their p53 KO derivatives. We used class I FINs to define the mechanism, as they showed the best suppression with MDM2-MDMX antagonists.

All classes of FINs are dependent on the presence of labile iron, as iron chelators are able to block ferroptosis (Stockwell et al. 2017). Using FIP1, a cellular FRET-based iron probe, Aron et al. reported that erastin treatment causes an increase in the cellular levels of labile iron, which are brought back to basal levels by co-treatment with the iron chelator DFO. On the other hand, fer-1 can block ferroptosis without changing labile iron levels (compared to erastin treatment alone), demonstrating that the reduction in iron levels is not the only means by which ferroptosis can be blocked (Aron et al. 2016). With the help of our collaborators, Allegra Aron and Christopher Chang, we obtained the FIP1 probe to test in our system. When FIP1 was used to test the impact of MDM2 and MDMX inhibition on iron levels, we found that, unlike DFO, neither MEL23 nor the MDMX inhibitor was able to lower the levels of labile iron in cells (Figs 4.1F and 4.S1F). This led us to conclude that, in order to promote ferroptosis, MDM2 and MDMX do not need to alter iron levels in cells, and that these compounds do not act like iron chelators.

4.2.4 MDM2 and MDMX prevent antioxidant responses during ferroptosis

4.2.4.1 MDM2 and MDMX alter the lipid metabolism of cells undergoing ferroptosis

Having ruled out the above mechanisms of suppressing ferroptosis, an untargeted lipidomic profiling was originally performed in collaboration with UC Denver's metabolic core headed by

Angelo D'Alessandro. Subsequently these results were further validated and extended in-house in the Stockwell lab, by Fereshteh Zandkarimi. We wanted to evaluate whether inhibition of MDM2 and MDMX changed the profile of lipids present in cells in order to disfavor lipid peroxidation. Co-treatment of cells with erastin and either MDM2 or MDMX inhibitors did indeed alter the lipid profile of cells. We observed two main trends in the lipid profile.

The first trend showed that these inhibitors caused an upregulation of the abundance of many lipid species, including phosphatidylcholines (PC), phosphatidylethanolamines (PE), and free fatty acids (FA) (Figs 4.2A and 4.S2A). This accumulation of lipids could indicate impaired catabolism, such as through β-oxidation. When there is incomplete β-oxidation, intermediate chain acyl carnitines (C5-C14) accumulate, while long chain acyl carnitines (C16-C22) are unaffected (Afshinnia et al. 2018), but we did not observe such an alteration (Figs 4.S2B and 4.S2C). Instead, in addition to C5 and C16 carnitines, others such as C2 carnitines (derived from acetyl CoA obtained by metabolic breakdown products) and C4 carnitines (derived from both amino acid and lipid catabolism) (Koves et al. 2008) were all increased in abundance upon MDM2-X inhibition. Additionally, when we blocked β-oxidation using etomoxir, which did indeed increase ferroptotic sensitivity as previously reported (Miess et al. 2018), there was no effect on the ability of MDM2/X antagonists to suppress ferroptosis (Fig 4.S2D). Therefore, we conclude that altered β-oxidation is not the sole effect of MDM2 and MDMX inhibition. Instead, we assume that blocking these proteins led both to increased lipid anabolism and impaired lipid catabolism, and that the altered levels of acyl-carnitines are simply markers of this global regulation of lipid metabolism.

In the lipid profile analysis, we observed a second trend pertaining to triacylglycerides. In fact, both triacylglycerides and diacylglycerides were upregulated upon erastin treatment, but were brought back to normal by the MDM2 and MDMX antagonists (Figs 4.2B and 4.S2E). Blocking diacylglycerol acyltransferase (DGAT) to lower the triacyl glyceride levels directly was not able to block ferroptosis (Figs 4.S2F and 4.S2G). Therefore, the altered levels of triacylglycerides can also be viewed as a casualty of the altered lipid metabolism due to MDM2-X inhibition.

We hypothesized that cells treated with MDM2 and MDMX antagonists may upregulate lipid metabolism pathways to combat oxidative stress. Among the upregulated lipids upon MDM2-X inhibition were monounsaturated lipids (Fig 4.2B), which were reported to be able to counteract ferroptosis (Magtanong et al. 2019). In a second line of evidence that is presented below, we also found the ability of MDM2-X to regulate another key component of anti-oxidant defense of cells, CoQ_{10}. Taken together, these lipidomic data led us to consider the possibility that one or more master regulators of lipids might be under the control of MDM2 and MDMX.

4.2.4.2 PPARα activity plays a key role in facilitating the abilities of MDM2 and MDMX to promote ferroptosis

In order to identify the candidate master regulator, we first examined if ferroptosis altered the localization of MDM2/X. We observed no consistent localization changes upon ferroptosis induction with erastin, or suppression using DFO, MEL23 and MDMX inhibitor (Fig 4.S3A).

We then examined some previously known targets of MDM2 that have potential links to lipid metabolism (Table 4.1). The knockdown of two such targets (DHFR or FANCD2) did not prevent the activity of MDM2/X antagonists in ferroptosis (Figs 4.S3B and 4.S3C).

Along with Nicholas A O'Brien in the Prives lab, we then evaluated the role of PPARα, a transcription factor whose activity has been previously reported to be regulated by MDM2 under some conditions (Gopinathan et al. 2009). In fact, the PPAR family of transcription factors are known to be involved in large-scale rewiring of lipid homeostasis, particularly in response to stress (Gervois et al. 2000; van Raalte et al. 2004; Kersten 2008). PPARα is also reported to regulate carnitine palmitoyl transferases to promote the formation of acyl-carnitines (Song et al. 2010; Chen, Wang, Huang, et al. 2017) and in fact, pharmacological fibrates that function by enhancing PPARα activity are frequently used as triglyceride-lowering drugs (Auwerx et al. 1996; van Raalte et al. 2004; Kersten 2008). Recently, it was also found that PPARα activation can promote the synthesis of monounsaturated fatty acids (Tian et al. 2020). Since we saw a decrease in abundance of triacylglycerides and an increase in abundance of acylcarnitines and monounsaturated fatty acids, in addition to large-scale changes to the lipid profile of cells treated with the MDM2 and MDMX antagonists, we hypothesized that this effect of MDM2 and MDMX on ferroptosis might be mediated by PPARα.

To test this, we evaluated whether altering PPARα activity altered the sensitivity of cells to ferroptosis. To this end, we used both a PPARα-specific agonist (pirinixic acid) and a PPARα antagonist (GW6471). We confirmed the effectiveness of these compounds by testing their respective effects on select transcriptional targets of PPARα (Figs 4.S4A and 4.S4B). In the p53

KO derivatives of both HT-1080 and SK-Hep1 cells, increased PPARα activity suppressed ferroptosis (Figs 4.2C and 4.2D), while decreased PPARα activity increased their sensitivity to ferroptosis (Figs 4.2E and 4.2F). Akin to the effect of the PPARα agonist, the ectopic overexpression of PPARα also suppressed ferroptotic death (Figs 4.S3D and 4.S3E). On the other hand, PPARγ antagonist (GW9662) was able to decrease the ferroptotic sensitivity (Figs 4.S4C and 4.S4D) in line with reports indicating that the α and γ isoforms of PPAR have opposing cellular functions (Kersten 2008). Despite a lot of effort, we were unable to eliminate the PPARα protein using RNA interference or CRISPR technology.

Nevertheless, we tested if MEL23 and MDMX inhibition were able to rescue ferroptosis when PPARα activity was reduced. Strikingly, in the absence of PPARα activity, neither MDM2-MDMX antagonist was effective in suppressing ferroptosis. As a control, the ability of fer-1 to inhibit ferroptosis was unaffected by the lack of PPARα activity (Figs 4.3A-C, 4.S4E-4.S4G). We verified that the effects seen were not due to increased toxicity of compounds, such that the combination of either MEL23 or the MDMX inhibitor with the PPARα antagonist did not significantly decrease viability (Figs 4.S4H and 4.S4I), nor did co-treatment with the antagonist result in any changes in the ability of the antagonists to block or ablate MDM2 and MDMX (Figs 4.3B, 4.3C, 4.S4E and 4.S4G). Importantly, both MEL23 and the MDMX inhibitor themselves acted as agonists of PPARα activity, as seen by the upregulation of known PPARα transcriptional targets (Figs 4.3D and 4.S5A). This corroborates the published report that MDM2 can regulate PPARα activity (Gopinathan et al. 2009), and also suggests that the MDM2-MDMX complex is able to regulate this activity.

The exact mode of regulation of PPARα activity by MDM2-X is nonetheless unclear. These MDM2/X antagonists did not significantly or consistently alter the protein levels of PPARα (Fig 4.S5B). Since PPARα is a transcription factor, nuclear exclusion could also alter its activity; we did not detect any change in localization of PPARα upon MDM2-X inhibition (Fig 4.S5D), even in the context of ferroptosis (Fig 4.S5C). This suggests that MDM2 and MDMX do not need to control the protein stability or nuclear localization of PPARα in order to regulate its transcriptional activity. On the other hand, both MDM2 and MDMX were detected when we immunoprecipitated PPARα, and this binding was not abrogated by the MDM2-X antagonists (Figs 4.3E, 4.S5E and 4.S5F). These results suggest that the MDM2-X complex may post-translationally modify PPARα and alter its activity without inducing its degradation or nuclear exclusion.

4.2.4.3 MDM2/X alter the antioxidant responses of cells through PPARα activity

We evaluated whether heightened PPARα activity under MDM2-X antagonistic conditions could enhance other key defenses of cells. Stockwell lab member, Fereshteh Zandkarimi measured the levels of CoQ_{10}, the lipophilic antioxidant. Treatment with MDM2-X antagonists elicited a markedly increased ratio of reduced to oxidized CoQ_{10} during ferroptosis (Figs 4.3F and 4.S5G). In fact, these inhibitors not only suppressed the reduction in the ratio resulting from erastin treatment, but enhanced it further beyond the levels of the vehicle control due to an increase in the levels of reduced CoQ_{10} (Fig 4.S5G right panel). This finding is in line with our hypothesis of large-scale rewiring of lipid metabolism caused by MDM2 and MDMX to favor pro-oxidant cellular pathways.

Further, as described in Chapter 1, FSP1/AIFM2 can block ferroptosis independent of GPX4 by increasing the amount of reduced CoQ_{10} (Bersuker et al. 2019; Doll et al. 2019). We found that MDM2/X inhibition causes an increase in FSP1 levels, which likely in turn regenerates reduced CoQ_{10} to block ferroptosis. We also observed that, in order to achieve the complete induction of FSP1 by MDM2-X inhibition, the full PPARα activity is required in either cell line (Figs 4.3G and 4.S5H).

These results thus indicate that lowered PPARα activity is a key conduit for MDM2/X to suppress the antioxidant defenses of cells and thereby promote ferroptosis. We provide a model in Fig 4.3H depicting our proposed scheme of the roles of MDM2 and MDMX in preventing the normal ability of cancer cells to resist the lipid peroxidation that drives ferroptosis.

4.3 Discussion

Our data show that MDM2 and MDMX control ferroptosis sensitivity through their ability to regulate lipid homeostasis. Blocking the MDM2-MDMX complex causes an accumulation of monounsaturated lipids and reduced CoQ_{10}, as well as changes in the abundance of acyl carnitines and tri/diacylglycerides. This indicates that inhibition of MDM2-MDMX complex activity leads to a coordinated rewiring of lipid metabolism to suppress ferroptosis. Of note, oleaginous microorganisms accumulate lipids in response to ROS (Shi et al. 2017), suggesting a similar stress response upon inhibition of MDMX and MDM2.

The increase in reduced CoQ_{10} due to altered regulation of FSP1 has also been shown to be a strong defense against lipid peroxidation (Bersuker et al. 2019; Doll et al. 2019). It is unlikely, however, that the increase in CoQ_{10} levels is the only means by which MDM2 and MDMX suppress ferroptosis, as MDM2 and MDMX inhibition also suppresses death induced by the class III FIN, FIN56, which can inhibit mevalonate pathway-derived CoQ_{10} production (Shimada et al. 2016). It is therefore probable that additional defenses against ferroptosis are upregulated in the absence of MDM2 and MDMX activity. Taken together, we assume that MDM2 and MDMX normally function to coordinate lipid metabolism, perhaps through one or more master regulators, in a manner that favors ferroptosis.

One such regulator is PPARα, the activity of which is modulated by the MDM2-MDMX antagonists and in turn this activity can mediate the role of MDM2 and MDMX in ferroptosis. Altered PPARα activity by MDM2 and MDMX disables the antioxidant defenses of cells, as well as effects other changes to the lipidome that together favor ferroptosis. The PPAR family of receptors, which are master regulators of cellular metabolism, particularly that of lipids, have been

implicated in several diseases (Tyagi et al. 2011). PPARα activity in particular has been targeted to control hyperlipidemia (Auwerx et al. 1996), but of direct relevance here, it has also been implicated in controlling oxidative homeostasis of cells with implications in inflammation (van Raalte et al. 2004; Tyagi et al. 2011). It was reported that MDM2 can regulate the transcriptional activity of PPARα, and the direction of regulation was dependent on their relative expression levels (Gopinathan et al. 2009). While the previous paper mainly focused on MDM2 behaving like a PPARα agonist, in our cell lines, both MDM2 and MDMX actually behave like PPARα antagonists and this is just one example of the complex nature of this regulatory mechanism.

Since our results indicate that MDM2 and MDMX do not alter the PPARα protein levels, their inhibitory effect on PPARα is not due to its degradation. Yet, the results with MEL23, which is an inhibitor of the E3 ligase activity of the MDM2-MDMX complex, suggests either the possibility that blocking ubiquitination of PPARα (but not its degradation) affects its activity, or that degradation of a regulator of PPARα leads to its altered activity. Given that MDM2 and MDMX associate with PPARα, it is more likely that its activity is kept at bay through ubiquitination by the MDM2-X complex. Future studies will hopefully illuminate better how MDM2 and MDMX control PPARα in cells undergoing ferroptosis.

There are numerous other proteins that can potentially be modulated to render cells susceptible to ferroptosis (Yang and Stockwell 2016), either through PPARα or independently. For example, FSP1 protein levels were still induced, albeit to a lesser degree, even when PPARα activity was inhibited. It is possible that the MDM2-X complex can also directly control the stability of FSP1, along with regulating its transcription through PPARα or that there are other target proteins

involved in this process. E3 ligase targets of MDM2, other than p53, have been discovered (Riley and Lozano 2012), but there are no confirmed targets of the MDM2-MDMX heterocomplex other than p53 and p21. Since we found that the role of the MDM2-MDMX complex in ferroptosis is independent of p53 and p21, other targets (as yet unknown) can likely mediate these effects on lipid metabolism. Our experiments indicated that some other known targets of MDM2, could actually be targets of the MDM2-X complex and have a role in ferroptosis, but are not involved in mediating the role of MDM2-X in ferroptosis. Identifying more targets of the MDM2-MDMX complex and especially those that can modulate the cellular lipid profile changes poses a substantial challenge for the future.

In the previous chapter we had a puzzling finding with MDMX overexpression, which suggests that MDMX may have additional MDM2-independent role(s) in promoting ferroptosis. Given that we now know the mechanism by which MDM2/X exert their effects on ferroptosis, we can suggest a potential explanation for this result. It is possible that MDMX can coordinate additional changes in lipid metabolism possibly through different master regulators. This is in agreement with a recent report showing that MDMX might control obesity in mice by preventing lipid accumulation (Kon et al. 2018).

Identifying the mechanism by which MDM2 and MDMX regulate ferroptosis may also provide some additional therapeutic benefits apart from those mentioned in the previous chapter. Some cancer therapies that activate p53 and cause unintended organ damage might be doing so through the induction of MDM2/X mediated ferroptosis in those organs. For example, some studies suggest that the cardiotoxicity associated with doxorubicin treatment for breast cancer, can be counteracted

with CoQ_{10} supplementation (Conklin 2005). Such therapies might benefit from combinations with ferroptosis inhibitors, to allow for higher doses of the therapy to be safely administered. Also, PPARα inducing fibrates that are already being used to treat patients with lipid based disorders (Auwerx et al. 1996; van Raalte et al. 2004), could potentially be used in treating disorders such as neurodegeneration and organ damage, which implicate ferroptosis as mentioned in the previous chapter. On the other hand, PPARα activity in tumors may also be a predictor of ferroptosis sensitivity. Thus, combining inhibitors of PPARα with FINs might enable targeting of ferroptosis-resistant cancers that display high PPARα activity.

4.4 Methods

4.4.1 Immunoblot

The same methodology as described in 2.4.5 was used except the lysis buffer was RIPA buffer (0.05M Tris-HCL pH:8.0, 0.5% Sodium deoxycholate, 0.1% SDS, 1% NP-40 and 0.15 M Sodium hydrochloride). PPARα was only detected when samples were lysed with RIPA buffer. Actin or GAPDH was used as the loading control.

The following primary antibodies were additionally used from those listed in 2.4.5 and 3.4.2: PPARα (H-2, Santa Cruz biotech cat# sc-398394 or Abcam cat# ab24509); GAPDH (CST cat# 5174S); FSP1 (mAB produced in Dr. Marcus Conrad's lab).

4.4.2 Chemicals

The following chemicals were additionally used apart from those listed in 2.4.3 and 3.4.3: PPARα agonist (Pirinixic acid, Selleckchem, cat# S8029), PPARα antagonist (GW6471, Santa Cruz Biotechnology, CAS 436159-64-7), PPARγ antagonist (GW9662, Santa Cruz Biotechnology, CAS 22978-25-2) and DGAT1 inhibitor (Cayman Chemicals A-922500). All compounds were dissolved in DMSO (Sigma-Aldrich, cat# D8418).

4.4.3 Transfection-siRNA

The same methodology and reagents as described in 2.4.6 and 3.4.4 was used, except for that TransIT-X2 Transfection Reagent (Mirus) was used instead of lipofectamine to lower the interference of exogenous lipids from altering the activity of PPARα.

4.4.4 Transfection- plasmids

The same methodology as described in 2.4.7 and 3.4.5 was used, except TransIT-X2 Transfection Reagent (Mirus) was used instead of lipofectamine for all experiments related to PPARα.

Full length PPARα plasmids were obtained from Origene (Myc-DDK-tagged-Human peroxisome proliferator-activated receptor alpha (PPARA), transcript variant 5, cat #RC216176).

4.4.5 Immunoprecipitation

The same methodology as described in 3.4.7 was used.

For PPARα IP: 1.5 million SK-HEP1 p53 KO cells or 1 million HT-1080 p53 KO cells were plated in 10 cm dishes. The next day they were treated with MDM2-X antagonistic drugs (MEL23, MDMX inhibitor) or DMSO control for 24 h before harvesting. RIPA lysis buffer was used for the steps described above. We used 4 μg of the H-2 (Santa Cruz biotech cat# sc-398394) or ab24509 (Abcam) antibodies against PPARα.

4.4.6 Cell viability assay

The same methodology as described in 3.4.8 was used.

4.4.7 Quantitative reverse transcription PCR

The same methodology as described in 2.4.4 was used.

Primer sequences:

L32 F: TTCCTGGTCCACAACGTCAAG, L32 R: TGTGAGCGATCTCGGCAC;

CPT1A F: ATC AAT CGG ACT CTG GAA ACG G, CPT1A R: TCA GGG AGT AGC GCA TGG T;

ACOX1 F: GGA ACT CAC CTT CGA GGC TTG, ACOX1 R: TTC CCC TTA GTG ATG AGC TGG;

ABCA1 F: TCA GAG ACG ACC CTG GAA GA, ABCA1 R: TGGCAAGGTACCATCTGAGG;

ECH1 F: TTC AAC AAG ATT TCG AGA GAC GC, ECH1 R: TCC TGG TAT CGA GTG ATG ATG T

4.4.8 Cell cycle analysis by flow cytometry

HT-1080 cells (3×10^5) were plated in each well of a 6-well plate and treated with compounds the next day. The cells were harvested using trypsin. The cell pellets were washed with phosphate buffered saline (PBS) and fixed/permeabilized with 50% ice-cold ethanol. The pellets were further washed with PBS and resuspended in PBS containing solution of 50 μg/ml ribonuclease A and 62.5 μg/ml propidium iodide (Sigma-Aldrich, St Louis, MO, USA). Samples were analyzed using FACSCalibur (Becton Dickinson, Franklin Lakes, NJ, USA). FlowJo Version 10.4.2 was used to determine the percent of cells in each stage of the cell cycle.

4.4.9 Reduced glutathione measurement

HT-1080 cells were plated in 10 cm dishes (2×10^6) and treated with compounds the next day. Cells were harvested and lysed using ice-cold PBS containing 0.5% Nonidet P-40. Samples were

centrifuged for 15 min at 4 °C at 13,000 g. The supernatant was deproteinized using a deproteinizing kit (ab2047080, Abcam) while on ice. Reduced GSH levels were determined using GSH/GSSG Ratio Detection Assay Kit (Fluorometric - Green) (ab138881, Abcam) following the manufacturer's protocol.

4.4.10 Measurement of Iron levels

The measurement of iron levels was performed using the iron probe developed by the lab of Dr. Christopher J Chang. The protocol described in Aron et al (Aron et al. 2016) for measuring the labile iron pool during erastin-induced ferroptosis was used for conducting the experiment and for the imaging approach. HT-1080 cells(2×10^4) were plated into each well of the 4-chambered cover glass slides. The following day, cells were treated with compounds for 4 h, then washed with HBSS. The cells with incubated with HBSS containing 2.5-5 μM of the iron probe for 90 min at 37 °C in the dark. The cells were then washed several times with HBSS before a second incubation with HBSS containing 1 μM of Hoescht 33342 (Thermo Fisher Scientific) for 10 min at 37 °C in the dark. The cells were again washed several times with HBSS and imaged using the 20X objective of a confocal microscope (LSM 700; Carl Zeiss). The cells thus were images after a total period of 6.5 h post compound treatment.

4.4.11 Lipid ROS measurement using C11-BODIPY 581/591

HT-1080 cells were plated in 6-well plates (3 x 10^5) and were treated with the compounds the following day for 6.5-7 h. Cells were harvested using trypsin and washed using HBSS. Cells were centrifuged briefly and the pellet was resuspended in HBSS containing 10 μM C11-BODIPY 581/591 (ThermoFisher) and incubated at 37 °C for 20 min. Fluorescence intensity was measured

on the FL1 and FL2 channels using FACSCalibur (Becton Dickinson, Franklin Lakes, NJ, USA). FlowJo Version 10.4.2 was used to generate the histograms and quantify the mean fluorescence intensity of the FL1 and FL2 channel. The intensity of FL1 channel was normalized to that of the FL2 channel to account for any differences in uptake of reagent due to compound treatment. A minimum of 2 x 10^4 cells was analyzed per condition.

4.4.12 Lipid profiling

Coenzyme Q_{10} detection and characterization: Mass spectrometry based targeted lipid profiling was done as previously described in (Kraft et al. 2020)

Lipid Profile Analysis used for estimation of lipids and acyl carnitines (UC Denver): Mass spectrometry based untargeted lipid profiling was done as previously described in (Reisz et al. 2019)

Lipid Profile Analysis used for estimation of triacyl and diacyl glycerides: Mass spectrometry based untargeted lipid profiling was done as previously described in (Zhang et al. 2019)

4.4.13 Statistical analysis

Prism (version 8, GraphPad) was used to make all the graphs in the paper and for performing all the statistical analysis shown. The GraphPad style (0.1234(ns), <0.0332(*), < 0.0021(**), <0.0002(***)) was used to represent the p values. The p values were calculated by ANOVA and appropriate multiple testing correction was done where required.

4.5 Tables

Table 4.1 Evaluation of key ferroptosis modulators and MDM2-associated proteins

In order to identify the mechanism of regulation of ferroptosis by MDM2/X, multiple proteins were tested for their roles as modulators of this pathway. Different known modulators of ferroptosis, as well as certain known targets of MDM2 with potential roles in ferroptosis were found to not modulate the roles of MDM2/X in ferroptosis.

Type of target	Target	Evaluation
Ferroptosis modulators	GPX4	Protein levels are not altered by MDM2/X antagonists.
	SLC7A11	
	FTH1	MDM2/X antagonists stabilize the protein, but role of FTH1 is unclear as MDM2/X antagonists do not lower labile iron levels during ferroptosis.
	Uptake of components of the serum	MDM2/X antagonists are able to suppress ferroptosis equally in media supplemented with either high or low levels of serum.
p53-independent MDM2 targets/MDM2-associated proteins with biological roles relevant to ferroptosis	DHFR	DHFR ablation or inhibition basally increases ferroptosis sensitivity. DHFR inhibitors Methotrexate and Pemtrexed seem to partially lower the ability of MDM2/X antagonists to block ferroptosis. But DHFR ablation has no effect on this ability.
	FANCD2	FANCD2 ablation increases basal ferroptosis sensitivity. MDM2/X antagonists do not seem to stabilize the protein, and FANCD2 ablation has no effect on the ability of MDM2/X antagonists to suppress ferroptosis.
	ATF3	ATF3 ablation increases basal ferroptosis sensitivity. MDM2/X antagonists stabilize the protein, but ATF3 ablation has no effect on the ability of MDM2/X antagonists to suppress ferroptosis.
	E2F1	MDM2/X antagonists do not stabilize these proteins.
	FOXO1,3	

4.6 Figures

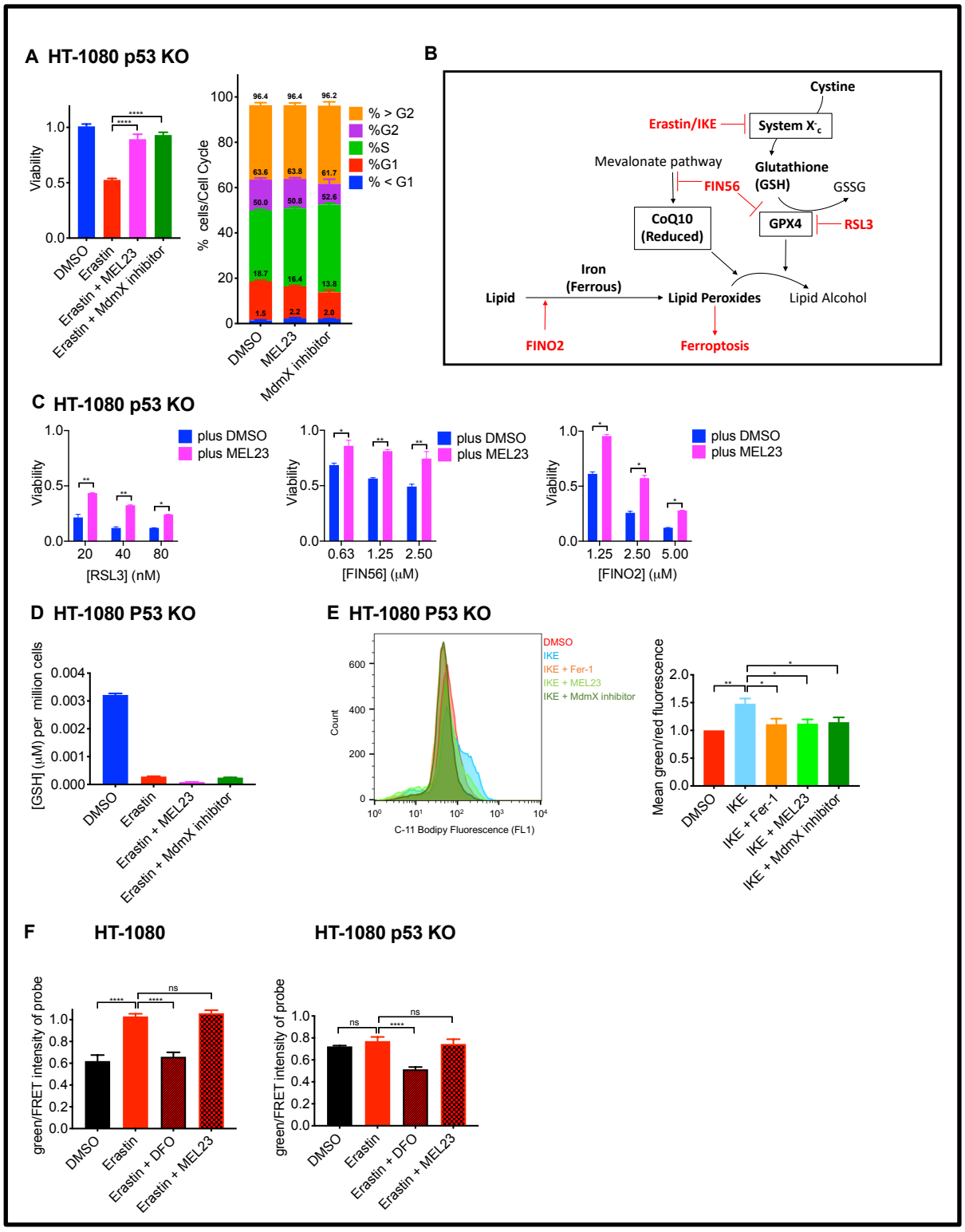
A HT-1080 p53 KO
Viability
DMSO
Erastin
Erastin + MEL23
Erastin + MdmX inhibitor
% cells/Cell Cycle
% > G2
%G2
%S
%G1
% < G1
MdmX inhibitor
B
Cystine
Erastin/IKE
System X-c
Mevalonate pathway
FIN56
Glutathione (GSH)
GSSG
CoQ10 (Reduced)
GPX4
RSL3
Iron (Ferrous)
Lipid
Lipid Peroxides
Lipid Alcohol
FINO2
Ferroptosis
C HT-1080 p53 KO
plus DMSO
plus MEL23
[RSL3] (nM)
[FIN56] (μM)
[FINO2] (μM)
D HT-1080 P53 KO
[GSH] (μM) per million cells
E HT-1080 P53 KO
DMSO
IKE
IKE + Fer-1
IKE + MEL23
IKE + MdmX inhibitor
Count
C-11 Bodipy Fluorescence (FL1)
Mean green/red fluorescence
F
HT-1080
HT-1080 p53 KO
green/FRET intensity of probe
Erastin + DFO
Erastin + MEL23

Figure 4.1 MDM2 and MDMX control a central checkpoint of ferroptosis

(A) The influence of MDM2 and MDMX antagonists (MEL23 and MDMX inhibitor) on the cell cycle profile of HT-1080 derived p53 KO cells after 7-8 h of treatment. The left panel shows the viability of cells treated for this duration with erastin (10μM) in combination with the antagonists. The right panel depicts the cell cycle profile assessed by flow cytometry using propidium iodide when cells were treated with the antagonists for this duration.

(B) Schematic depicting the previously established mechanisms of various FINs (Stockwell et al. 2017).

(C) Inhibitory effect of MEL23 on the response of HT-1080 derived p53 KO cells to various classes of FINs: RSL3, FIN56 and FINO2.

(D) Assessment of reduced glutathione levels in HT-1080 derived p53 KO cells treated with erastin, with or without MEL23 or MDMX inhibitor.

(E) Lipid ROS levels in HT-1080 derived p53 KO cells were measured by flow cytometry using C-11 Bodipy 581/591. The cells were treated with IKE in combination with either ferrostatin-1 or MDM2/X antagonists. The left panel represents the histogram showing the green fluorescence and the right panel represents the quantification of the normalized fluorescence.

(F) The levels of labile (ferrous) iron in HT-1080 derived cells were measured using the FIP-1 probe. The cells were treated with erastin, either alone or in combination with DFO or MEL23.

Cells in (C) were treated with drugs for 24 h. Cells in (D-F) were treated with erastin/IKE (10 μM) for 6.5 h. The data in left panel of (A) represent the mean ± SE for three independent experiments, and in right panel of (A) represent the mean ± SE for three biological replicates. The data in (C) represent the mean ± SE for two out of four independent experiments. The data in (D) represent

the mean ± SE for three biological replicates. The data in the right panel of (E) represent the mean ± SE for three independent experiments. The data in (F) is from one representative experiment out of three independent experiments. The data in (F) show the mean ± SE obtained from analyzing at least 100 different cells (from a minimum of five different fields) for each treatment condition. The viability data have been measured using ATP based CellTiter-Glo reagent and have been normalized to the DMSO control.

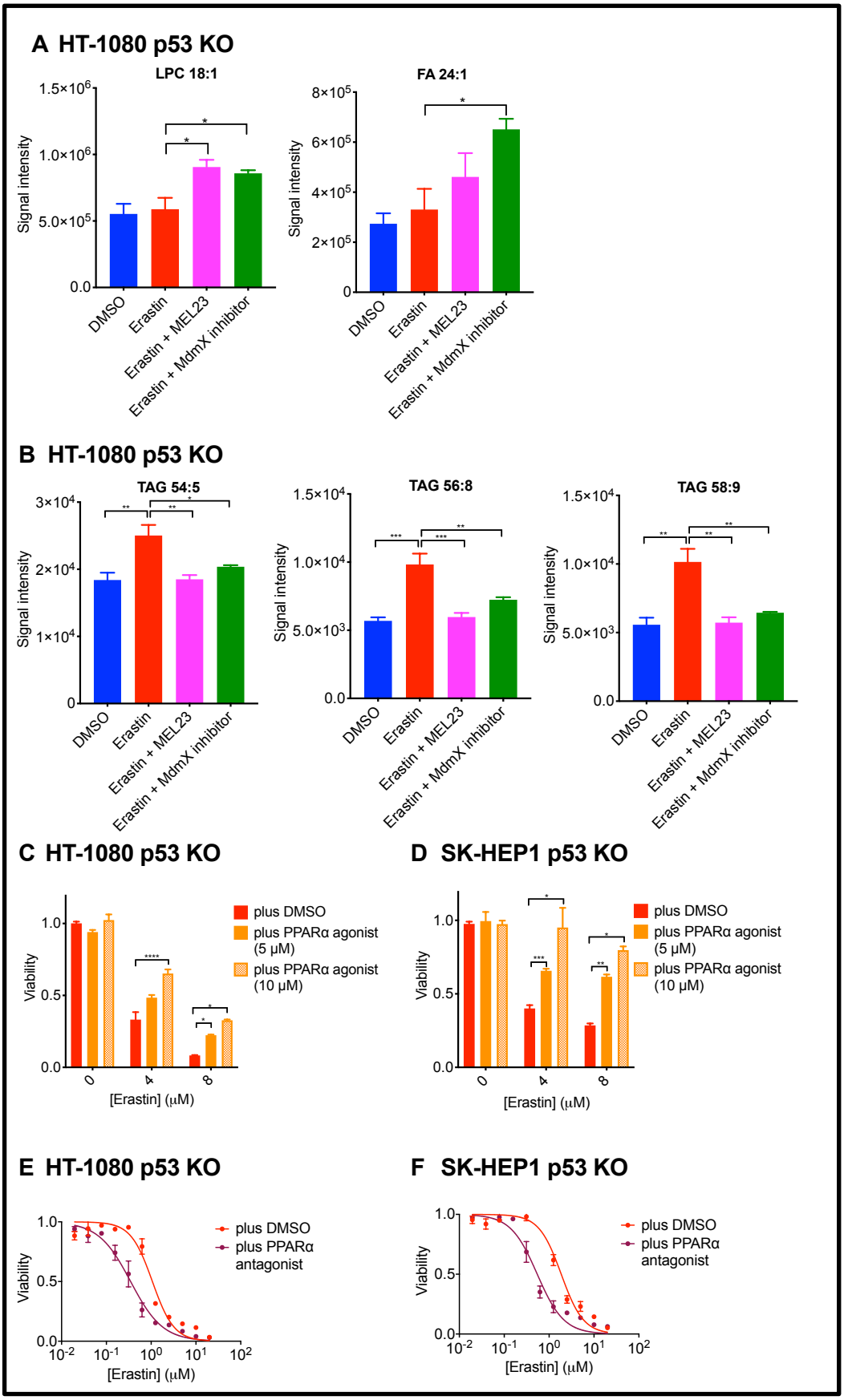
A HT-1080 p53 KO
LPC 18:1
FA 24:1
Signal intensity
DMSO
Erastin
Erastin + MEL23
Erastin + MdmX inhibitor
B HT-1080 p53 KO
TAG 54:5
TAG 56:8
TAG 58:9
C HT-1080 p53 KO
D SK-HEP1 p53 KO
Viability
plus DMSO
plus PPARα agonist (5 μM)
plus PPARα agonist (10 μM)
[Erastin] (μM)
E HT-1080 p53 KO
F SK-HEP1 p53 KO
plus PPARα antagonist

Figure 4.2 MDM2 and MDMX regulate lipid metabolism to favor ferroptosis

(A, B) Signal intensities of (A) lipids and (B) triacyl glycerides (TAG) in HT-1080 derived p53 KO cells were measured by LC-MS and analyzed as significantly altered by ANOVA. The cells were treated with erastin in combination with MDM2 and MDMX antagonists.

(C-F) The cell death due to erastin was assessed when PPARα activity was modulated using an agonist, pirinixic acid, or an antagonist, GW6471, in two different cell lines. Pirinixic acid blocks the lethal dose of erastin in (C) HT-1080 derived p53 KO cells and (D) SK-Hep1 derived p53 KO cells. GW6471 enhances the dose-response to erastin in (E) HT-1080 derived p53 KO cells and (F) SK-Hep1 derived p53 KO cells.

Cells in (A, B) were treated with erastin (10μM) for 6.5 h. Cells in (C, D) were treated with erastin and pirinixic acid for 16 h. Cells in (E, F) were treated with erastin for 24 h and with GW6471 for 48 h. The data in (A, B) represent the mean ± SE for three biological replicates. The data in (C, D) represent the mean ± SE for three or two of three independent experiments respectively. The data in (E, F) represent the mean ± SE for two out of four independent experiments. The viability data have been measured using ATP based CellTiter-Glo reagent and have been normalized to the DMSO control.

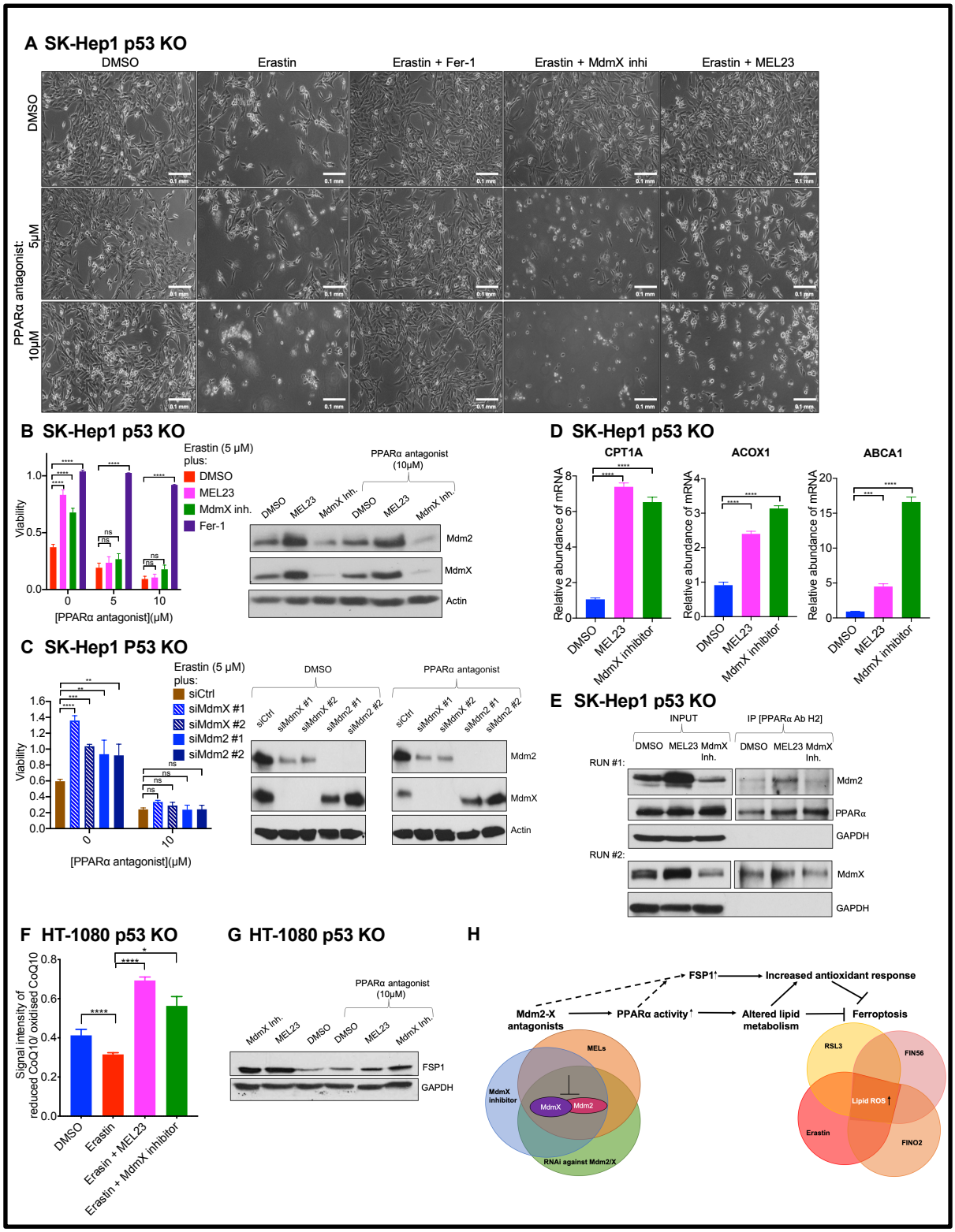

Figure 4.3 PPARα activity plays a key role in facilitating the abilities of MDM2 and MDMX to dampen the antioxidant responses of cells and promote ferroptosis

(A, B) Effect of PPARα antagonist GW6471 on the ability of MEL23, MDMX inhibitor, and fer-1 to block ferroptosis in SK-HEP1 derived p53 KO cells. (B) Left panel: the relative cell death due to erastin when in combination with these inhibitors and GW6471. (B) Right panel: the effect of MEL23 and MDMX inhibitor on the protein levels of MDM2 and MDMX is unaffected by cotreatment with GW6471. (A) Visualization of the aforementioned changes in cell viability at 10X magnification.

(C) PPARα antagonist GW6471 suppresses the ability of siMDMX and siMDM2 to block ferroptosis in SK-HEP1 derived p53 KO cells. Two different siRNAs (#1 and #2) were used against each protein and compared against a scrambled siRNA negative control (siCtrl). The right panel shows the corresponding decrease in the protein levels of MDM2 and MDMX upon RNA interference. The transfection was done using 20nM of siRNA in media with GW4671 and the cells were treated with drugs 24 h after transfection.

(D) MEL23 and MDMX inhibitor upregulate the mRNA levels of some known PPARα downstream targets in SK-HEP1 derived p53 KO cells.

(E) Immunoprecipitation using PPARα antibody in SK-HEP1 derived p53 KO cells shows binding to MDM2 and MDMX even under treatment with MDM2-X antagonists.

(F) Ratio of reduced to oxidized CoQ_{10} levels in HT-1080 derived p53 KO cells treated with erastin in combination with MDM2 and MDMX antagonists.

(G) PPARα activity modulates the levels and extent of increase of FSP1 protein in cells treated with the MDM2/X antagonists in HT-1080 p53 KO cells.

(H) Summary schematic depicting the hypothesized role of MDM2 and MDMX in ferroptosis.

Cells in (A-C, E, G) were treated with erastin/MEL23/MDMX inhibitor for 16 h and (A- C, G) also with GW6471 for 40 h. Cells in (D, F) were treated with erastin (10μM) for 6.5 h. The data in (B, C) represent the mean ± SE for three or two of three independent experiments respectively. The data in (D, F) represent the mean ± SE for three biological replicates. The viability data have been measured using ATP based CellTiter-Glo reagent and have been normalized to either the DMSO control or the GW6471 control respectively in (B), and to each transfection's respective control that is not treated with erastin in (C).

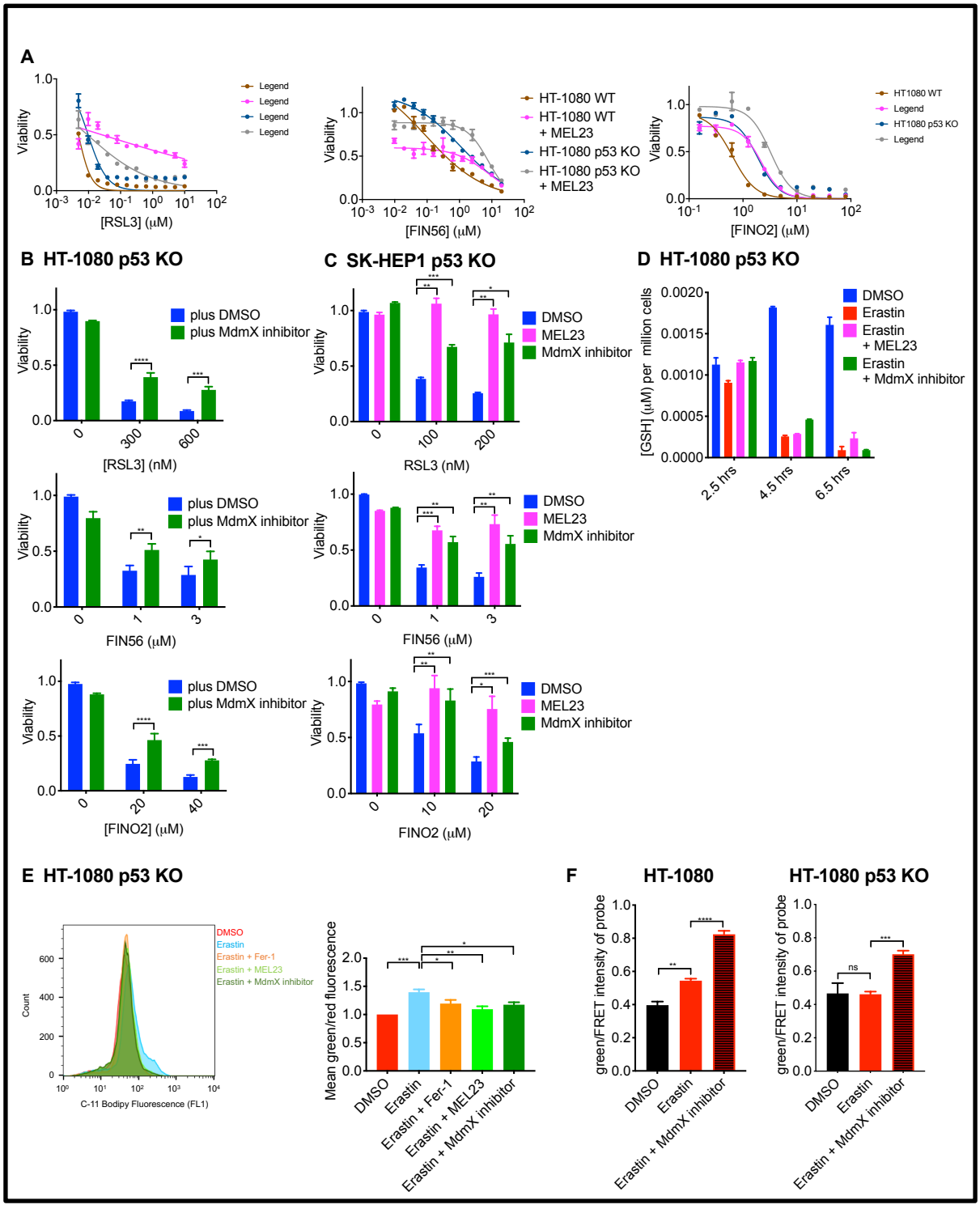

Figure 4.S1 The inhibition of MDM2 and MDMX suppresses ferroptosis induced by any of the four classes of FINs (Relating to Figure 4.2)

(A-C) Inhibitory effect of MDM2 and MDMX antagonists (MEL23, MDMX inhibitor) on the response of two different cell lines to various classes of FINs. HT-1080 derived cells have been treated with a combination of (A) MEL23 or (B) MDMX inhibitor, each with RSL3, FIN56 or FINO2 respectively. (C) SK-Hep1 derived cells have been treated with either MEL23 or MDMX inhibitor, each in combination with either RSL3, FIN56 or FINO2.

(D) Assessment of reduced glutathione levels of HT-1080 derived p53 KO cells over different time points (2.5, 4.5 and 6.5 h). The cells were treated with erastin with or without either MEL23 or MDMX inhibitor.

(E) Lipid ROS levels in HT-1080 derived p53 KO cells were measured by flow cytometry using C-11 Bodipy 581/591. The cells were treated with erastin in combination with either fer-1 or MDM2 and MDMX antagonists. The left panel represents the histogram showing the green fluorescence for one representative experiment and the right panel represents the quantification of the normalized fluorescence.

(F) The levels of labile (ferrous) iron levels in HT-1080 derived cells were measured using the FIP-1 probe. The cells were treated with erastin, either alone or in combination with MDMX inhibitor.

Cells in (A) were treated with drugs for 24 h. Cells in (B, C) were treated with drugs for 16 h. Cells in (D-F) were treated with erastin (10μM) for 6.5 h. The data in (A) represent the mean ± SE for two out of four independent experiments. The data in (B, C) represent the mean ± SE for two of three independent experiments. The data in (D) represent the mean ± SE for three biological replicates. The data in the right panel of (E) represent the mean ± SE for four independent experiments. The data in (F) show the mean ± SE obtained from analyzing at least 100 different

cells (from a minimum of five different fields) for each treatment condition and is one representative experiment out of three independent experiments. The viability data have been measured using ATP based CellTiter-Glo reagent and have been normalized to the DMSO control.

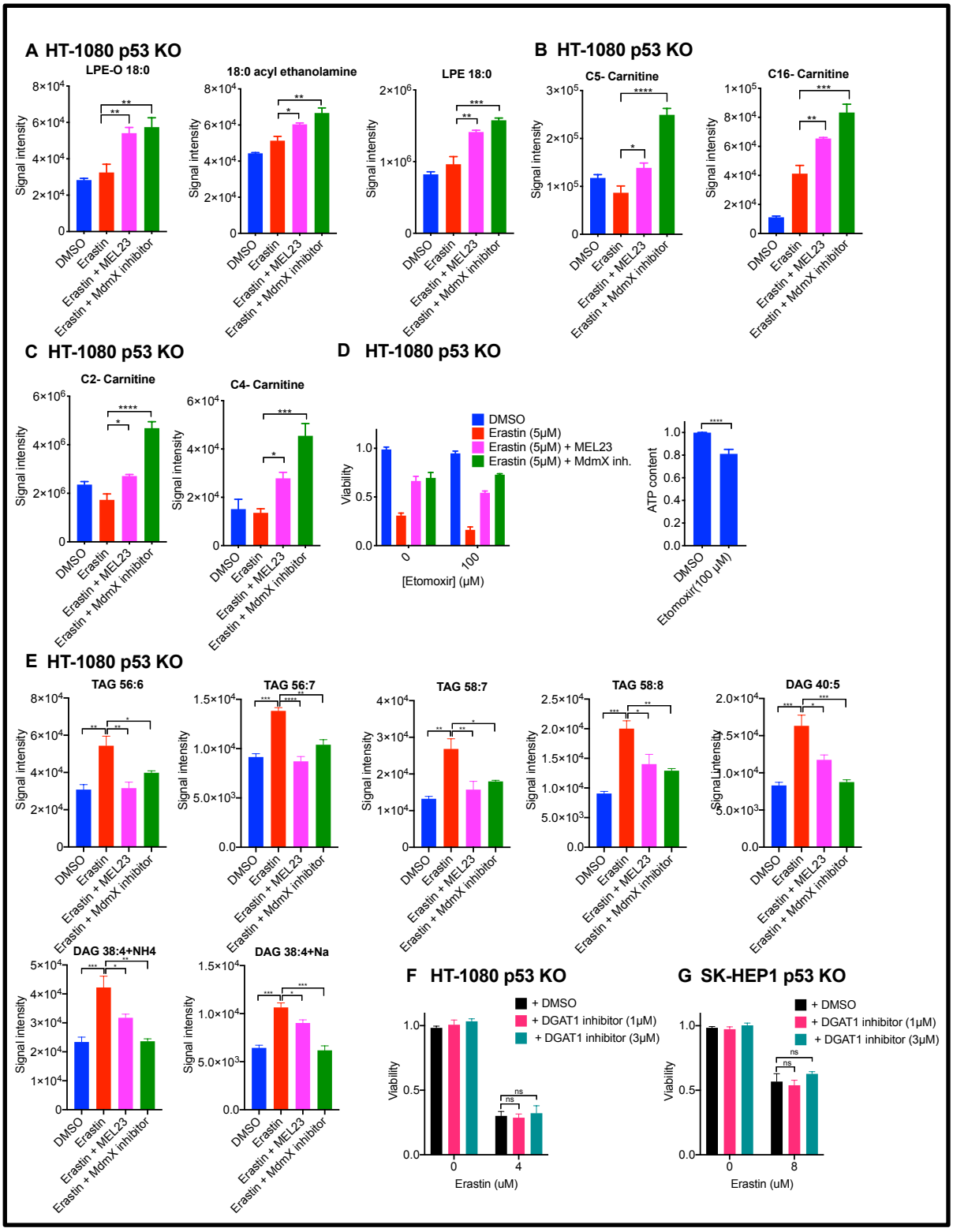
A HT-1080 p53 KO
LPE-O 18:0
18:0 acyl ethanolamine
LPE 18:0
B HT-1080 p53 KO
C5- Carnitine
C16- Carnitine
C HT-1080 p53 KO
C2- Carnitine
C4- Carnitine
D HT-1080 p53 KO
DMSO
Erastin (5μM)
Erastin (5μM) + MEL23
Erastin (5μM) + MdmX inh.
Viability
[Etomoxir] (μM)
ATP content
DMSO
Etomoxir(100 μM)
E HT-1080 p53 KO
TAG 56:6
TAG 56:7
TAG 58:7
TAG 58:8
DAG 40:5
DAG 38:4+NH4
DAG 38:4+Na
Signal intensity
DMSO
Erastin
Erastin + MEL23
Erastin + MdmX inhibitor
F HT-1080 p53 KO
+ DMSO
+ DGAT1 inhibitor (1μM)
+ DGAT1 inhibitor (3μM)
Viability
Erastin (uM)
G SK-HEP1 p53 KO
+ DMSO
+ DGAT1 inhibitor (1μM)
+ DGAT1 inhibitor (3μM)
Viability
Erastin (uM)

Figure 4.S2 MDM2 or MDMX inhibitors alter the abundance of various lipid species in cells undergoing ferroptosis (Relating to Figure 4.3)

(A-C, E) Signal intensities of (A) lipids, (B, C) acyl carnitines, (E) triacyl glycerides (TAG), and diacyl glycerides (DAG) in HT-1080 derived p53 KO cells were measured by LC-MS and analyzed as significantly altered by ANOVA. The cells were treated with erastin in combination with MDM2 and MDMX antagonists.

(D) The β-oxidation inhibitor, etomoxir does not block the ferroptotic activity of MEL23 or MDMX inhibitor in HT-1080 derived p53 KO cells. Right panel- etomoxir lowers the ATP content of cells, as previously reported.

(F, G) The DGAT1 inhibitor (A-922500) does not alter the ferroptotic sensitivity of (F) HT-1080 derived p53 KO cells and (G) SK-HEP1 derived p53 KO cells.

Cells in (A-C, E) were treated with erastin (10μM) for 6.5 h. Cells in (D, F, G) were treated with erastin for 16 h and (F, G) were also treated with the inhibitor for the same time. The data in (A-C, E) represent the mean ± SE for three biological replicates. The data in (D, F, G) represent the mean ± SE for two independent experiments. The viability data in (D) have been measured using PrestoBlue reagent and in (F, G) ATP based CellTiter-Glo reagent. The viability data have been normalized to the DMSO control.

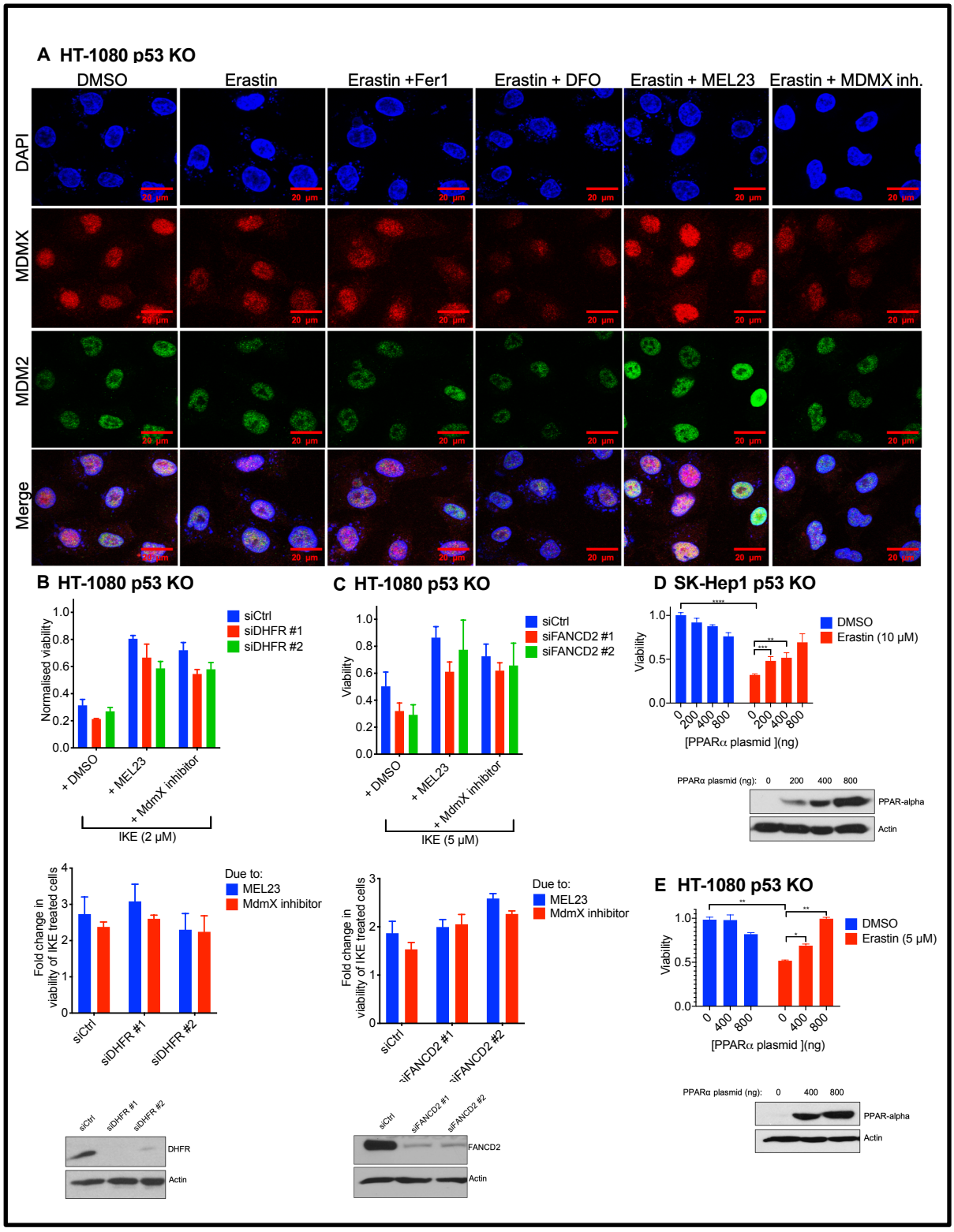
A HT-1080 p53 KO
DMSO
Erastin
Erastin +Fer1
Erastin + DFO
Erastin + MEL23
Erastin + MDMX inh.
DAPI
MDMX
MDM2
Merge
20 µm
B HT-1080 p53 KO
Normalised viability
siCtrl
siDHFR #1
siDHFR #2
+ DMSO
+ MEL23
+ MdmX inhibitor
IKE (2 µM)
Fold change in viability of IKE treated cells
Due to:
MEL23
MdmX inhibitor
DHFR
Actin
C HT-1080 p53 KO
Viability
siCtrl
siFANCD2 #1
siFANCD2 #2
IKE (5 µM)
FANCD2
Actin
D SK-Hep1 p53 KO
DMSO
Erastin (10 µM)
[PPARα plasmid](ng)
PPARα plasmid (ng): 0 200 400 800
PPAR-alpha
Actin
E HT-1080 p53 KO
DMSO
Erastin (5 µM)
[PPARα plasmid](ng)
PPARα plasmid (ng): 0 400 800
PPAR-alpha
Actin

Figure 4.S3 PPARα, but not DHFR or FANCD2, mediates the role of MDM2 and MDMX in ferroptosis (Relating to Figure 4.3)

(A) The localization pattern of MDM2 and MDMX was visualized at 20X magnification. DAPI was used to label the nucleus.

(B, C) Knockdown of (B) DHFR or (C) FANCD2 does not significantly suppress the ability of MEL23 or the MDMX inhibitor to block ferroptosis. The top panel shows the viability changes under the various conditions. The middle panel highlights the change in fold change of cell death due to ferroptosis when co treated with the MDM2-X antagonists. The bottom panel depicts the corresponding decrease in the protein levels of DHFR/FANCD2 upon RNA interference. The transfection was done using 20nM of siRNA. The cells were treated with drugs 24 h after transfection.

(D, E) PPARα overexpression suppresses ferroptosis in (D) SK-HEP1 derived p53 KO cells and (E) HT-1080 derived p53 KO cells. The top panels show the effect of PPARα overexpression on the cell death response to erastin. The bottom panels show the corresponding expression levels of PPARα in the cells.

Cells in (A) were treated with erastin (10μM) for 6.5 h. Cells in (B, C) were treated with IKE for 18 h. Cells in (D, E) were treated with erastin for 16 h. The data in (A) show one representative experiment of three independent experiments. The data in (B, C) represent the mean ± SE for two independent experiments. The data in (D, E) represent the mean ± SE for two of three independent experiments. The viability data have been measured using ATP based CellTiter-Glo reagent and have been normalized to each transfection's respective control that is not treated with erastin.

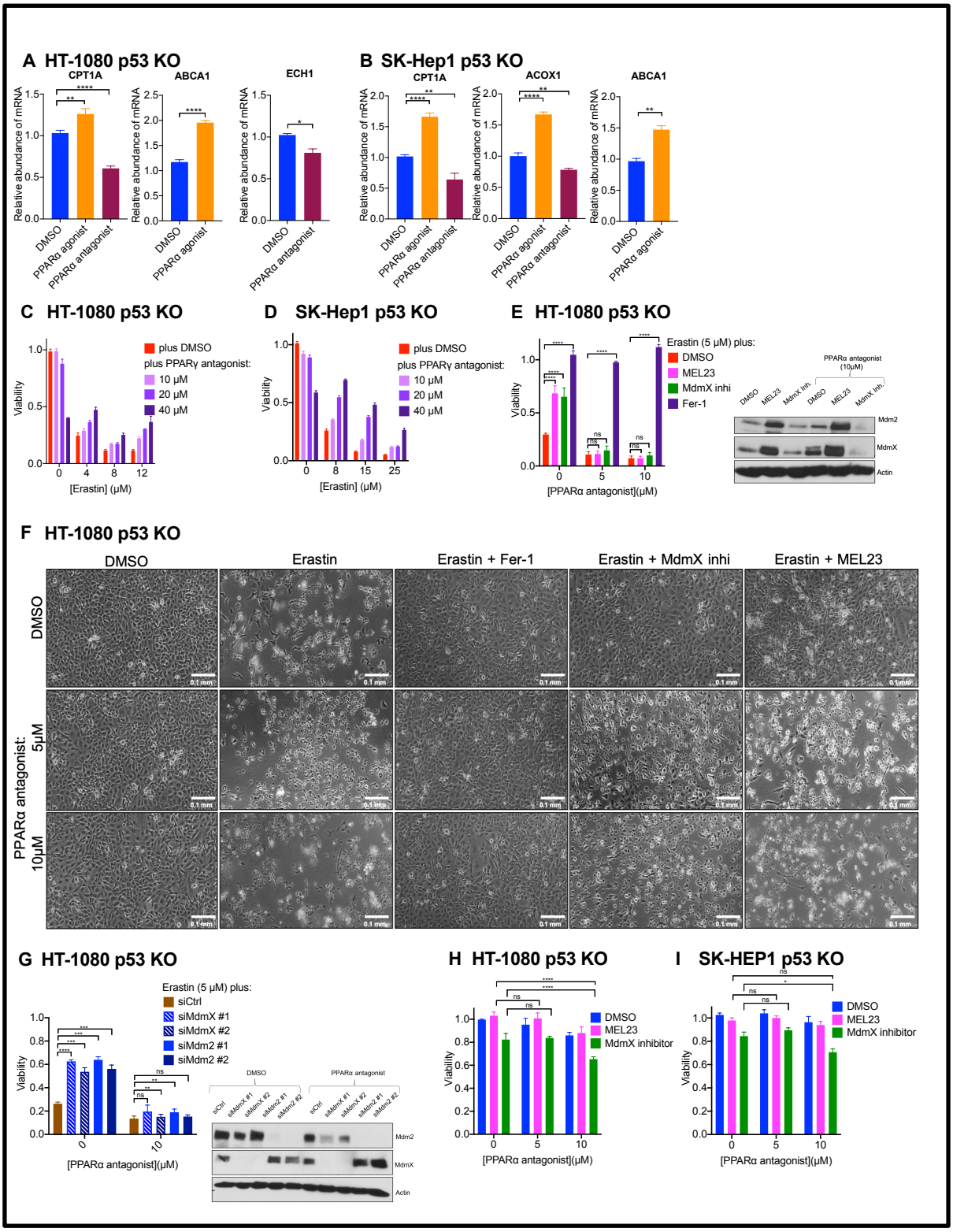
A HT-1080 p53 KO
CPT1A
ABCA1
ECH1
Relative abundance of mRNA
DMSO
PPARα agonist
PPARα antagonist
B SK-Hep1 p53 KO
CPT1A
ACOX1
ABCA1
C HT-1080 p53 KO
plus DMSO
plus PPARγ antagonist:
10 μM
20 μM
40 μM
Viability
[Erastin] (μM)
D SK-Hep1 p53 KO
E HT-1080 p53 KO
Erastin (5 μM) plus:
DMSO
MEL23
MdmX inhi
Fer-1
[PPARα antagonist](μM)
PPARα antagonist (10μM)
MdmX inh.
Mdm2
MdmX
Actin
F HT-1080 p53 KO
DMSO
Erastin
Erastin + Fer-1
Erastin + MdmX inhi
Erastin + MEL23
PPARα antagonist:
5μM
10μM
G HT-1080 p53 KO
Erastin (5 μM) plus:
siCtrl
siMdmX #1
siMdmX #2
siMdm2 #1
siMdm2 #2
[PPARα antagonist](μM)
H HT-1080 p53 KO
MdmX inhibitor
I SK-HEP1 p53 KO

Figure 4.S4 MDM2 and MDMX behave as antagonists of PPARα in order to promote ferroptosis (Relating to Figure 4.4)

(A, B) The change in the mRNA levels of some known PPARα downstream targets by the PPARα agonist, pirinixic acid, and the PPARα antagonist, GW6471, in (A) HT-1080 derived p53 KO cells and (B) SK-Hep1 derived p53 KO cells.

(C, D) The PPAR γ antagonist (GW9662) blocks ferroptosis in a concentration dependent manner in both (C) HT-1080 derived p53 KO cells and (D) SK-HEP1 derived p53 KO cells.

(E, F) Effect of PPARα antagonist GW6471 on the ability of MEL23, MDMX inhibitor, and fer-1 to block ferroptosis in HT-1080 derived p53 KO cells. (E) Left panel: The relative cell death due to erastin when in combination with GW6471 and either MEL23, MDMX inhibitor, or fer-1. (E) Right panel: The effect of MEL23 and MDMX inhibitor on the protein levels of MDM2 and MDMX is unaffected by co-treatment with GW6471. (F) Visualization of the aforementioned changes in cell viability at 10X magnification.

(G) PPARα antagonist GW6471 suppresses the ability of siMDMX and siMDM2 to block ferroptosis in HT-1080 derived p53 KO cells. Two different siRNAs (#1 and #2) were used against each protein and compared against a scrambled siRNA negative control (siCtrl). The right panel shows the corresponding decrease in the protein levels of MDM2 and MDMX upon RNA interference. The transfection was done using 20nM of siRNA in media containing GW4671. The cells were treated with drugs 24 h after transfection.

(H, I) PPARα antagonist GW6471 only slightly increases the basal toxicity when co-treated with either MEL23 or MDMX inhibitor in (H) HT-1080 derived p53 KO and (I) SK-HEP1 derived p53 KO cells.

Cells in (A, B) were treated with pirinixic acid (10μM) for 24 h and with GW6471 (10μM) for 40 h. Cells in (C-I) were treated with erastin for 16 h and also treated with GW9662/GW6471 for 40 h. The data in (A, B) represent the mean ± SE for three biological replicates. The data in (C, D) represent the mean ± SD for one representative of three independent experiments. The data in (E, G-I) represent the mean ± SE for three independent experiments.

The viability data have been measured using ATP based CellTiter-Glo reagent and have been normalized to either the DMSO control or the GW6471 control respectively in (E), to each transfection's respective control that is not treated with erastin in (G), and to the DMSO control in (C, D, H, I).

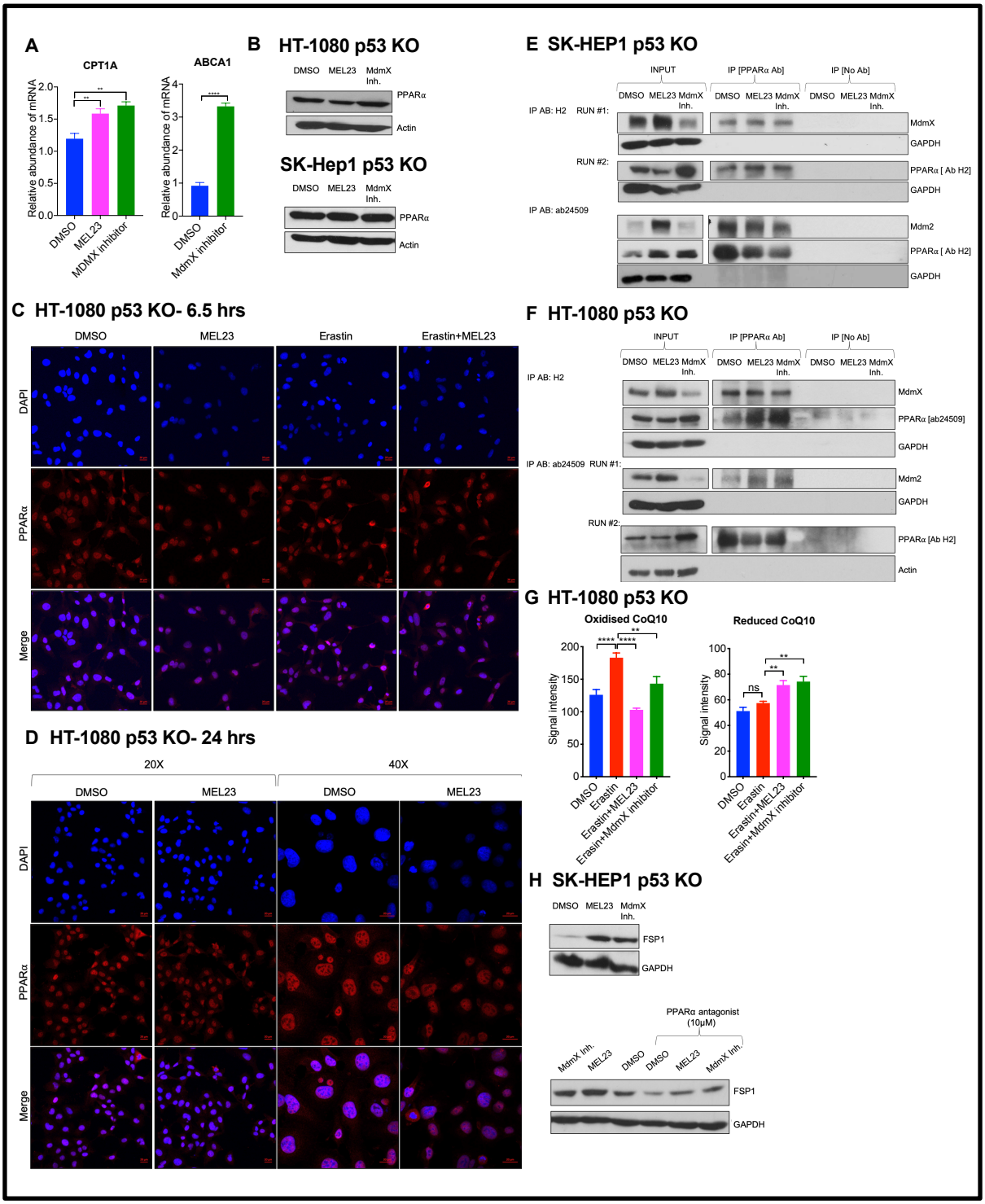
A
CPT1A
ABCA1
Relative abundance of mRNA
DMSO
MEL23
MDMX inhibitor
MdmX inhibitor
B HT-1080 p53 KO
DMSO MEL23 MdmX Inh.
PPARα
Actin
SK-Hep1 p53 KO
C HT-1080 p53 KO- 6.5 hrs
DMSO
MEL23
Erastin
Erastin+MEL23
DAPI
PPARα
Merge
D HT-1080 p53 KO- 24 hrs
20X
40X
E SK-HEP1 p53 KO
INPUT
IP [PPARα Ab]
IP [No Ab]
IP AB: H2
RUN #1:
RUN #2:
MdmX
GAPDH
PPARα [Ab H2]
IP AB: ab24509
Mdm2
F HT-1080 p53 KO
PPARα [ab24509]
PPARα [Ab H2]
Actin
G HT-1080 p53 KO
Oxidised CoQ10
Reduced CoQ10
Signal intensity
ns
Erastin
Erastin+MEL23
Erasin+MdmX inhibitor
H SK-HEP1 p53 KO
FSP1
PPARα antagonist (10μM)
MdmX Inh.

Figure 4.S5 Inhibition of MDM2/X does not need to alter the stability or localization of PPARα in order to limit its ability to promote antioxidant defenses against ferroptosis (Relating to Figure 4.3)

(A) MEL23 and MDMX inhibitor upregulate the mRNA levels of some of the known PPARα downstream targets in HT-1080 derived p53 KO cells.

(B) MEL23 and MDMX inhibitor, do not significantly or consistently alter the levels of PPARα. Note that PPARα protein levels tend to vary between experiments.

(C, D) The localization pattern of PPARα was visualized under treatment conditions. DAPI was used to label the nucleus. (C) 20X magnification was used and the cells were treated for 6.5 h in the context of ferroptosis. (D) Cells under MEL23 treatment were also examined at 24 h post treatment at both 20X and 40X magnifications.

(E, F) Immunoprecipitation using two different PPARα antibodies in (E) SK-HEP1 derived p53 KO cells and (F) HT-1080 derived p53 KO cells shows binding to MDM2 and MDMX even under treatment with MDM2-X antagonists. The condition with no antibody represents the IgG control to show the specificity of the binding.

(G) The levels of CoQ_{10} in HT-1080 derived p53 KO cells was measured by LC-MS. The cells were treated with erastin in combination with MDM2 and MDMX antagonists. The left panel depicts the levels of the oxidized form of CoQ_{10} while the right panels shows the levels of the reduced form of CoQ_{10} under these treatment conditions.

(H) PPARα activity modulates the levels and extent of increase of FSP1 protein in cells treated with the MDM2/X antagonists in SK-HEP1 p53 KO cells. The top panel shows the increase in FSP1 levels due to MDM2/X antagonists and the bottom panel compares the change in FSP1 levels due to the MDM2/X antagonist with or without the addition of the PPARα antagonists (GW6471).

Cells in (A, G) were treated with the drugs for 6.5 h. Cells in (B, E, F, H) were treated with MEL23 or MDMX inhibitor for 16 h and lower panel of (H) also with GW6471 for 40 h . The data in (A, G) represent the mean ± SE for three biological replicates.

Chapter 5: Perspectives and future directions

Multiple reports have demonstrated the importance of p53 in determining the extent of cancerous death through ferroptosis. In this dissertation we take an alternative route to examine the relevance of p53 to ferroptosis. Instead of examining the direct effect of presence or absence of p53 on the ferroptotic sensitivity of cancer cells, we have focused on evaluating the ability of other proteins in the p53 network to modulate ferroptosis. The original aim of this project was two pronged: one, to identify downstream targets of p53 that can alter the rate of ferroptosis; two, to then use that knowledge to unravel the complexity in defining the direction of regulation of ferroptosis by p53. We were indeed successful in identifying three proteins of the p53 network, namely p21, MDM2 and MDMX, which can modulate ferroptosis. While Chapter 2 describes p21 as a potential conduit of the suppressive roles of p53 on ferroptosis, Chapters 3 and 4 mainly show a p53-independent pro-ferroptotic role for MDM2 and MDMX. Chapters 3 and 4, do suggest that MDM2/X might be able to mediate the ability of p53 to promote ferroptosis, at least in some settings. Nevertheless, the second aim of the project does not yet have a clear answer. In the future, we need to compare the levels or activities of MDM2/X and p21 in various contexts to evaluate if either can determine the extent of ferroptosis upon perturbation to p53 levels. Based on the availability of substrates and in co-operation with other ferroptosis modulators, it is more likely that p53 activates different or multiple targets, that together determine the final effect on ferroptosis. Therefore, there is need to identify more members of the p53 network with roles in ferroptosis, in order to fully satisfy this goal.

Chapters 3 and 4 also add to the growing literature regarding p53-independent roles of MDM2, MDMX and especially the MDM2-X complex. While being novel, it is in line with the previous

reports highlighted in Chapter 1 that demonstrate the abilities of MDM2 and MDMX to regulate cellular metabolism independent of p53. Particularly, our work demonstrates a molecular pathway to further the suggested role of MDM2/X in being capable of altering the cellular lipid metabolism.

In addition, we have uncovered MDM2, MDMX and PPARα as the upstream regulators of the newly discovered ferroptosis suppressor, FSP1. This finding suggests that perhaps, many of the regulators listed in Chapter 1, could have more of a crosstalk and interdependence than we currently appreciate. In the future, when more regulators of ferroptosis are uncovered due to ongoing research efforts, a more comprehensive molecular map of the drivers of ferroptosis can be developed.

In order to better understand the p53-independent roles of MDM2-X complex in ferroptosis, as well as in regulating other aspects of cell survival, the most important next step of this project lies in uncovering new targets of the complex that are independent of p53. This includes both direct ubiquitination targets of the MDM2-X complex as well as its binding partners outside the context of p53. Strategies to identify such targets will be discussed in the sections below.

5.1 A role for p53 target genes in mediating ferroptosis

Owing to our discovery in Chapter 3, that MDM2 and its E3 ligase activity are key promoters of ferroptosis, one of the results in Chapter 2 assumes more importance. In Chapter 2, upon ferroptosis induction a reduction in the protein levels of the E3 ligase targets of MDM2 (p53, p21 and MDM2 itself) was observed only in the sensitive cells. This reduction was suppressed by the use of MEL23, the inhibitor of the E3 ligase activity of MDM2 that also blocked ferroptosis. On

the other hand, in ferroptosis-resistant cells, p53 and p21 accumulated and this is potentially an indication of suppressed MDM2 E3 ligase activity, which could be contributing to their resistance. These results taken together with the apparent dephosphorylation of MDM2 observed in sensitive cells due to FIN treatment, suggest that MDM2 E3 ligase activity is hyperactive in cells sensitive to ferroptosis. The possibility that FINs actually lead to this activation since this activity is needed to promote ferroptosis, is very pertinent at this point.

First, the change in the phosphorylation status of MDM2 upon ferroptosis induction needs to be confirmed in order to further explore this hypothesis. While it is well known that phosphorylation of MDM2 can alter its activity and stability, the phosphorylated residue dictates the type of alteration. Different upstream effectors are responsible for the phosphorylation of MDM2 at specific residues (Chen 2012). For example, DNA damage can lead to the phosphorylation of MDM2 at various sites through different downstream sensors, in order to compromise the ability of MDM2 to regulate p53 in multiple ways. While the phosphorylation at S395 through ATM inhibits the E3 ligase activity of MDM2 (Maya et al. 2001), the phosphorylation at S407 through ATR can prevent MDM2-mediated nuclear export of p53 (Shinozaki et al. 2003) and the phosphorylation at Y394 through c-Abl blocks both these functions of MDM2 against p53 (Sionov et al. 2001). On the other hand, phosphorylation of the serines in the acidic domain of MDM2 through mediators such as GSK3 can enhance the degradation of p53 without directly affecting the E3 ligase activity of MDM2. Thus, this role of GSK3 is downregulated upon DNA damage (Blattner et al. 2002; Kulikov, Boehme, and Blattner 2005).

MDMX phosphorylation can also play a role in determining the E3 ligase activity of the MDM2-X heterocomplex. For example, Chk-2 phosphorylation in proximity of the RING domain of MDMX can enhance MDM2-X heterodimerization and hence activity (Chen et al. 2005). Conversely, WIP1 can dephosphorylate MDM2 at S395 to enhance its E3 ligase activity. Interestingly, if WIP1 dephosphorylates MDMX, then it has the opposite effect of lowering the MDM2-X heterocomplex formation (Chen 2012).

Based on our data with the 2A10 antibody, we have some evidence that MDM2 is dephosphorylated on the S395 position upon ferroptosis induction. This needs to validated using site-specific phosphorylation antibodies, as well as mass-spectrometry-based protein studies. It will also be important to determine whether ferroptosis can lead to changes in the phosphorylation status of MDMX and if so, at what position(s). Identifying the site(s) of phosphorylation may also shed light on upstream modulators that might respond to FINs and in turn activate MDM2.

Second, it is yet unclear if the changes in MDM2/X phosphorylation status have any direct relevance to the ability of MDM2/X to promote ferroptosis. We had some preliminary data (data not shown) that an inhibitor of WIP1 can promote ferroptosis. This was counter-intuitive, since inhibition of WIP1-mediated MDM2 dephosphorylation would be expected to block ferroptosis. But this result suggests that in this context, WIP1 may favor MDMX dephosphorylation, the inhibition of which could then promote complex formation and hence ferroptosis. The extent of formation of the MDM2-X heterocomplex needs to be assessed in cells treated with this WIP1 inhibitor to confirm that the effect is specific to the MDM2-X E3 ligase activity. Further, the effects of MDM2/X mutants, with altered ability to undergo phosphorylation, on the ferroptosis sensitivity

of cancer cells need to be evaluated. These variants would be mutated at the identified phosphorylation sites to either be resistant to phosphorylation or be constitutively phosphorylated.

Finally, the phosphorylation status of MDM2/X needs to be assessed using ferroptosis inhibitors that inhibit the various stages of the ferroptosis pathway, in order to determine which checkpoint is involved in this alteration and if it could possibly be key to triggering excessive death.

5.2 MDM2 and MDMX promote ferroptosis in a p53-independent manner

Our findings in Chapter 3 used multiple approaches (small molecule and genetic) in various contexts to show that MDM2 and MDMX are bona fide regulators of ferroptosis. While this indicates the robustness of this regulation, we are unaware if it is context-specific. Since we used cancer cell lines derived from different tissues of origin (even those without a MDM2/X amplification), this argues against a clear contextual effect. Nevertheless, it is important to extend this analysis to other cancer cell lines, both with and without p53. The key question is, can we use techniques to enhance MDM2-X activity? for example, can MDMX overexpression be a tool to convert some of the ferroptosis-resistant cells identified in Chapter 2, to be more responsive to ferroptosis?

In line with this, it is also important to evaluate whether MDM2-X can be used as biomarkers of ferroptosis across tumors. While our results with glioblastoma patient models provide one context while this would be true, we did not observe a strong correlation between the expression levels of *MDM2/X* and the ferroptosis sensitivity of NC1-60 cancer cell lines (data not shown). The limitation of this analysis is that the expression levels were represented by mRNA levels and they may not always correlate with protein levels. Proteomic analyses of cancers are necessary to be

able to reach firmer conclusions. Additionally, we do not yet have a quantitative assay to measure the E3 ligase activity of MDM2-X complex, which might serve as a better biomarker in various contexts. While a luciferase-based reporter assay was used in the discovery of the MELs, this only measured the E3 ligase activity of ectopic constructs. Instead, a reporter assay based on the use of exogenously provided tagged-substrates of the E3 ligase activity could enable the measurement of endogenous activity. Developing such an assay would be a substantial challenge for future studies.

Regarding the E3 ligase activity of the MDM2-X complex, while our data does indicate that it is important for ferroptosis, we were limited by the available tools to determine the extent of its requirement for the role of MDM2 and MDMX in ferroptosis. There is a need to develop more inhibitors of this activity that do not affect complex formation, as MELs are the only such inhibitors available currently. The other inhibitors of the E3 ligase activity of the complex do so either by inhibiting the formation of the complex (E.g.: MMRi compounds) or are only known to affect the E3 ligase activity of MDM2 without necessarily being specific towards that of the MDM2-X complex (E.g.: HLI98, Sempervine). Additionally, the exact molecular mechanism of inhibition by MEL23 or the precise binding site is also unclear. Biophysical studies to minimally determine the binding of MELs to MDM2-X are needed to better understand the complex's role in ferroptosis. Further, it has not yet been established whether MELs can inhibit protein-protein interactions of the complex that are independent of its E3 ligase activity. The main bottleneck here is the lack of known binding partners of the MDM2-X complex outside the context of p53. We need to perform affinity-based proteomic studies to identify binding partners of the MDM2-X complex to truly assess the extent of impact of the MELs on the biological roles of MDM2 and MDMX.

5.3 MDM2/X lower PPARα activity to dampen the antioxidant defenses of cells against ferroptosis

We identified PPARα and PPARɣ as new regulators of ferroptosis in Chapter 4, and these seem to function in opposition to each other. It is not yet clear if their effects are truly independent of each other, as they are known to have cross-talk at times (Song et al. 2010; Kersten 2008). An earlier report did indicate that PPARɣ stability can be regulated by MDM2 through Neddylation (Park et al. 2016). But another report showed that MDM2 seems to alter the activity of PPARα but not PPARɣ (Gopinathan et al. 2009). These contrasting reports suggest two things that can be evaluated in our context: (1) MDM2/X may control the activity of PPARα through NEDDylation, which can be assessed using NEDDylation inhibitors and a NEDDylation assay, (2) even though the agonistic/antagonistic molecules of PPARα and PPARɣ that were used were supposed to be specific to each isoform, we need to also evaluate the effect of MDM2-X inhibition on the activity of PPARɣ in our cells. It is possible that the MDM2-X complex is able to lower the activity of PPARα, as well as enhance the activity of PPARɣ to effect the final change in ferroptotic sensitivity.

In this chapter, we faced the arduous task of identifying the mediator of the role of MDM2-X complex in ferroptosis, without the knowledge of p53-independent targets of the complex. While we did discover PPARα and FSP1 to be two key mediators of this mechanism, the exact mode of their regulation by MDM2-X still remains a mystery.

In regard to FSP1, the next step is to determine if the level of regulation of its protein expression is transcriptional or translational. Our preliminary data indicated that FSP1 protein is controlled by a combination of altered stability through MDM2-X E3 ligase activity and altered transcription through PPARα activity. In order to validate this hypothesis, more follow-up experiments are required. RT-PCR can be used to assess the change in *FSP1* mRNA levels in response to MDM2/X/ PPARα inhibition while a cycloheximide chase upon MDM2/X inhibition will help to separate effects on FSP1 protein stability vs synthesis. An ubiquitination assay can determine if FSP1 protein's ubiquitination status is altered upon MDM2-X inhibition. CHIP of PPARα on FSP1 promoter region will shed more light on whether FSP1 transcription is likely under the control of PPARα activity.

It is possible that in addition to changes in the protein levels of FSP1, its activity is also altered when the MDM2-X complex is inhibited. For example, since MDM2 has been known to alter the mitochondrial dynamics as described in Chapter 1, it is possible that the MDM2-X complex alters the availability of NADPH, the substrate of FSP1. This possibility can be studied by minimally measuring the levels of NADPH in the cells and if positive, then followed up by tracing which upstream pathways might be altered to effect this change.

It is also likely that other MDM2-X targets are involved in mediating the regulation of PPARα, FSP1 and other aspects of ferroptosis. Thus, the knowledge of a list of proteins affected by the MDM2-X complex, independent of their effects on p53, would aid further study into understanding the full molecular pathway involved. The proteomics study mentioned previously, would yield a list of proteins affected by the MDM2-X complex, but only some of these targets would be expected to be direct ubiquitination targets. Direct targets would then need to be further identified

using a “ligase trap” which can specifically affinity-purify the ubiquitination targets of a given E3-ligase (Mark, Loveless, and Toczyski 2016) or by ubiquitylome analysis, that enriches for ubiquitinated substrates only in a proteomic screen (Theurillat et al. 2014). It is likely that these proteomics studies need to also be performed in the context of ferroptosis, as it is possible that induction of this cell death mechanism can vary the functionality of MDM2-X complex.

The comprehensive list of MDM2-X targets (ubiquitin dependent and independent), obtained through this two-stage analysis, can then be used to mount an arrayed-CRISPR screen to identify further regulators of ferroptosis. These targets can also be subjected to pathway analysis to identify affected pathways beyond ferroptosis and can thus provide, a gold mine for future studies.

This thesis details one of the first studies that implicate MDM2 and MDMX in being facilitators of a cell death process in a p53-independent manner. Hopefully, further study into generating MDM2-X complex inhibitors as well as identifying more targets of MDM2-X will lead to the discovery of different roles of MDM2 and MDMX in regulating cell survival, outside the context of p53 regulation.

References

Abbas, Tarek, and Anindya Dutta. 2009. 'p21 in cancer: intricate networks and multiple activities', *Nature reviews. Cancer*, 9: 400-14.

Afshinnia, Farsad, Thekkelnaycke M. Rajendiran, Tanu Soni, Jaeman Byun, Stefanie Wernisch, Kelli M. Sas, Jennifer Hawkins, Keith Bellovich, Debbie Gipson, George Michailidis, and Subramaniam Pennathur. 2018. 'Impaired β-Oxidation and Altered Complex Lipid Fatty Acid Partitioning with Advancing CKD', *Journal of the American Society of Nephrology*, 29: 295.

Alarcon-Vargas, Dania, and Ze'ev Ronai. 2002. 'p53-Mdm2--the affair that never ends.', *Carcinogenesis*, 23: 541-47.

Arena, Giuseppe, Madi Yann Cissé, Samuel Pyrdziak, Laurent Chatre, Romain Riscal, Maryse Fuentes, Jamie Jon Arnold, Markus Kastner, Laurie Gayte, Christelle Bertrand-Gaday, Kevin Nay, Claire Angebault-Prouteau, Kerren Murray, Beatrice Chabi, Christelle Koechlin-Ramonatxo, Béatrice Orsetti, Charles Vincent, François Casas, Jean-Christophe Marine, Sandrine Etienne-Manneville, Florence Bernex, Anne Lombès, Craig Eugene Cameron, Hervé Dubouchaud, Miria Ricchetti, Laetitia Karine Linares, and Laurent Le Cam. 2018. 'Mitochondrial MDM2 Regulates Respiratory Complex I Activity Independently of p53', *Molecular Cell*, 69: 594-609.e8.

Armstrong, Jane F., Matthew H. Kaufman, David J. Harrison, and Alan R. Clarke. 1995. 'High-frequency developmental abnormalities in p53-deficient mice', *Current Biology*, 5: 931-36.

Aron, A. T., M. O. Loehr, J. Bogena, and C. J. Chang. 2016. 'An Endoperoxide Reactivity-Based FRET Probe for Ratiometric Fluorescence Imaging of Labile Iron Pools in Living Cells', *J Am Chem Soc*, 138: 14338-46.

Atatreh, Noor, Mohammad A. Ghattas, Sanaa K. Bardaweel, Sara Al Rawashdeh, and Mohammad Al Sorkhy. 2018. 'Identification of new inhibitors of Mdm2-p53 interaction via pharmacophore and structure-based virtual screening', *Drug design, development and therapy*, 12: 3741-52.

Attardi, L. D., and T. Jacks. 1999. 'The role of p53 in tumour suppression: lessons from mouse models', *Cellular and Molecular Life Sciences CMLS*, 55: 48-63.

Auwerx, Johan, Kristina Schoonjans, J. C Fruchart, and Bart Staels. 1996. *Regulation of Triglyceride Metabolism by PPARs : Fibrates and Thiazolidinediones have Distinct Effects*.

Baker, Suzanne J., Antonette C. Preisinger, J. Milburn Jessup, Christos Paraskeva, Sanford Markowitz, J. K. V. Willson, Stanley Hamilton, and Bert Vogelstein. 1990. 'p53 Gene Mutations Occur in Combination with 17p Allelic Deletions as Late Events in Colorectal Tumorigenesis', *Cancer research*, 50: 7717.

Barboza, Juan A., Tomoo Iwakuma, Tamara Terzian, Adel K. El-Naggar, and Guillermina Lozano. 2008. 'Mdm2 and Mdm4 loss regulates distinct p53 activities', *Molecular cancer research : MCR*, 6: 947-54.

Beckerman, Rachel, and Carol Prives. 2010. "Transcriptional regulation by p53." In *Cold Spring Harbor perspectives in biology*.

Belmokhtar, Chafké Ahmed, Josette Hillion, and Evelyne Ségal-Bendirdjian. 2001. 'Staurosporine induces apoptosis through both caspase-dependent and caspase-independent mechanisms', *Oncogene*, 20: 3354.

Berkson, Rachel G., Jonathan J. Hollick, Nicholas J. Westwood, Julie A. Woods, David P. Lane, and Sonia Lain. 2005. 'Pilot screening programme for small molecule activators of p53', *International Journal of Cancer*, 115: 701-10.

Bersuker, Kirill, Joseph M. Hendricks, Zhipeng Li, Leslie Magtanong, Breanna Ford, Peter H. Tang, Melissa A. Roberts, Bingqi Tong, Thomas J. Maimone, Roberto Zoncu, Michael C. Bassik, Daniel K. Nomura, Scott J. Dixon, and James A. Olzmann. 2019. 'The CoQ oxidoreductase FSP1 acts parallel to GPX4 to inhibit ferroptosis', *Nature*.

Biderman, Lynn, James L. Manley, and Carol Prives. 2012. 'Mdm2 and MdmX as Regulators of Gene Expression', *Genes & Cancer*, 3: 264-73.

Blattner, Christine, Trevor Hay, David W. Meek, and David P. Lane. 2002. 'Hypophosphorylation of Mdm2 augments p53 stability', *Molecular and Cellular Biology*, 22: 6170-82.

Bohlman, Stephen, and James J. Manfredi. 2014. 'p53-independent effects of Mdm2', *Sub-cellular biochemistry*, 85: 235-46.

Bowen, Margot E., and Laura D. Attardi. 2019. 'The role of p53 in developmental syndromes', *Journal of molecular cell biology*, 11: 200-11.

Bunz, Fred, Christine Fauth, Michael R. Speicher, Annie Dutriaux, John M. Sedivy, Kenneth W. Kinzler, Bert Vogelstein, and Christoph Lengauer. 2002. 'Targeted Inactivation of p53 in Human Cells Does Not Result in Aneuploidy', *Cancer research*, 62: 1129.

Carrillo, Alexia M., Alyssa Bouska, Maria Pia Arrate, and Christine M. Eischen. 2015. 'Mdmx promotes genomic instability independent of p53 and Mdm2', *Oncogene*, 34: 846-56.

Chang, Ling-Chu, Shih-Kai Chiang, Shuen-Ei Chen, Yung-Luen Yu, Ruey-Hwang Chou, and Wei-Chao Chang. 2018. 'Heme oxygenase-1 mediates BAY 11–7085 induced ferroptosis', *Cancer Letters*, 416: 124-37.

Chen, Jiandong. 2012. 'The Roles of MDM2 and MDMX Phosphorylation in Stress Signaling to p53', *Genes & Cancer*, 3: 274-82.

Chen, Lihong, Daniele M. Gilkes, Yu Pan, William S. Lane, and Jiandong Chen. 2005. 'ATM and Chk2-dependent phosphorylation of MDMX contribute to p53 activation after DNA damage', *The EMBO Journal*, 24: 3411-22.

Chen, Xiaofeng, Jinrong Qiu, Dapeng Yang, Jianlei Lu, Caiyun Yan, Xiaoming Zha, and Yongmei Yin. 2013. 'MDM2 Promotes Invasion and Metastasis in Invasive Ductal Breast Carcinoma by Inducing Matrix Metalloproteinase-9', *PLoS One*, 8: e78794.

Chen, Ying, Dan-Dan Wang, Ye-Ping Wu, Dan Su, Tian-Yi Zhou, Ren-Hua Gai, Ying-Ying Fu, Lin Zheng, Qiao-Jun He, Hong Zhu, and Bo Yang. 2017. 'MDM2 promotes epithelial-mesenchymal transition and metastasis of ovarian cancer SKOV3 cells', *British journal of cancer*, 117: 1192-201.

Chen, Yixin, Yongtao Wang, Yaoyao Huang, Hang Zeng, Bingfang Hu, Lihuan Guan, Huizhen Zhang, Ai-Ming Yu, Caroline H. Johnson, Frank J. Gonzalez, Min Huang, and Huichang Bi. 2017. 'PPARα regulates tumor cell proliferation and senescence via a novel target gene carnitine palmitoyltransferase 1C', *Carcinogenesis*, 38: 474-83.

Cheng, Qian, and Jiandong Chen. 2011. 'The phenotype of MDM2 auto-degradation after DNA damage is due to epitope masking by phosphorylation', *Cell cycle (Georgetown, Tex.)*, 10: 1162-66.

Cheok, Chit Fang, and David Philip Lane. 2017. 'Exploiting the p53 Pathway for Therapy', *Cold Spring Harbor Perspectives in Medicine*, 7: a026310.

Chonghaile, Tríona Ní. 2018. 'Ironing out dedifferentiation in melanoma', *Science Translational Medicine*, 10: eaau0461.
Conklin, Kenneth A. 2005. 'Coenzyme Q10 for Prevention of Anthracycline-Induced Cardiotoxicity', *Integrative Cancer Therapies*, 4: 110-30.
Connor, Patrick M., Joany Jackman, Insoo Bae, Timothy G. Myers, Saijun Fan, Masato Mutoh, Dominic A. Scudiero, Ann Monks, Edward A. Sausville, John N. Weinstein, Stephen Friend, Albert J. Fornace, and Kurt W. Kohn. 1997. 'Characterization of the p53 Tumor Suppressor Pathway in Cell Lines of the National Cancer Institute Anticancer Drug Screen and Correlations with the Growth-Inhibitory Potency of 123 Anticancer Agents', *Cancer research*, 57: 4285.
Conrad, Marcus, and José Pedro Friedmann Angeli. 2015. 'Glutathione peroxidase 4 (Gpx4) and ferroptosis: what's so special about it?', *Molecular & Cellular Oncology*, 2: e995047-e47.
Danovi, Davide, Erik Meulmeester, Diego Pasini, Domenico Migliorini, Maria Capra, Ruth Frenk, Petra de Graaf, Sarah Francoz, Patrizia Gasparini, Alberto Gobbi, Kristian Helin, Pier Giuseppe Pelicci, Aart G. Jochemsen, and Jean-Christophe Marine. 2004. 'Amplification of Mdmx (or Mdm4) directly contributes to tumor formation by inhibiting p53 tumor suppressor activity', *Molecular and Cellular Biology*, 24: 5835-43.
de Oca Luna, Roberta Montes, Daniel S. Wagner, and Guillermina Lozano. 1995. 'Rescue of early embryonic lethality in mdm2-deficient mice by deletion of p53', *Nature*, 378: 203-06.
Deb, S. P. 2002. 'Function and dysfunction of the human oncoprotein mdm2', *Front. Biosci.*, 7: d235–d43.
Deb, Swati Palit. 2003. 'Cell Cycle Regulatory Functions of the Human Oncoprotein MDM2 ', *Molecular Cancer Research*, 1: 1009.
Deben, Christophe, An Wouters, Ken Op de Beeck, Jolien van Den Bossche, Julie Jacobs, Karen Zwaenepoel, Marc Peeters, Jan Van Meerbeeck, Filip Lardon, Christian Rolfo, Vanessa Deschoolmeester, and Patrick Pauwels. 2015. 'The MDM2-inhibitor Nutlin-3 synergizes with cisplatin to induce p53 dependent tumor cell apoptosis in non-small cell lung cancer', *Oncotarget*, 6: 22666-79.
Dixon, Scott J, Darpan N Patel, Matthew Welsch, Rachid Skouta, Eric D Lee, Miki Hayano, Ajit G Thomas, Caroline E Gleason, Nicholas P Tatonetti, Barbara S Slusher, and Brent R Stockwell. 2014. 'Pharmacological inhibition of cystine–glutamate exchange induces endoplasmic reticulum stress and ferroptosis', *eLife*, 3: 1-25.
Dixon, Scott J, and Brent R Stockwell. 2014. 'The role of iron and reactive oxygen species in cell death', *Nature chemical biology*, 10: 9-17.
Dixon, Scott J., Kathryn M. Lemberg, Michael R. Lamprecht, Rachid Skouta, Eleina M. Zaitsev, Caroline E. Gleason, Darpan N. Patel, Andras J. Bauer, Alexandra M. Cantley, Wan Seok Yang, Barclay Morrison, and Brent R. Stockwell. 2012. 'Ferroptosis: An iron-dependent form of nonapoptotic cell death', *Cell*, 149: 1060-72.
Dodson, Matthew, Raul Castro-Portuguez, and Donna D. Zhang. 2019. 'NRF2 plays a critical role in mitigating lipid peroxidation and ferroptosis', *Redox biology*, 23: 101107-07.
Doll, Sebastian, Florencio Porto Freitas, Ron Shah, Maceler Aldrovandi, Milene Costa da Silva, Irina Ingold, Andrea Goya Grocin, Thamara Nishida Xavier da Silva, Elena Panzilius, Christina H. Scheel, André Mourão, Katalin Buday, Mami Sato, Jonas Wanninger, Thibaut Vignane, Vaishnavi Mohana, Markus Rehberg, Andrew Flatley, Aloys Schepers, Andreas Kurz, Daniel White, Markus Sauer, Michael Sattler, Edward William Tate,

Werner Schmitz, Almut Schulze, Valerie O'Donnell, Bettina Proneth, Grzegorz M. Popowicz, Derek A. Pratt, José Pedro Friedmann Angeli, and Marcus Conrad. 2019. 'FSP1 is a glutathione-independent ferroptosis suppressor', *Nature*.

Dubois, Vanessa, Jérôme Eeckhoute, Philippe Lefebvre, and Bart Staels. 2017. 'Distinct but complementary contributions of PPAR isotypes to energy homeostasis', *The Journal of Clinical Investigation*, 127: 1202-14.

Eischen, Christine M. 2017. 'Role of Mdm2 and Mdmx in DNA repair', *Journal of molecular cell biology*, 9: 69-73.

Elkholi, Rana, Ioana Abraham-Enachescu, Andrew P. Trotta, Camila Rubio-Patiño, Jarvier N. Mohammed, Mark P. A. Luna-Vargas, Jesse D. Gelles, Joshua R. Kaminetsky, Madhavika N. Serasinghe, Cindy Zou, Sumaira Ali, Gavin P. McStay, Cathie M. Pfleger, and Jerry Edward Chipuk. 2019. 'MDM2 Integrates Cellular Respiration and Apoptotic Signaling through NDUFS1 and the Mitochondrial Network', *Molecular Cell*, 74: 452-65.e7.

Ewen, Mark E., and Susan J. Miller. 1996. 'p53 and translational control', *Biochimica et Biophysica Acta (BBA) - Reviews on Cancer*, 1242: 181-84.

Fåhraeus, R., and V. Olivares-Illana. 2013. 'MDM2's social network', *Oncogene*, 33: 4365.

Fakharzadeh, S. S., S. P. Trusko, and D. L. George. 1991. 'Tumorigenic potential associated with enhanced expression of a gene that is amplified in a mouse tumor cell line', *The EMBO Journal*, 10: 1565-69.

Fang, Shengyun, Jane P. Jensen, Robert L. Ludwig, Karen H. Vousden, and Allan M. Weissman. 2000. 'Mdm2 Is a RING Finger-dependent Ubiquitin Protein Ligase for Itself and p53', *Journal of Biological Chemistry*, 275: 8945-51.

Fang, Xuexian, Hao Wang, Dan Han, Enjun Xie, Xiang Yang, Jiayu Wei, Shanshan Gu, Feng Gao, Nali Zhu, Xiangju Yin, Qi Cheng, Pan Zhang, Wei Dai, Jinghai Chen, Fuquan Yang, Huang-Tian Yang, Andreas Linkermann, Wei Gu, Junxia Min, and Fudi Wang. 2019. 'Ferroptosis as a target for protection against cardiomyopathy', *Proceedings of the National Academy of Sciences of the United States of America*, 116: 2672-80.

Feeley, Kyle P., Clare M. Adams, Ramkrishna Mitra, and Christine M. Eischen. 2017. 'Mdm2 Is Required for Survival and Growth of p53-Deficient Cancer Cells', *Cancer research*, 77: 3823-33.

Feng, Huizhong, Kenji Schorpp, Jenny Jin, Carrie E. Yozwiak, Benjamin G. Hoffstrom, Aubrianna M. Decker, Presha Rajbhandari, Michael E. Stokes, Hannah G. Bender, Joleen M. Csuka, Pavan S. Upadhyayula, Peter Canoll, Koji Uchida, Rajesh K. Soni, Kamyar Hadian, and Brent R. Stockwell. 2020. 'Transferrin Receptor Is a Specific Ferroptosis Marker', *Cell Reports*, 30: 3411-23.e7.

Feng, Huizhong, and Brent R. Stockwell. 2018. 'Unsolved mysteries: How does lipid peroxidation cause ferroptosis?', *PLOS Biology*, 16: e2006203.

Ferré, Pascal. 2004. 'The Biology of Peroxisome Proliferator-Activated Receptors', *Diabetes*, 53: S43.

Fitzgerald, a L, a a Osman, T-X Xie, a Patel, H Skinner, V Sandulache, and J N Myers. 2015. 'Reactive oxygen species and p21Waf1/Cip1 are both essential for p53-mediated senescence of head and neck cancer cells', *Cell Death and Disease*, 6: e1678.

Friedmann Angeli, Jose Pedro, Manuela Schneider, Bettina Proneth, Yulia Y. Tyurina, Vladimir A. Tyurin, Victoria J. Hammond, Nadja Herbach, Michaela Aichler, Axel Walch, Elke Eggenhofer, Devaraj Basavarajappa, Olof Rådmark, Sho Kobayashi, Tobias Seibt, Heike

Beck, Frauke Neff, Irene Esposito, Rüdiger Wanke, Heidi Förster, Olena Yefremova, Marc Heinrichmeyer, Georg W. Bornkamm, Edward K. Geissler, Stephen B. Thomas, Brent R. Stockwell, Valerie B. O'Donnell, Valerian E. Kagan, Joel A. Schick, and Marcus Conrad. 2014. 'Inactivation of the ferroptosis regulator Gpx4 triggers acute renal failure in mice', *Nature Cell Biology*, 16: 1180.

Ganguli, Gitali, and Bohdan Wasylyk. 2003. 'p53-Independent Functions of MDM2', *Molecular Cancer Research*, 1: 1027.

Gao, Minghui, Prashant Monian, Nosirudeen Quadri, Ravichandran Ramasamy, and Xuejun Jiang. 2015. 'Glutaminolysis and Transferrin Regulate Ferroptosis', *Molecular Cell*, 59: 298-308.

Gaschler, Michael M., Alexander A. Andia, Hengrui Liu, Joleen M. Csuka, Brisa Hurlocker, Christopher A. Vaiana, Daniel W. Heindel, Dylan S. Zuckerman, Pieter H. Bos, Eduard Reznik, Ling F. Ye, Yulia Y. Tyurina, Annie J. Lin, Mikhail S. Shchepinov, Amy Y. Chan, Eveliz Peguero-Pereira, Maksim A. Fomich, Jacob D. Daniels, Andrei V. Bekish, Vadim V. Shmanai, Valerian E. Kagan, Lara K. Mahal, K. A. Woerpel, and Brent R. Stockwell. 2018. 'FINO2 initiates ferroptosis through GPX4 inactivation and iron oxidation', *Nature chemical biology*, 14: 507-15.

Gervois, Philippe, Pineda Torra Inés, Jean-Charles Fruchart, and Bart Staels. 2000. "Regulation of Lipid and Lipoprotein Metabolism by PPAR Activators." In *Clinical Chemistry and Laboratory Medicine*, 3.

Giovannini, Catia, Michele Baglioni, Marco Baron Toaldo, Cristiano Ventrucci, Stefania D'Adamo, Mario Cipone, Pasquale Chieco, Laura Gramantieri, and Luigi Bolondi. 2013. 'Notch3 inhibition enhances sorafenib cytotoxic efficacy by promoting GSK3b phosphorylation and p21 down-regulation in hepatocellular carcinoma.', *Oncotarget*, 4: 1618-31.

Gnanapradeepan, Keerthana, Subhasree Basu, Thibaut Barnoud, Anna Budina-Kolomets, Che-Pei Kung, and Maureen E. Murphy. 2018. 'The p53 Tumor Suppressor in the Control of Metabolism and Ferroptosis', *Frontiers in Endocrinology*, 9: 124.

Gopinathan, Lakshmi, Daniel B. Hannon, Jeffrey M. Peters, and John P. Vanden Heuvel. 2009. 'Regulation of peroxisome proliferator-activated receptor-alpha by MDM2', *Toxicological sciences : an official journal of the Society of Toxicology*, 108: 48-58.

Gu J, Kawai H, Nie L, Kitao H, Wiederschain D, Jochemsen AG, et al. 2002. 'Mutual dependence of Mdm2 and MdmX in their functional inactivation of p53', *J Biol Chem*: 3.

Guha, Tanya, and David Malkin. 2017. 'Inherited TP53 Mutations and the Li-Fraumeni Syndrome', *Cold Spring Harbor Perspectives in Medicine*, 7: a026187.

Hager, Kayla M., and Wei Gu. 2013. 'Understanding the non-canonical pathways involved in p53-mediated tumor suppression', *Carcinogenesis*, 35: 740-46.

Herman, Ariel G., Miki Hayano, Masha V. Poyurovsky, Kenichi Shimada, Rachid Skouta, Carol Prives, and Brent R. Stockwell. 2011. 'Discovery of Mdm2-MdmX E3 ligase inhibitors using a cell-based ubiquitination assay', *Cancer Discovery*, 1: 312-25.

Hientz, Karin, André Mohr, Dipita Bhakta-Guha, and Thomas Efferth. 2017. 'The role of p53 in cancer drug resistance and targeted chemotherapy', *Oncotarget*, 8: 8921-46.

Ho, J., and S. Benchimol. 2003. 'Transcriptional repression mediated by the p53 tumour suppressor', *Cell Death & Differentiation*, 10: 404-08.

Hoe, Khoo Kian, Chandra S. Verma, and David P. Lane. 2014. 'Drugging the p53 pathway: understanding the route to clinical efficacy', *Nat Rev Drug Discov*, 13: 217-36.

Hooper, Claudie, Eirini Meimaridou, Mahvash Tavassoli, Gerry Melino, Simon Lovestone, and Richard Killick. 2007. 'p53 is upregulated in Alzheimer's disease and induces tau phosphorylation in HEK293a cells', *Neuroscience letters*, 418: 34-37.

Hou, W., Y. Xie, X. Song, X. Sun, M. T. Lotze, H. J. Zeh, 3rd, R. Kang, and D. Tang. 2016. 'Autophagy promotes ferroptosis by degradation of ferritin', *Autophagy*: 1-4.

Hu, Wenwei, Cen Zhang, Rui Wu, Yvonne Sun, Arnold Levine, and Zhaohui Feng. 2010. 'Glutaminase 2, a novel p53 target gene regulating energy metabolism and antioxidant function', *Proceedings of the National Academy of Sciences*, 107: 7455.

Huang, Lei, Zheng Yan, Xiaodong Liao, Yuan Li, Jie Yang, Zhu-Gang Wang, Yong Zuo, Hidehiko Kawai, Miriam Shadfan, Suthakar Ganapathy, and Zhi-Min Yuan. 2011. 'The p53 inhibitors MDM2/MDMX complex is required for control of p53 activity in vivo', *Proceedings of the National Academy of Sciences of the United States of America*, 108: 12001-06.

Inguaggiato, Paola, Luis Gonzalez-Michaca, Anthony J. Croatt, Jill J. Haggard, Jawed Alam, and Karl A. Nath. 2001. 'Cellular overexpression of heme oxygenase-1 up-regulates p21 and confers resistance to apoptosis', *Kidney International*, 60: 2181-91.

Issaeva, Natalia, Przemyslaw Bozko, Martin Enge, Marina Protopopova, Lisette G. G. C. Verhoef, Maria Masucci, Aladdin Pramanik, and Galina Selivanova. 2004. 'Small molecule RITA binds to p53, blocks p53–HDM-2 interaction and activates p53 function in tumors', *Nature Medicine*, 10: 1321-28.

Iwakuma, Tomoo, and Guillermina Lozano. 2003. 'MDM2, An Introduction', *Molecular Cancer Research*, 1: 993.

Iyappan, Saravanakumar, Hans-Peter Wollscheid, Alejandro Rojas-Fernandez, Andreas Marquardt, Hao-Cheng Tang, Rajesh K. Singh, and Martin Scheffner. 2010. 'Turning the RING Domain Protein MdmX into an Active Ubiquitin-Protein Ligase', *Journal of Biological Chemistry*, 285: 33065-72.

Jain, Abhinav K, and Michelle C Barton. 2016. 'Outside the p53 RING: Transcription Regulation by Chromatin-Bound MDM2', *Molecular Cell*, 62: 805-07.

Jain, Abhinav K., and Michelle Craig Barton. 2018. 'p53: emerging roles in stem cells, development and beyond', *Development*, 145: dev158360.

Jennis, Matthew, Che-Pei Kung, Subhasree Basu, Anna Budina-Kolomets, Julia I. Ju Leu, Sakina Khaku, Jeremy P. Scott, Kathy Q. Cai, Michelle R. Campbell, Devin K. Porter, Xuting Wang, Douglas A. Bell, Xiaoxian Li, David S. Garlick, Qin Liu, Monica Hollstein, Donna L. George, and Maureen E. Murphy. 2016. 'An African-specific polymorphism in the TP53 gene impairs p53 tumor suppressor function in a mouse model', *Genes & Development*, 30: 918-30.

Jiang, Le, Ning Kon, Tongyuan Li, Shang-Jui Wang, Tao Su, Hanina Hibshoosh, Richard Baer, and Wei Gu. 2015. 'Ferroptosis as a p53-mediated activity during tumour suppression', *Nature*, 520: 57-62.

Jin, Y., S. X. Zeng, X. X. Sun, H. Lee, C. Blattner, Z. Xiao, and H. Lu. 2008. 'MDMX promotes proteasomal turnover of p21 at G1 and early S phases independently of, but in cooperation with, MDM2', *Mol Cell Biol*, 28: 1218-29.

Jin, Yetao, Hunjoo Lee, Shelya X. Zeng, Mu-Shui Dai, and Hua Lu. 2003. 'MDM2 promotes p21waf1/cip1 proteasomal turnover independently of ubiquitylation', *The EMBO Journal*, 22: 6365-77.

Jones, Stephen N., Amy E. Roe, Lawrence A. Donehower, and Allan Bradley. 1995. 'Rescue of embryonic lethality in Mdm2-deficient mice by absence of p53', *Nature*, 378: 206-08.
Kadakia, Madhavi, Thomas L. Brown, Molly M. McGorry, and Steven J. Berberich. 2002. 'MdmX inhibits Smad transactivation', *Oncogene*, 21: 8776.
Kaplan, Anna, Michael M. Gaschler, Denise E. Dunn, Ryan Colligan, Lewis M. Brown, Arthur G. Palmer, Donald C. Lo, and Brent R. Stockwell. 2015. 'Small molecule-induced oxidation of protein disulfide isomerase is neuroprotective', *Proceedings of the National Academy of Sciences*, 112: E2245.
Karni-Schmidt, O., M. Lokshin, and C. Prives. 2016. 'The Roles of MDM2 and MDMX in Cancer', *Annu Rev Pathol*, 11: 617-44.
Kersten, S. 2008. 'Peroxisome proliferator activated receptors and lipoprotein metabolism', *PPAR Res*, 2008: 132960.
Kon, Ning, Donglai Wang, Tongyuan Li, Le Jiang, Li Qiang, and Wei Gu. 2018. 'Inhibition of Mdmx (Mdm4) in vivo induces anti-obesity effects', *Oncotarget*, 9: 7282-97.
Koves, Timothy R., John R. Ussher, Robert C. Noland, Dorothy Slentz, Merrie Mosedale, Olga Ilkayeva, James Bain, Robert Stevens, Jason R. B. Dyck, Christopher B. Newgard, Gary D. Lopaschuk, and Deborah M. Muoio. 2008. 'Mitochondrial Overload and Incomplete Fatty Acid Oxidation Contribute to Skeletal Muscle Insulin Resistance', *Cell Metabolism*, 7: 45-56.
Kraft, Vanessa A. N., Carla T. Bezjian, Susanne Pfeiffer, Larissa Ringelstetter, Constanze Müller, Fereshteh Zandkarimi, Juliane Merl-Pham, Xuanwen Bao, Natasa Anastasov, Johanna Kössl, Stefanie Brandner, Jacob D. Daniels, Philippe Schmitt-Kopplin, Stefanie M. Hauck, Brent R. Stockwell, Kamyar Hadian, and Joel A. Schick. 2020. 'GTP Cyclohydrolase 1/Tetrahydrobiopterin Counteract Ferroptosis through Lipid Remodeling', *ACS Central Science*, 6: 41-53.
Kulikov, Roman, Karen A. Boehme, and Christine Blattner. 2005. 'Glycogen synthase kinase 3-dependent phosphorylation of Mdm2 regulates p53 abundance', *Molecular and Cellular Biology*, 25: 7170-80.
Kwon, Min-Young, Eunhee Park, Seon-Jin Lee, and Su Wol Chung. 2015. 'Heme oxygenase-1 accelerates erastin-induced ferroptotic cell death', *Oncotarget*, 6: 24393-403.
Lachaier, Emma, Christophe Louandre, Corinne Godin, Zuzana Saidak, Université De Picardie, Jules Verne, and Amiens Cedex. 2014. 'Sorafenib Induces Ferroptosis in Human Cancer Cell Lines Originating from Different Solid Tumors', *Anticancer research*, 34: 6417-22.
Larraufie, Marie-Helene, Wan Seok Yang, Elise Jiang, Ajit G. Thomas, Barbara S. Slusher, and Brent R. Stockwell. 2015. 'Incorporation of metabolically stable ketones into a small molecule probe to increase potency and water solubility', *Bioorganic & Medicinal Chemistry Letters*, 25: 4787-92.
Lefebvre, Philippe, Giulia Chinetti, Jean-Charles Fruchart, and Bart Staels. 2006. 'Sorting out the roles of PPAR alpha in energy metabolism and vascular homeostasis', *The Journal of Clinical Investigation*, 116: 571-80.
Lei, Guang, Yilei Zhang, Pranavi Koppula, Xiaoguang Liu, Jie Zhang, Steven H. Lin, Jaffer A. Ajani, Qin Xiao, Zhongxing Liao, Hui Wang, and Boyi Gan. 2020. 'The role of ferroptosis in ionizing radiation-induced cell death and tumor suppression', *Cell Research*, 30: 146-62.
Lessel, Davor, Danyi Wu, Carlos Trujillo, Thomas Ramezani, Ivana Lessel, Mohammad K. Alwasiyah, Bidisha Saha, Fuki M. Hisama, Katrin Rading, Ingrid Goebel, Petra Schütz,

Günter Speit, Josef Högel, Holger Thiele, Gudrun Nürnberg, Peter Nürnberg, Matthias Hammerschmidt, Yan Zhu, David R. Tong, Chen Katz, George M. Martin, Junko Oshima, Carol Prives, and Christian Kubisch. 2017. 'Dysfunction of the MDM2/p53 axis is linked to premature aging', *The Journal of Clinical Investigation*, 127: 3598-608.

Levine, Beth, and John Abrams. 2008. 'p53: The Janus of autophagy?', *Nature Cell Biology*, 10: 637-9.

Li, Jie, Feng Cao, He-liang Yin, Zi-jian Huang, Zhi-tao Lin, Ning Mao, Bei Sun, and Gang Wang. 2020. 'Ferroptosis: past, present and future', *Cell Death & Disease*, 11: 88.

Liang, S.X. 2003. 'The effect of potent iron chelators on the regulation of p53: examination of the expression, localization and DNA-binding activity of p53 and the transactivation of WAF1', *Carcinogenesis*, 24: 1601-14.

Lin, Tongxiang, and Yi Lin. 2017. 'p53 switches off pluripotency on differentiation', *Stem cell research & therapy*, 8: 44-44.

Liu, Bin, Yumin Chen, and Daret K. St Clair. 2008. 'ROS and p53: a versatile partnership', *Free radical biology & medicine*, 44: 1529-35.

Liu, David S., Cuong P. Duong, Sue Haupt, Karen G. Montgomery, Colin M. House, Walid J. Azar, Helen B. Pearson, Oliver M. Fisher, Matthew Read, Glen R. Guerra, Ygal Haupt, Carleen Cullinane, Klas G. Wiman, Lars Abrahmsen, Wayne A. Phillips, and Nicholas J. Clemons. 2017. 'Inhibiting the system x(C)(-)/glutathione axis selectively targets cancers with mutant-p53 accumulation', *Nature communications*, 8: 14844-44.

Liu, Yan, Shannon E. Elf, Yasuhiko Miyata, Goro Sashida, Yuhui Liu, Gang Huang, Silvana Di Giandomenico, Jennifer M. Lee, Anthony Deblasio, Silvia Menendez, Jack Antipin, Boris Reva, Andrew Koff, and Stephen D. Nimer. 2009. 'p53 regulates hematopoietic stem cell quiescence', *Cell stem cell*, 4: 37-48.

Liu, Zhuohao, Leigang Jin, Jin-Kui Yang, Baile Wang, Kelvin K. L. Wu, Philip Hallenborg, Aimin Xu, and Kenneth K. Y. Cheng. 2018. 'The Dysfunctional MDM2–p53 Axis in Adipocytes Contributes to Aging-Related Metabolic Complications by Induction of Lipodystrophy', *Diabetes*, 67: 2397.

Löhr, Kristina, Constanze Möritz, Ana Contente, and Matthias Dobbelstein. 2003. 'p21/CDKN1A Mediates Negative Regulation of Transcription by p53', *Journal of Biological Chemistry*, 278: 32507-16.

Lu, Xiangdong, Caiyun Yan, Yi Huang, Dongmin Shi, Ziyi Fu, Jinrong Qiu, and Yongmei Yin. 2016. 'Mouse double minute 2 (MDM2) upregulates Snail expression and induces epithelial-to-mesenchymal transition in breast cancer cells in vitro and in vivo', *Oncotarget*, 7: 37177-91.

Magtanong, Leslie, Pin-Joe Ko, Milton To, Jennifer Yinuo Cao, Giovanni C. Forcina, Amy Tarangelo, Carl C. Ward, Kevin Cho, Gary J. Patti, Daniel K. Nomura, James A. Olzmann, and Scott J. Dixon. 2019. 'Exogenous Monounsaturated Fatty Acids Promote a Ferroptosis-Resistant Cell State', *Cell Chemical Biology*.

Mancini, Francesca, Emanuela Teveroni, Giusy Di Conza, Valentina Monteleone, Ivan Arisi, Marsha Pellegrino, Marianna Buttarelli, Luisa Pieroni, Mara D'Onofrio, Andrea Urbani, Alfredo Pontecorvi, Massimiliano Mazzone, and Fabiola Moretti. 2017. 'MDM4 actively restrains cytoplasmic mTORC1 by sensing nutrient availability', *Molecular Cancer*, 16: 55.

Manfredi, James J. 2010. 'The Mdm2–p53 relationship evolves: Mdm2 swings both ways as an oncogene and a tumor suppressor', *Genes & Development*, 24: 1580-89.

Marine, Jean-Christophe W., Michael A. Dyer, and Aart G. Jochemsen. 2007. 'MDMX: from bench to bedside', *Journal of Cell Science*, 120: 371.

Mark, Kevin G., Theresa B. Loveless, and David P. Toczyski. 2016. 'Isolation of ubiquitinated substrates by tandem affinity purification of E3 ligase–polyubiquitin-binding domain fusions (ligase traps)', *Nature Protocols*, 11: 291-301.

Martin-Sanchez, Diego, Olga Ruiz-Andres, Jonay Poveda, Susana Carrasco, Pablo Cannata-Ortiz, Maria D. Sanchez-Niño, Marta Ruiz Ortega, Jesus Egido, Andreas Linkermann, Alberto Ortiz, and Ana B. Sanz. 2017. 'Ferroptosis, but Not Necroptosis, Is Important in Nephrotoxic Folic Acid–Induced AKI', *Journal of the American Society of Nephrology*, 28: 218.

Martinez, Alejandra M., Ahryun Kim, and Wan Seok Yang. 2020. 'Detection of Ferroptosis by BODIPY™ 581/591 C11.' in Ivana Vancurova and Yan Zhu (eds.), *Immune Mediators in Cancer: Methods and Protocols* (Springer US: New York, NY).

Martinez, Alejandra M., Jovan Mirkovic, Zofia A. Stanisz, Fahmida S. Patwari, and Wan Seok Yang. 2019. 'NSC-34 motor neuron-like cells are sensitized to ferroptosis upon differentiation', *FEBS open bio*, 9: 582-93.

Matijasevic, Z., A. Krzywicka-Racka, G. Sluder, J. Gallant, and S. N. Jones. 2016. 'The Zn-finger domain of MdmX suppresses cancer progression by promoting genome stability in p53-mutant cells', *Oncogenesis*, 5: e262-e62.

Matijasevic, Zdenka, Heather A. Steinman, Kathleen Hoover, and Stephen N. Jones. 2008. 'MdmX promotes bipolar mitosis to suppress transformation and tumorigenesis in p53-deficient cells and mice', *Molecular and Cellular Biology*, 28: 1265-73.

Matsushita, Mai, Stefan Freigang, Christoph Schneider, Marcus Conrad, Georg W. Bornkamm, and Manfred Kopf. 2015. 'T cell lipid peroxidation induces ferroptosis and prevents immunity to infection', *Journal of Experimental Medicine*, 212: 555-68.

Maya, R., M. Balass, S. T. Kim, D. Shkedy, J. F. Leal, O. Shifman, M. Moas, T. Buschmann, Z. Ronai, Y. Shiloh, M. B. Kastan, E. Katzir, and M. Oren. 2001. 'ATM-dependent phosphorylation of Mdm2 on serine 395: role in p53 activation by DNA damage', *Genes & Development*, 15: 1067-77.

McMullen, Patrick D., Sudin Bhattacharya, Courtney G. Woods, Bin Sun, Kathy Yarborough, Susan M. Ross, Manda E. Miller, Mary T. McBride, Edward L. LeCluyse, Rebecca A. Clewell, and Melvin E. Andersen. 2014. 'A map of the PPARα transcription regulatory network for primary human hepatocytes', *Chemico-Biological Interactions*, 209: 14-24.

Meletis, Konstantinos, Valtteri Wirta, Sanna-Maria Hede, Monica Nistér, Joakim Lundeberg, and Jonas Frisén. 2006. 'p53 suppresses the self-renewal of adult neural stem cells', *Development*, 133: 363.

Melo, Alexia N., and Christine M. Eischen. 2012. 'Protecting the genome from mdm2 and mdmx', *Genes & Cancer*, 3: 283-90.

Menon, Vijay, and Lawrence Povirk. 2014. 'Involvement of p53 in the repair of DNA double strand breaks: multifaceted Roles of p53 in homologous recombination repair (HRR) and non-homologous end joining (NHEJ)', *Sub-cellular biochemistry*, 85: 321-36.

Miess, Heike, Beatrice Dankworth, Arvin M. Gouw, Mathias Rosenfeldt, Werner Schmitz, Ming Jiang, Becky Saunders, Michael Howell, Julian Downward, Dean W. Felsher, Barrie Peck, and Almut Schulze. 2018. 'The glutathione redox system is essential to prevent ferroptosis caused by impaired lipid metabolism in clear cell renal cell carcinoma', *Oncogene*, 37: 5435-50.

Mobarra, Naser, Mehrnoosh Shanaki, Hassan Ehteram, Hajar Nasiri, Mehdi Sahmani, Mohsen Saeidi, Mehdi Goudarzi, Hoda Pourkarim, and Mehdi Azad. 2016. 'A Review on Iron Chelators in Treatment of Iron Overload Syndromes', *International journal of hematology-oncology and stem cell research*, 10: 239-47.

Molchadsky, Alina, Igor Shats, Naomi Goldfinger, Meirav Pevsner-Fischer, Melissa Olson, Ariel Rinon, Eldad Tzahor, Guillermina Lozano, Dov Zipori, Rachel Sarig, and Varda Rotter. 2008. 'p53 plays a role in mesenchymal differentiation programs, in a cell fate dependent manner', *PLoS One*, 3: e3707-e07.

Moll, Ute M., Sonja Wolff, Daniel Speidel, and Wolfgang Deppert. 2005. 'Transcription-independent pro-apoptotic functions of p53', *Current Opinion in Cell Biology*, 17: 631-36.

Moon, Sung-Hwan, Chun-Hao Huang, Shauna L. Houlihan, Kausik Regunath, William A. Freed-Pastor, John P. th Morris, Darjus F. Tschaharganeh, Edward R. Kastenhuber, Anthony M. Barsotti, Rachel Culp-Hill, Wen Xue, Yu-Jui Ho, Timour Baslan, Xiang Li, Allison Mayle, Elisa de Stanchina, Lars Zender, David R. Tong, Angelo D'Alessandro, Scott W. Lowe, and Carol Prives. 2019. 'p53 Represses the Mevalonate Pathway to Mediate Tumor Suppression', *Cell*, 176: 564-80.e19.

Muir, Ryan K., Ning Zhao, Junnian Wei, Yung-hua Wang, Anna Moroz, Yangjie Huang, Ying-Chu Chen, Renuka Sriram, John Kurhanewicz, Davide Ruggero, Adam R. Renslo, and Michael J. Evans. 2019. 'Measuring Dynamic Changes in the Labile Iron Pool in Vivo with a Reactivity-Based Probe for Positron Emission Tomography', *ACS Central Science*, 5: 727-36.

Mulay, Shrikant R., Dana Thomasova, Mi Ryu, and Hans-Joachim Anders. 2012. 'MDM2 (murine double minute-2) links inflammation and tubular cell healing during acute kidney injury in mice', *Kidney International*, 81: 1199-211.

Müller, Tammo, Christin Dewitz, Jessica Schmitz, Anna Sophia Schröder, Jan Hinrich Bräsen, Brent R. Stockwell, James M. Murphy, Ulrich Kunzendorf, and Stefan Krautwald. 2017. 'Necroptosis and ferroptosis are alternative cell death pathways that operate in acute kidney failure', *Cellular and molecular life sciences : CMLS*, 74: 3631-45.

Mungamuri, Sathish Kumar, Rui F. Qiao, Shen Yao, James J. Manfredi, Wei Gu, and Stuart A. Aaronson. 2016. 'USP7 Enforces Heterochromatinization of p53 Target Promoters by Protecting SUV39H1 from MDM2-Mediated Degradation', *Cell Reports*, 14: 2528-37.

Murphy, Maureen E. 2016. 'Ironing out how p53 regulates ferroptosis', *Proceedings of the National Academy of Sciences*, 113: 12350-52.

Olivier, Magali, Monica Hollstein, and Pierre Hainaut. 2010. 'TP53 mutations in human cancers: origins, consequences, and clinical use', *Cold Spring Harbor perspectives in biology*, 2: a001008-a08.

Ou, Yang, Shang-Jui Wang, Dawei Li, Bo Chu, and Wei Gu. 2016. 'Activation of SAT1 engages polyamine metabolism with p53-mediated ferroptotic responses', *Proceedings of the National Academy of Sciences*, 113: E6806-E12.

Parant, John, Arturo Chavez-Reyes, Natalie A. Little, Wen Yan, Valerie Reinke, Aart G. Jochemsen, and Guillermina Lozano. 2001. 'Rescue of embryonic lethality in Mdm4-null mice by loss of Trp53 suggests a nonoverlapping pathway with MDM2 to regulate p53', *Nature Genetics*, 29: 92-95.

Park, H. S., U. I. Ju, J. W. Park, J. Y. Song, D. H. Shin, K. H. Lee, L. S. Jeong, J. Yu, H. W. Lee, J. Y. Cho, S. Y. Kim, S. W. Kim, J. B. Kim, K. S. Park, and Y. S. Chun. 2016. 'PPARγ

neddylation essential for adipogenesis is a potential target for treating obesity', *Cell death and differentiation*, 23: 1296-311.
Parrales, Alejandro, and Tomoo Iwakuma. 2016. 'p53 as a Regulator of Lipid Metabolism in Cancer', *International journal of molecular sciences*, 17: 2074.
Patton, J. T., L. D. Mayo, A. D. Singhi, A. V. Gudkov, G. R. Stark, and M. W. Jackson. 2006. 'Levels of HdmX expression dictate the sensitivity of normal and transformed cells to Nutlin-3', *Cancer Res*, 66: 3169-76.
Pishas, Kathleen I., Alaknanda Adwal, Susan J. Neuhaus, Mark T. Clayer, Gelareh Farshid, Alexander H. Staudacher, and David F. Callen. 2015. 'XI-006 induces potent p53-independent apoptosis in Ewing sarcoma', *Scientific reports*, 5: 11465-65.
Poyurovsky, Masha V., Christina Priest, Alex Kentsis, Katherine L. B. Borden, Zhen-Qiang Pan, Nikola Pavletich, and Carol Prives. 2007. 'The Mdm2 RING domain C-terminus is required for supramolecular assembly and ubiquitin ligase activity', *The EMBO Journal*, 26: 90-101.
Qi, Chao, Yijun Zhu, and Janardan K. Reddy. 2000. 'Peroxisome proliferator-activated receptors, coactivators, and downstream targets', *Cell Biochemistry and Biophysics*, 32: 187.
Qian, Yingjuan, and Xinbin Chen. 2013. 'Senescence regulation by the p53 protein family', *Methods in molecular biology (Clifton, N.J.)*, 965: 37-61.
Quartararo, Christine E., Eduard Reznik, Ana C. deCarvalho, Tom Mikkelsen, and Brent R. Stockwell. 2015. 'High-Throughput Screening of Patient-Derived Cultures Reveals Potential for Precision Medicine in Glioblastoma', *ACS medicinal chemistry letters*, 6: 948-52.
Ranjan, Atul, and Tomoo Iwakuma. 2016. 'Non-Canonical Cell Death Induced by p53', *International journal of molecular sciences*, 17: 2068.
———. 2018. 'Emerging Non-Canonical Functions and Regulation of p53', *International journal of molecular sciences*, 19: 1015.
Reinhart, Peter H., Linda S. Kaltenbach, Christian Essrich, Denise E. Dunn, Joshua A. Eudailey, C. Todd DeMarco, Gregory J. Turmel, Jennifer C. Whaley, Andrew Wood, Seongeun Cho, and Donald C. Lo. 2011. 'Identification of anti-inflammatory targets for Huntington's disease using a brain slice-based screening assay', *Neurobiology of disease*, 43: 248-56.
Reisz, Julie A., Connie Zheng, Angelo D'Alessandro, and Travis Nemkov. 2019. 'Untargeted and Semi-targeted Lipid Analysis of Biological Samples Using Mass Spectrometry-Based Metabolomics.' in Angelo D'Alessandro (ed.), *High-Throughput Metabolomics: Methods and Protocols* (Springer New York: New York, NY).
Riley, Maurisa F., and Guillermina Lozano. 2012. 'The Many Faces of MDM2 Binding Partners', *Genes & Cancer*, 3: 226-39.
Riley, Todd, Eduardo Sontag, Patricia Chen, and Arnold Levine. 2008. 'Transcriptional control of human p53-regulated genes', *Nature Reviews Molecular Cell Biology*, 9: 402-12.
Ringshausen, Ingo, Clodagh C. O'Shea, Andrew J. Finch, Lamorna Brown Swigart, and Gerard I. Evan. 2006. 'Mdm2 is critically and continuously required to suppress lethal p53 activity in vivo', *Cancer Cell*, 10: 501-14.
Rinon, Ariel, Alina Molchadsky, Elisha Nathan, Gili Yovel, Varda Rotter, Rachel Sarig, and Eldad Tzahor. 2011. 'p53 coordinates cranial neural crest cell growth and epithelial-mesenchymal transition/delamination processes', *Development*, 138: 1827.

Riscal, Romain, Emilie Schrepfer, Giuseppe Arena, Madi Y Cissé, Floriant Bellvert, Maud Heuillet, Florian Rambow, Eric Bonneil, Frédérique Sabourdy, Charles Vincent, Imade Ait-Arsa, Thierry Levade, Pierre Thibaut, Jean-Christophe Marine, Jean-Charles Portais, Jean-Emmanuel Sarry, Laurent Le Cam, and Laetitia K Linares. 2016. 'Chromatin-Bound MDM2 Regulates Serine Metabolism and Redox Homeostasis Independently of p53', *Molecular Cell*, 62: 890-902.

Sanjana, Neville E., Ophir Shalem, and Feng Zhang. 2014. 'Improved vectors and genome-wide libraries for CRISPR screening', *Nature methods*, 11: 783-84.

Sato, Mami, Ryosuke Kusumi, Shinji Hamashima, Sho Kobayashi, Satoru Sasaki, Yuhei Komiyama, Takuji Izumikawa, Marcus Conrad, Shiro Bannai, and Hideyo Sato. 2018. 'The ferroptosis inducer erastin irreversibly inhibits system xc− and synergizes with cisplatin to increase cisplatin's cytotoxicity in cancer cells', *Scientific reports*, 8: 968.

Seiler, Alexander, Manuela Schneider, Heidi Förster, Stephan Roth, Eva K. Wirth, Carsten Culmsee, Nikolaus Plesnila, Elisabeth Kremmer, Olof Rådmark, Wolfgang Wurst, Georg W. Bornkamm, Ulrich Schweizer, and Marcus Conrad. 2008. 'Glutathione Peroxidase 4 Senses and Translates Oxidative Stress into 12/15-Lipoxygenase Dependent- and AIF-Mediated Cell Death', *Cell Metabolism*, 8: 237-48.

Shadfan, Miriam, Vanessa Lopez-Pajares, and Zhi-Min Yuan. 2012. 'MDM2 and MDMX: Alone and together in regulation of p53', *Translational cancer research*, 1: 88-89.

Shah, Ron, Luke A. Farmer, Omkar Zilka, Antonius T. M. Van Kessel, and Derek A. Pratt. 2019. 'Beyond DPPH: Use of Fluorescence-Enabled Inhibited Autoxidation to Predict Oxidative Cell Death Rescue', *Cell Chemical Biology*, 26: 1594-607.e7.

Shah, Ron, Mikhail S. Shchepinov, and Derek A. Pratt. 2018. 'Resolving the Role of Lipoxygenases in the Initiation and Execution of Ferroptosis', *ACS Central Science*, 4: 387-96.

Shen, Jia, Xiangpeng Sheng, ZeNan Chang, Qian Wu, Sheng Wang, Zongliang Xuan, Dan Li, Yalan Wu, Yongjia Shang, Xiangtao Kong, Long Yu, Lin Li, Kangchen Ruan, Hongyu Hu, Ying Huang, Lijian Hui, Dong Xie, Fudi Wang, and Ronggui Hu. 2014. 'Iron Metabolism Regulates p53 Signaling through Direct Heme-p53 Interaction and Modulation of p53 Localization, Stability, and Function', *Cell Reports*, 7: 180-93.

Shi, Dingding, and Wei Gu. 2012. 'Dual Roles of MDM2 in the Regulation of p53: Ubiquitination Dependent and Ubiquitination Independent Mechanisms of MDM2 Repression of p53 Activity', *Genes & Cancer*, 3: 240-48.

Shi, Kun, Zhen Gao, Tian-Qiong Shi, Ping Song, Lu-Jing Ren, He Huang, and Xiao-Jun Ji. 2017. 'Reactive Oxygen Species-Mediated Cellular Stress Response and Lipid Accumulation in Oleaginous Microorganisms: The State of the Art and Future Perspectives', *Frontiers in Microbiology*, 8: 793.

Shimada, Kenichi, Rachid Skouta, Anna Kaplan, Wan Seok Yang, Miki Hayano, Scott J. Dixon, Lewis M. Brown, Carlos A. Valenzuela, Adam J. Wolpaw, and Brent R. Stockwell. 2016. 'Global survey of cell death mechanisms reveals metabolic regulation of ferroptosis', *Nature chemical biology*, 12: 497-503.

Shinozaki, Tomomi, Ayumi Nota, Yoichi Taya, and Koji Okamoto. 2003. 'Functional role of Mdm2 phosphorylation by ATR in attenuation of p53 nuclear export', *Oncogene*, 22: 8870-80.

Shvarts, A., W. T. Steegenga, N. Riteco, T. van Laar, P. Dekker, M. Bazuine, R. C. van Ham, W. van der Houven van Oordt, G. Hateboer, A. J. van der Eb, and A. G. Jochemsen. 1996.

'MDMX: a novel p53-binding protein with some functional properties of MDM2', *The EMBO Journal*, 15: 5349-57.

Shvarts, Avi, Merlijn Bazuine, Patrick Dekker, Yolande F. M. Ramos, Wilma T. Steegenga, Gerard Merckx, Reinier C. A. van Ham, Willemien van der Houven van Oordt, Alex J. van der Eb, and A. G. Jochemsen. 1997. 'Isolation and Identification of the Human Homolog of a New p53-Binding Protein, Mdmx', *Genomics*, 43: 34-42.

Sionov, R. V., S. Coen, Z. Goldberg, M. Berger, B. Bercovich, Y. Ben-Neriah, A. Ciechanover, and Y. Haupt. 2001. 'c-Abl regulates p53 levels under normal and stress conditions by preventing its nuclear export and ubiquitination', *Molecular and Cellular Biology*, 21: 5869-78.

Sionov, Ronit Vogt, and Ygal Haupt. 1999. 'The cellular response to p53: the decision between life and death', *Oncogene*, 18: 6145-57.

Skouta, Rachid, Scott J. Dixon, Jianlin Wang, Denise E. Dunn, Marina Orman, Kenichi Shimada, Paul A. Rosenberg, Donald C. Lo, Joel M. Weinberg, Andreas Linkermann, and Brent R. Stockwell. 2014. 'Ferrostatins Inhibit Oxidative Lipid Damage and Cell Death in Diverse Disease Models', *Journal of the American Chemical Society*, 136: 4551-56.

Song, Shulan, Ramy R. Attia, Sara Connaughton, Melissa I. Niesen, Gene C. Ness, Marshall B. Elam, Roderick T. Hori, George A. Cook, and Edwards A. Park. 2010. 'Peroxisome proliferator activated receptor α (PPARα) and PPAR gamma coactivator (PGC-1α) induce carnitine palmitoyltransferase IA (CPT-1A) via independent gene elements', *Molecular and Cellular Endocrinology*, 325: 54-63.

Soria, G., O. Podhajcer, C. Prives, and V. Gottifredi. 2006. 'P21Cip1/WAF1 downregulation is required for efficient PCNA ubiquitination after UV irradiation', *Oncogene*, 25: 2829-38.

Stad, R., N. A. Little, D. P. Xirodimas, R. Frenk, A. J. van der Eb, D. P. Lane, M. K. Saville, and A. G. Jochemsen. 2001. 'Mdmx stabilizes p53 and Mdm2 via two distinct mechanisms', *EMBO reports*, 2: 1029-34.

Steffan, J. S., A. Kazantsev, O. Spasic-Boskovic, M. Greenwald, Y. Z. Zhu, H. Gohler, E. E. Wanker, G. P. Bates, D. E. Housman, and L. M. Thompson. 2000. 'The Huntington's disease protein interacts with p53 and CREB-binding protein and represses transcription', *Proceedings of the National Academy of Sciences of the United States of America*, 97: 6763-68.

Stockwell, Brent R. 2019. 'Dawn of a New Era of Targeted Antioxidant Therapies', *Cell Chemical Biology*, 26: 1483-85.

Stockwell, Brent R., José Pedro Friedmann Angeli, Hülya Bayir, Ashley I. Bush, Marcus Conrad, Scott J. Dixon, Simone Fulda, Sergio Gascón, Stavroula K. Hatzios, Valerian E. Kagan, Kay Noel, Xuejun Jiang, Andreas Linkermann, Maureen E. Murphy, Michael Overholtzer, Atsushi Oyagi, Gabriela C. Pagnussat, Jason Park, Qitao Ran, Craig S. Rosenfeld, Konstantin Salnikow, Daolin Tang, Frank M. Torti, Suzy V. Torti, Shinya Toyokuni, K. A. Woerpel, and Donna D. Zhang. 2017. 'Ferroptosis: A Regulated Cell Death Nexus Linking Metabolism, Redox Biology, and Disease', *Cell*, 171: 273-85.

Sullivan, Kelly D., Matthew D. Galbraith, Zdenek Andrysik, and Joaquin M. Espinosa. 2018. 'Mechanisms of transcriptional regulation by p53', *Cell death and differentiation*, 25: 133-43.

Surget, Sylvanie, Marie P. Khoury, and Jean-Christophe Bourdon. 2013. 'Uncovering the role of p53 splice variants in human malignancy: a clinical perspective', *OncoTargets and therapy*, 7: 57-68.

Suzuki, Sawako, Tomoaki Tanaka, Masha V. Poyurovsky, Hidekazu Nagano, Takafumi Mayama, Shuichi Ohkubo, Maria Lokshin, Hiroyuki Hosokawa, Toshinori Nakayama, Yutaka Suzuki, Sumio Sugano, Eiichi Sato, Toshitaka Nagao, Koutaro Yokote, Ichiro Tatsuno, and Carol Prives. 2010. 'Phosphate-activated glutaminase (GLS2), a p53-inducible regulator of glutamine metabolism and reactive oxygen species', *Proceedings of the National Academy of Sciences*, 107: 7461.

Tackmann, Nicole R., and Yanping Zhang. 2017. 'Mouse modelling of the MDM2/MDMX−p53 signalling axis', *Journal of molecular cell biology*, 9: 34-44.

Tarangelo, Amy, Leslie Magtanong, Kathryn T. Bieging-Rolett, Yang Li, Jiangbin Ye, Laura D. Attardi, and Scott J. Dixon. 2018. 'p53 Suppresses Metabolic Stress-Induced Ferroptosis in Cancer Cells', *Cell Reports*, 22: 569-75.

Teissier, Elisabeth, Atsushi Nohara, Giulia Chinetti, Réjane Paumelle, Bertrand Cariou, Jean-Charles Fruchart, P. Brandes Ralf, Ajay Shah, and Bart Staels. 2004. 'Peroxisome Proliferator–Activated Receptor α Induces NADPH Oxidase Activity in Macrophages, Leading to the Generation of LDL with PPAR-α Activation Properties', *Circulation Research*, 95: 1174-82.

Theurillat, Jean-Philippe P., Namrata D. Udeshi, Wesley J. Errington, Tanya Svinkina, Sylvan C. Baca, Marius Pop, Peter J. Wild, Mirjam Blattner, Anna C. Groner, Mark A. Rubin, Holger Moch, Gilbert G. Prive, Steven A. Carr, and Levi A. Garraway. 2014. 'Prostate cancer. Ubiquitylome analysis identifies dysregulation of effector substrates in SPOP-mutant prostate cancer', *Science (New York, N.Y.)*, 346: 85-89.

Tian, Huibin, Jun Luo, Hengbo Shi, Xiaoying Chen, Jiao Wu, Yusheng Liang, Cong Li, and Juan J. Loor. 2020. 'Role of peroxisome proliferator-activated receptor-α on the synthesis of monounsaturated fatty acids in goat mammary epithelial cells', *Journal of Animal Science*.

Turunen, Mikael, Jerker Olsson, and Gustav Dallner. 2004. 'Metabolism and function of coenzyme Q', *Biochimica et Biophysica Acta (BBA) - Biomembranes*, 1660: 171-99.

Tyagi, Sandeep, Paras Gupta, Arminder Singh Saini, Chaitnya Kaushal, and Saurabh Sharma. 2011. 'The peroxisome proliferator-activated receptor: A family of nuclear receptors role in various diseases', *Journal of advanced pharmaceutical technology & research*, 2: 236-40.

Uldrijan, Stjepan, Willem-Jan Pannekoek, and Karen H. Vousden. 2007. 'An essential function of the extreme C-terminus of MDM2 can be provided by MDMX', *The EMBO Journal*, 26: 102-12.

Urist, Marshall, Tomoaki Tanaka, Masha V. Poyurovsky, and Carol Prives. 2004. 'p73 induction after DNA damage is regulated by checkpoint kinases Chk1 and Chk2', *Genes & Development*, 18: 3041-54.

Van Nostrand, Jeanine L., Colleen A. Brady, Heiyoun Jung, Daniel R. Fuentes, Margaret M. Kozak, Thomas M. Johnson, Chieh-Yu Lin, Chien-Jung Lin, Donald L. Swiderski, Hannes Vogel, Jonathan A. Bernstein, Tania Attié-Bitach, Ching-Pin Chang, Joanna Wysocka, Donna M. Martin, and Laura D. Attardi. 2014. 'Inappropriate p53 activation during development induces features of CHARGE syndrome', *Nature*, 514: 228-32.

van Raalte, Daniel H., Min Li, P. Haydn Pritchard, and Kishor M. Wasan. 2004. 'Peroxisome Proliferator-Activated Receptor (PPAR)-α: A Pharmacological Target with a Promising Future', *Pharmaceutical Research*, 21: 1531-38.
Vassilev, Lyubomir T., Binh T. Vu, Bradford Graves, Daisy Carvajal, Frank Podlaski, Zoran Filipovic, Norman Kong, Ursula Kammlott, Christine Lukacs, Christian Klein, Nader Fotouhi, and Emily A. Liu. 2004. 'In Vivo Activation of the p53 Pathway by Small-Molecule Antagonists of MDM2', *Science*, 303: 844-48.
Vogelstein, Bert, David Lane, and Arnold J. Levine. 2000. 'Surfing the p53 network', *Nature*, 408: 307-10.
Vousden, Karen H., and Xin Lu. 2002. 'Live or let die: the cell's response to p53', *Nature Reviews Cancer*, 2: 594-604.
Wade, M., Y. C. Li, A. S. Matani, S. M. G. Braun, F. Milanesi, L. W. Rodewald, and G. M. Wahl. 2012. 'Functional analysis and consequences of Mdm2 E3 ligase inhibition in human tumor cells', *Oncogene*, 31: 4789-97.
Wade, M., E. T. Wong, M. Tang, J. M. Stommel, and G. M. Wahl. 2006. 'Hdmx modulates the outcome of p53 activation in human tumor cells', *J Biol Chem*, 281: 33036-44.
Wade, Mark, Yao-Cheng Li, and Geoffrey M. Wahl. 2013. 'MDM2, MDMX and p53 in oncogenesis and cancer therapy', *Nature Reviews Cancer*, 13: 83.
Wade, Mark, Yunyuan V. Wang, and Geoffrey M. Wahl. 2010. 'The p53 orchestra: Mdm2 and Mdmx set the tone', *Trends in cell biology*, 20: 299-309.
Waldman, Todd, Kenneth W. Kinzler, and Bert Vogelstein. 1995. 'p21 Is Necessary for the p53-mediated G1 Arrest in Human Cancer Cells', *Cancer Res.*, 55: 5187-90.
Wang, Hongbo, and Chunhong Yan. 2011. 'A small-molecule p53 activator induces apoptosis through inhibiting MDMX expression in breast cancer cells', *Neoplasia (New York, N.Y.)*, 13: 611-19.
Wang, S., E. A. Konorev, S. Kotamraju, J. Joseph, S. Kalivendi, and B. Kalyanaraman. 2004. 'Doxorubicin induces apoptosis in normal and tumor cells via distinctly different mechanisms. intermediacy of H(2)O(2)- and p53-dependent pathways', *J Biol Chem*, 279: 25535-43.
Wang, Shang-Jui, Dawei Li, Yang Ou, Le Jiang, Yue Chen, Yingming Zhao, and Wei Gu. 2016. 'Acetylation Is Crucial for p53-Mediated Ferroptosis and Tumor Suppression', *Cell Reports*, 17: 366-73.
Wang, Shu-Ping, Wen-Lung Wang, Yih-Leong Chang, Chen-Tu Wu, Yu-Chih Chao, Shih-Han Kao, Ang Yuan, Chung-Wu Lin, Shuenn-Chen Yang, Wing-Kai Chan, Ker-Chau Li, Tse-Ming Hong, and Pan-Chyr Yang. 2009. 'p53 controls cancer cell invasion by inducing the MDM2-mediated degradation of Slug', *Nature Cell Biology*, 11: 694.
Wang, Wei, Jiang-Jiang Qin, Sukesh Voruganti, Kalkunte S. Srivenugopal, Subhasree Nag, Shivaputra Patil, Horrick Sharma, Ming-Hai Wang, Hui Wang, John K. Buolamwini, and Ruiwen Zhang. 2014. 'The pyrido[b]indole MDM2 inhibitor SP-141 exerts potent therapeutic effects in breast cancer models', *Nature communications*, 5: 5086-86.
Wang, Weimin, Michael Green, Jae Eun Choi, Miguel Gijón, Paul D. Kennedy, Jeffrey K. Johnson, Peng Liao, Xueting Lang, Ilona Kryczek, Amanda Sell, Houjun Xia, Jiajia Zhou, Gaopeng Li, Jing Li, Wei Li, Shuang Wei, Linda Vatan, Hongjuan Zhang, Wojciech Szeliga, Wei Gu, Rebecca Liu, Theodore S. Lawrence, Candice Lamb, Yuri Tanno, Marcin Cieslik, Everett Stone, George Georgiou, Timothy A. Chan, Arul

Chinnaiyan, and Weiping Zou. 2019. 'CD8+ T cells regulate tumour ferroptosis during cancer immunotherapy', *Nature*, 569: 270-74.
Wang, Zhen, and Yi Sun. 2010. 'Targeting p53 for Novel Anticancer Therapy', *Translational oncology*, 3: 1-12.
Warfel, Noel a., and Wafik S. El-Deiry. 2013. 'p21WAF1 and tumourigenesis', *Current Opinion in Oncology*, 25: 52-58.
Warner, Wayne A., Ricardo Sanchez, Alex Dawoodian, Esther Li, and Jamil Momand. 2012. 'Identification of FDA-approved drugs that computationally bind to MDM2', *Chemical biology & drug design*, 80: 631-37.
Wienken, Magdalena, Ute M. Moll, and Matthias Dobbelstein. 2017. 'Mdm2 as a chromatin modifier', *Journal of molecular cell biology*, 9: 74-80.
Wu, Jia-rui, Qing-zhang Tuo, and Peng Lei. 2018. 'Ferroptosis, a Recent Defined Form of Critical Cell Death in Neurological Disorders', *Journal of Molecular Neuroscience*, 66: 197-206.
Wu, W., C. Xu, X. Ling, C. Fan, B. P. Buckley, M. V. Chernov, L. Ellis, F. Li, I. G. Muñoz, and X. Wang. 2015. 'Targeting RING domains of Mdm2-MdmX E3 complex activates apoptotic arm of the p53 pathway in leukemia/lymphoma cells', *Cell Death & Disease*, 6: e2035-e35.
Xia, M., D. Knezevic, C. Tovar, B. Huang, D. C. Heimbrook, and L. T. Vassilev. 2008. 'Elevated MDM2 boosts the apoptotic activity of p53-MDM2 binding inhibitors by facilitating MDMX degradation', *Cell Cycle*, 7: 1604-12.
Xie, Yangchun, Shan Zhu, Xinxin Song, Xiaofang Sun, Yong Fan, Jinbao Liu, Meizuo Zhong, Hua Yuan, Lin Zhang, Timothy R. Billiar, Michael T. Lotze, Herbert J. Zeh, Rui Kang, Guido Kroemer, and Daolin Tang. 2017. 'The Tumor Suppressor p53 Limits Ferroptosis by Blocking DPP4 Activity', *Cell Reports*, 20: 1692-704.
Xiong, Shunbin, Vinod Pant, Yun Zhang, Neeraj K. Aryal, M. James You, Donna Kusewitt, and Guillermina Lozano. 2017. 'The p53 inhibitor Mdm4 cooperates with multiple genetic lesions in tumourigenesis', *The Journal of pathology*, 241: 501-10.
Yang, Wan Seok, Rohitha SriRamaratnam, Matthew E Welsch, Kenichi Shimada, Rachid Skouta, Vasanthi S Viswanathan, Jaime H Cheah, Paul A Clemons, Alykhan F Shamji, Clary B Clish, Lewis M Brown, Albert W Girotti, Virginia W Cornish, Stuart L Schreiber, and Brent R Stockwell. 2014. 'Regulation of Ferroptotic Cancer Cell Death by GPX4', *Cell*, 156: 317-31.
Yang, Wan Seok, and Brent R. Stockwell. 2008. 'Synthetic lethal screening identifies compounds activating iron-dependent, nonapoptotic cell death in oncogenic-RAS-harboring cancer cells', *Chemistry & biology*, 15: 234-45.
———. 2016. 'Ferroptosis: death by lipid peroxidation', *Trends in cell biology*, 26: 165-76.
Ye, Ling F., Kunal R. Chaudhary, Fereshteh Zandkarimi, Andrew D. Harken, Connor J. Kinslow, Pavan S. Upadhyayula, Athanassios Dovas, Dominique M. Higgins, Hui Tan, Yan Zhang, Manuela Buonanno, Tony J. C. Wang, Tom K. Hei, Jeffrey N. Bruce, Peter D. Canoll, Simon K. Cheng, and Brent R. Stockwell. 2020. 'Radiation-Induced Lipid Peroxidation Triggers Ferroptosis and Synergizes with Ferroptosis Inducers', *ACS Chemical Biology*.
Ye, Ling F., Eduard Reznik, Joshua M. Korn, Fallon Lin, Guizhi Yang, Kimberly Malesky, Hui Gao, Alice Loo, Raymond Pagliarini, Tom Mikkelsen, Donald C. Lo, Ana C. deCarvalho,

and Brent R. Stockwell. 2020. 'Patient-derived glioblastoma cultures as a tool for small-molecule drug discovery', *Oncotarget; Vol 11, No 4*.
Youssef, Jihan, and Mostafa Badr. 2004. 'Role of Peroxisome Proliferator-Activated Receptors in Inflammation Control', *Journal of biomedicine & biotechnology*, 2004: 156-66.
Yu, H., P. Guo, X. Xie, Y. Wang, and G. Chen. 2017. 'Ferroptosis, a new form of cell death, and its relationships with tumourous diseases', *J Cell Mol Med*, 21: 648-57.
Zanjirband, Maryam, Richard J. Edmondson, and John Lunec. 2016. 'Pre-clinical efficacy and synergistic potential of the MDM2-p53 antagonists, Nutlin-3 and RG7388, as single agents and in combined treatment with cisplatin in ovarian cancer', *Oncotarget*, 7: 40115-34.
Zhang, Yan, Hui Tan, Jacob D. Daniels, Fereshteh Zandkarimi, Hengrui Liu, Lewis M. Brown, Koji Uchida, Owen A. O'Connor, and Brent R. Stockwell. 2019. 'Imidazole Ketone Erastin Induces Ferroptosis and Slows Tumor Growth in a Mouse Lymphoma Model', *Cell Chemical Biology*.
Zhang, Yun, Shunbin Xiong, Qin Li, Sophia Hu, Mehrnoosh Tashakori, Carolyn Van Pelt, Mingjian James You, Laura Pageon, and Guillermina Lozano. 2014. 'Tissue-specific and age-dependent effects of global Mdm2 loss', *The Journal of pathology*, 233: 380-91.
Zhang, Z., H. Wang, M. Li, S. Agrawal, X. Chen, and R. Zhang. 2004. 'MDM2 is a negative regulator of p21WAF1/CIP1, independent of p53', *J Biol Chem*, 279: 16000-6.
Zhao, Yuhan, Haiyang Yu, and Wenwei Hu. 2014. 'The regulation of MDM2 oncogene and its impact on human cancers', *Acta biochimica et biophysica Sinica*, 46: 180-89.
Zhuang, Li, and Boyi Gan. 2019. 'BAP1 suppresses tumor development by inducing ferroptosis upon SLC7A11 repression AU - Zhang, Yilei', *Molecular & Cellular Oncology*, 6: 1536845.